esa

fiducial reference measurements for satellite ocean colour

D-60 Technical Report TR-1 "Measurement Requirements and Protocols when Operating Fiducial Reference Measurement (FRM) Ocean Colour Radiometers (OCR) used for Satellite Validation„

Title	Technical Report TR- 1 "Measurement Requirements and Protocols when Operating Fiducial Reference Measurement (FRM) Ocean Colour Radiometers (OCR) used for Satellite Validation"
Document reference	FRM4SOC-TR1
Project	ESA – FRM4SOC
Contract	ESRIN/Contract No. 4000117454/16/1-SBo
Deliverable	D-60 (Technical Report TR-1)
ATTN	Tânia Casal ESA/ESTEC Technical Officer Keplerlaan 1 2201 AZ Noordwijk The Netherlands
Version	1
Date issued	29.01.2018

	Prepared by	Contractor	Customer
Name:	Kevin Ruddick	Riho Vendt	Tânia Casal
Organisation:	RBINS	Tartu Observatory	ESA/ESTEC
Position:	WP leader	Project manager	Technical Officer
Date:	29.01.2018		
Signature:		Digitally signed by VENDT,RIHO,37201185216 DN: c=EE, o=ESTEID, ou=digital signature, cn=VENDT,RIHO,37201185216, sn=VENDT, givenName=RIHO, serialNumber=37201185216 Date: 2018.02.01 13:52:09 +02'00'	Tânia Casal 17 Apr 2018

A note on authorship: many scientists have made small or large contributions in preparation of the current document. The Document Change Record below lists most of these, but cannot be considered as an author list in the sense of an author list for a scientific publication because: a) some contributors have requested that their contribution not be considered for co-authorship; b) some contributors have made very significant contributions to certain sections/chapters, some have made small contributions; c) co-authorship may imply for some scientists or some organisations endorsement of or agreement with every word of the document. The latter is particularly difficult to achieve at this stage since many words or sentences have been changed at each successive version, implying that a final stabilised document draft would need to be re-read and accepted. A full author list and acknowledgements of all contributors will be proposed in a future version of this document and, when accepted, published as the final, consolidated FRM4SOC Technical Report. The FRM4SOC project is funded by the European Space Agency.

Responsibility: statements made in this report are the responsibility of the lead author and the FRM4SOC Project Team and do not necessarily represent the official views of the European Space Agency or the organisations of any of the scientists who contributed to this report.

Document Change Record

Index	Issue	Revision	Date	Brief description	Issued by
1.	0	4	14.03.2017	INCOMPLETE DRAFT	Kevin Ruddick
2.	0	9	21.04.2017	First draft of Chapters 1, 2, 3	Kevin Ruddick
3.	0	10	5.5.2017	Improving references and numbering	KR
4.	0	12	6.6.2017	Major reorganisation – Ed protocols split off to separate chapter and sunphotometry and reference plaque methods added	KR
5.	0	13	9.6.2017	Completed draft of Chapters 1-4	KR
6.	0	14	15.6.2017	Complete check and update of Chapters 1-4	KR
7.	0	15	14.7.2017	Updates of Chapters 1-4 following detailed comments from Ken Voss, references update from Giuseppe Zibordi Input from Tartu not yet incorporated	Input from Ken Voss
8.	0	16	12.9.2017	Further updates following comments of Robert Frouin, Tartu and NPL colleagues and ESA.	Input from Robert Frouin, Viktor Vabson, Riho Vendt, Joel Kuusk, Ilmar Ansko, Krista Alikas, Andrew Banks, Craig Donlon
9.	0	17	4.10.2017	Further update following comments of S3VT and some NOAA/VIIRS Validation Team members. Includes correction of mistake in equation (8) (Reflectance of plaque should be in denominator).	Input from Mike Ondrusek, Zhongping Lee.
10	0	19	3.11.2017	Further update from Round 2 of NOAA/VIIRS Validation Team comments	Input from Martin Hieronymi, Cédric Jamet,
11.	0	20	5.12.2017	Further updates especially reflectance plaque method	Inputs from Carol Johnson, Alex Gilerson and other NOAA/VIIRS cal/val team.
12.	0	21	8.12.2017	Addition of Chapter 5 on bidiretional effects and Chapter 6 on space-time impacts on matchup validation, including input from Q. Vanhellemont and A. Dogliotti	Kevin Ruddick
13.	0	22	11.12.2017	Final cleanup for delivery	Kevin Ruddick
14.	1	0	29.01.2018	Final version for submittion to ESA	Kevin Ruddick

Distribution List

Company/Organisation	Name	Format	No. of Copies
TO	Riho Vendt	Electronic file (DOCX, PDF)	1 DOCX, 1 PDF
RBINS	Kevin Ruddick	Electronic file (DOCX, PDF)	1 DOCX, 1 PDF
NPL	Andrew Banks	Electronic file (DOCX, PDF)	1 DOCX, 1 PDF
PML	Gavin Tilstone	Electronic file (DOCX, PDF)	1 DOCX, 1 PDF
ACRI-ST	Christophe Lerebourg	Electronic file (DOCX, PDF)	1 DOCX, 1 PDF
ESA ESTEC	Craig Donlon	Electronic file (DOCX, PDF)	1 DOCX, 1 PDF
ESA ESRIN	Silke Bode	Electronic file (DOCX,PDF)	1 DOCX, 1 PDF
ESA ESTEC	Tânia Casal	Electronic file (DOCX, PDF)	1 DOCX, 1 PDF

Acronyms and Abbreviations

Acronym	Abbreviation
AAOT	Aqua Alta Oceanographic Tower
ADC	Analogue Digital Converter
CCD	Charge Coupled Device
ESA	European Space Agency
EO	Earth Observation
ESRIN	European Space Research Institute
ESTEC	European Space Research and Technology Centre (of ESA)
FICE	Field Inter-Comparison Experiment
FOV	Field of View
FRM4SOC	Fiducial Reference Measurements for Satellite Ocean Colour
FWHM	Full Width Half Maximum
KO	Kick-Off
LCE	Laboratory Comparison Experiment
LOV	Laboratoire d'Océanographie de Villefranche
NPL	National Physical Laboratory
OC	Ocean Color
OCR	Ocean Color Radiometer
PML	Plymouth Marine Laboratory
RBINS	Royal Belgian Institute for Natural Sciences
SI	Systeme International d’Unites
SOW	Statement of Work
TO	Tartu Observatory
TR	Technical Report (long report > 50 pages)

Contents

Document Change Record 2
Distribution List 3
Acronyms and Abbreviations 4
Contents 5
List of Figures 8
List of Tables 11
1 Introduction 12
1.1 Scope of the document 12
1.1.1 Statement of Work 12
1.1.2 Broad range of validation conditions 13
1.1.3 Approach based on uncertainty estimates 14
1.2 Definition of Fiducial Reference Measurement (FRM) 15
1.3 Motivation – the needs for FRM for satellite validation 15
1.4 Key protocol documents and prior references 18
1.4.1 NASA Ocean Optics Protocols for Satellite Ocean Color Sensor Validation 18
1.4.2 REVAMP/MERIS protocols 19
1.4.3 MERIS Optical Measurement Protocols and MERMAID database 19
1.4.4 GLASS and MERIS Lake Water protocol documents 20
1.4.5 CEOS INSITU-OCR 21
2 Measurement Requirements 23
2.1 Required parameters 23
2.1.1 Essential geophysical radiance/reflectance product 23
2.1.2 Directionality of radiometric products 25
2.1.3 Auxiliary optical parameters 26
2.1.4 Other auxiliary parameters and information 29
2.2 Uncertainty estimation 31
2.3 Traceability 31
2.4 Protocol and Measurement Documentation 32
2.5 Quality Control and associated measurement and processing flags 32
2.6 Data Processing software 32
2.7 Data archiving and distribution 32
2.8 Data exploitation 32
2.9 Document structuration with separate chapters for Lw and Ed 32
3 Measurement Protocols for above water downwelling irradiance 35
3.1 Direct above water measurement of $Ed0+$ with an upward pointing irradiance sensor 35

3.1.1 Measurement equation 35

3.1.2 Protocol-dependent sources of uncertainty 38

3.1.3 Variants on the method of Direct above water measurement of $Ed0+$ with an upward pointing irradiance sensor 42

3.2 Estimation of $Ed0+$ from direct sunphotometry and a clear sky atmospheric model 42

3.2.1 Measurement equation 44

3.2.2 Protocol-dependent sources of uncertainty 45

3.2.3 Variants on the method of measurement of $Ed0+$ from direct sunphotometry and a clear sky atmospheric model 47

3.3 Estimation of $Ed0+$ using a downward pointing radiance sensor and a reflective plaque . 47

3.3.1 Measurement equation 47

3.3.2 Protocol-dependent sources of uncertainty 50

3.3.3 Variants on the method for measurement of $Ed0+$ using a downward pointing radiance sensor and a reflectance plaque....53

3.4 Estimation of $Ed0+$ from underwater measurements.... 53

4 Measurement Protocols for water-leaving radiance.... 54

4.1 Underwater radiometry – fixed depth measurements.... 54

4.1.1 Measurement equation 54

4.1.2 Protocol-dependent sources of uncertainty 58

4.1.3 Variants on the fixed depth underwater radiometric method 60

4.2 Underwater radiometery – vertical profiles.... 61

4.2.1 Measurement equation 64

4.2.2 Protocol-dependent sources of uncertainty 66

4.2.3 Variants on the vertical profiling underwater radiometric method 68

4.3 Above water radiometry with sky radiance measurement and skyglint removal 68

4.3.1 Measurement equation 68

4.3.2 Protocol-dependent sources of uncertainty 73

4.3.3 Variants on the above water radiometric method....77

4.4 Above water radiometry with Skylight-Blocked Approach 78

4.4.1 Measurement equation 78

4.4.2 Protocol-dependent sources of uncertainty 79

4.4.3 Variants on the above water radiometric with Skylight Blocked Approach 81

5 Bidirectional effects 81

6 In Situ/Satellite space-time match-up considerations....83

6.1 Space and time scales of natural optically-relevant processes....83

6.2 Definition of space and time scales for satellite data measurements 85

6.3 Definition of space and time scales for in situ data measurements....86

6.4 Approaches for dealing with space-time differences when comparing satellite with in situ measurements 90
6.4.1 Approaches to sub-pixel scale spatial variability 90
6.5 Approaches for dealing with time differences when comparing satellite with in situ measurements 94
7 Conclusions and Recommendations 97
7.1 Maturity of requirements and protocols 97
7.2 Recommendations for achieving FRM status from S3VT 97
7.3 Other Recommendations - terminology 98
7.4 Any remaining issues and gaps in knowledge 98
7.4.1 Rare and expensive tools and expertise 98
7.5 Future evolution of requirements and protocols 99
8 References 100

List of Figures

Figure 1-1 Processing steps from: a) calibrated TOA radiance ("Level 1"), which represents temporal (snapshot), spatial (image), spectral (bands) and radiometric (digitised) sampling of nature through b) Level 2 radiometric (L2R) data after atmospheric correction, to the c) Level 2 water (L2W) used as basis for applications. From (K. Ruddick et al. 2010)........................... 17
Figure 2-1 Illustration of definitions of water-leaving radiance, $\boldsymbol{Lw}$, above water upwelling radiance, $\boldsymbol{Lu0+}$, and downwelling irradiance. See also [http://www.oceanopticsbook.info/view/overview_of_optical_oceanography/reflectances] 24
Figure 2-2 Illustration of restructuring of NASA Ocean Optics Protocols into these FRM4SOC Protocols with separate Chapters for $\boldsymbol{Ed0+}$ and $\boldsymbol{Lw}$. 34
Figure 3-1 Schematic of direct above water measurement of $\boldsymbol{Ed0+}$ with an irradiance sensor (not drawn to scale).. 36
Figure 3-2 Typical deployment of above water irradiance sensors (top) Combined with a sunphotometer system on a mast, taken from (Hlaing et al. 2010) (bottom) combined with sea- and sky-viewing radiance sensors at the prow of a ship, as in (KG Ruddick et al. 2006) 37
Figure 3-3 Schematic showing how a fish-eye camera, preferably fully hemispherical, can be used to qualitatively check for superstructure contamination of $\boldsymbol{Ed0+}$ measurements........... 39
Figure 3-4 Example fish-eye photos taken to check for contamination of $\boldsymbol{Ed0+}$ measurements. (top) Contamination of field of view by other instuments, (middle) Contamination of field of view by a scientist in bottom of photo, (top) No obvious contamination of field of view by nearby obstructions. Radiance from the trees does contribute to $\boldsymbol{Ed0+}$ (and this may be deemed inappropriate for satellite validation in some contexts) but since these objects are distant the $\boldsymbol{Ed0+}$ measurement is representative of the $\boldsymbol{Ed0+}$ field illuminating the water target. In none of these cases are the sky/cloud conditions suitable for satellite validation..... 39
Figure 3-5 Schematic of direct sun measurement for estimation of $\boldsymbol{Ed0+}$.............................. 43
Figure 3-6 Typical deployment of instrumentation for estimation of $\boldsymbol{Ed0+}$ by sunphotometry. (left) SeaPRISM instrument [photo courtesy: Dimitry Van Der Zande], (right) handheld SIMBADA instrument. 44
Figure 3-7 Schematic showing indirect measurement of $\boldsymbol{Ed0+}$ using a downward pointing radiance sensor and a reflective plaque (sensor, plaque and holder not to scale).....................47
Figure 3-8 Typical measurement equpment and deployment for measurement of $\boldsymbol{Ed0+}$ using a downward pointing radiance sensor and a reflective plaque. Photo courtesy A. Ruiz-Verdu... 48
Figure 3-9 Location of fish-eye camera used for qualitative checking of shading of reflectance plaque, for comparison with Figure 3-3 for the direct measurement of $\boldsymbol{Ed0+}$ using an irradiance sensor, described in section 3.1..52
Figure 4-1 Schematic of fixed depth underwater measurements...55
Figure 4-2 Typical deployments of fixed depth underwater measurements. (left) BOUSSOLE buoy (D. Antoine et al. 2008); (right) MOBY buoy [https://moby.mlml.calstate.edu/photo-gallery/] 56
Figure 4-3 Schematic of underwater vertical profile measurements 63
Figure 4-4 Typical deployments of underwater profiling radiometers (left) Ship-tethered free-fall profiler measuring upwelling radiance and downwelling radiance [Photo courtesy Satlantic]; (right) Freely-drifting vertically profiling radiometr platform [Photo courtesy: Laboratoire Océnographique de Villefranche]... 64
Figure 4-5 Schematic of above water radiometry with sky radiance measurement and skyglint removal. Dashed arrows indicate that contributions to the skylight reflected at the air-water interface come from directions that are not directly measured by the $\boldsymbol{Ld}$ radiance sensor, including possible contributions from the direct sunglint direction. 69

Figure 4-6 Typical deployments of above water radiometry systems: (top-left) TRIOS/RAMSES; (top-right) Satlantic Suntracker system with rotating mount; (middle-left) CIMEL SeaPRISM system with robotic pointing (bottom right) WISP 3-radiometer handheld system. 70
Figure 4-7 Fresnel reflectance coefficient, $\boldsymbol{\rho F}$, for a flat air-water interface with refractive index $\boldsymbol{nw}$=1.34 for light incident on the interface from air, e.g. skylight reflection. 71
Figure 4-8 Schematic of above water radiometry with Skylight-Blocked Approach. Note that the radiometer fore-optics are in air, but the radiometer body is extended with a cone or shield (black lines) that extends below the water surface, ensuring blocking of skylight reflection.... 78
Figure 4-9 Typical deployment of radiometer using Skylight Blocked Approach, reproduced from (Z. Lee et al. 2013) (c) 2013 Optical Society of America. 79
Figure 6-1. A schematic showing space scales of some important aquatic processes with optical relevance. The space scales of satellite measurements from Medium Resolution (MR), High Resolution (HR) satellite sensors are also shown, together with Very High Resolution (VHR: metre-scale) and Low Resolution length scales. LR data is typically obtained from spatial averaging of MR data. Some significant space scales relating to human activities (and large mammals) are shown in red. The spatial scales typical of in situ measurements are shown in violet and are generally shorter than MR satellite measurements but similar to HR or VHR length scales. 84
Figure 6-2. A schematic showing time scales of some important aquatic processes with optical relevance. Satellite measurements have very short time scales (1-100ms). The time scales typical of in situ measurements are shown in violet, but there is often also a time difference between in situ and satellite measurements, which may overlap with significant temporal variability of aquatic processes. 85
Figure 6-3 Schematic illustrating horizontal length scale for typical measurements made with fixed depth radiometry. $\boldsymbol{KLu}$ is the diffuse attenuation coefficient for upwelling radiance, $\boldsymbol{\theta FOV}$ is the half-angle field of view of the radiance sensor. 88
Figure 6-4 Schematic illustrating horizontal length scale for typical measurements made with "free-fall" vertically profiling depth radiometry. $\boldsymbol{KLu}$ is the diffuse attenuation coefficient for upwelling radiance, $\boldsymbol{\theta FOV}$ is the half-angle field of view of the radiance sensor. $\boldsymbol{udrift}$ is the horizontal drift velocity (similar to current velocity) and $\Delta \boldsymbol{t}$ is the time interval for the whole measurement sequence. 89
Figure 6-5 Schematic illustrating horizontal length scale for typical measurements made above water radiometry. $\boldsymbol{h}$ is the height of the sensor above water level, $\boldsymbol{\theta FOV}$ is the half-angle field of view of the radiance sensor. , $\boldsymbol{\theta v}$ is the zenith angle of the sensor. 90
Figure 6-6 Subset of a Landsat-8 Top Of Atmosphere Red-Green-Blue image described in detail by (Q. Vanhellemont and Ruddick 2015). Pixel size is 30m. The small red pixel contains a ship. The larger red pixel simulates a 300m Sentinel3/OLCI pixel. The blue pixel containing unperturbed water, is considered as a reference pixel. A band of darker brown water is also visible across the top of the image – this turbidity front will clearly be under-resolved in 300m imagery. Some periodic structures can also be seen across the image caused by surface gravity waves. 92
Figure 6-7 Subset of a Landsat-8 Top Of Atmosphere Red-Green-Blue image described in detail by (Q. Vanhellemont and Ruddick 2015). Pixel size is 30m. The small red pixel contains a large red offshore platform ("OTS") – it's shadow is also visible two pixels further North. The larger red pixel simulates a 300m Sentinel3/OLCI pixel. The blue pixel containing unperturbed water, is considered as a reference pixel. Individual wind turbines and their shadows are also clearly visible in this 30m imagery and will impact on 300m pixels. Some turbid wakes are visible to the East of the structures – see also (Q. Vanhellemont and Ruddick 2014). 93

Figure 6-8. (left) Turbidity map from a Landsat-8 of 23/4/2015 in the La Plata estuary. (right) Rayleigh-corrected reflectance spectral difference between different window sizes and a single L8 pixel (30m). 94
Figure 6-9 Reproduced from (Kevin Ruddick et al. 2014): Comparison of turbidity data derived from SEVIRI and MODIS-AQUA on 15th April 2008 using the processing of (Neukermans, Ruddick, and Greenwood 2012): (top-left) daily average from 34 SEVIRI images,(top-right) single MODIS-AQUA acquisition at 12:45 UTC. Corresponding time series of in situ and remotely sensed turbidity at (bottom left) the mouth of the Thames river (51.5235°N,1.0240°E) and (bottom right) further offshore (51.9802°N, 2.0828°E). In the time series, SEVIRI data is given as grey dots, in situ optical data is given as blue or green dots according to location, and MODIS data is given as a single magenta dot for each location.) Full details of processing, including definition of the uncertainty bars for SEVIRI and in situ data, are given in (Neukermans, Ruddick, and Greenwood 2012) and (Neukermans 2012). 95
Figure 6-10 Reproduced from (Q. Vanhellemont, Neukermans, and Ruddick 2014): Comparison of MODIS derived turbidity with CEFAS/SmartBuoy turbidities from DOWS, WGAB and WARP (red, green and blue dots) at a) overpass time t0, b) two hours before, and c) three hours after t0. Matchups were extracted from mid-2002 to 2010, depending on buoy deployments. Red, green and blue dots are data from Dowsing, West Gabbard and Warp buoys respectively. 96

List of Tables

Table 1-1 MERMAID database Measurement Quality Control (MQC) flag criteria definition. Flag position is counted from the first numeric character after the leading 'M'. Unless otherwise specified: 0 = No / Not done, 1 = Yes / done/ provided, 2 = Unknown / not available / not applicable (N/A). Reproduced from (Barker et al. 2008). ... 20

Table 1-2. Processing Quality Ccontrol (PQC) flag criteria definition. Flag position is counted from the first numeric character after the leading 'P'. Unless otherwise specified: 0 = No / Not done, 1 = Yes / done/ provided, 2 = Unknown / not available. Reproduced from (Barker et al. 2008). ... 20

Table 2-1 Principal optical and biogeochemical *in situ* observations suggested by the NASA Ocean Optics Protocols (J. L. Mueller 2004) for satellite ocean color system validation, and algorithm development and validation. The right-hand column identifies and classifies measurements as: (a) required for minimal validation match-ups; (b) highly desired and important for general algorithm development and validation; (c) specialized measurements of important, but restricted, applicability to algorithm development and validation (for the present); and (d) calculated or derived quantities. Notation used in this Table is defined is detail in (Morel and Mueller 2003) but does not include all notation used in the present FRM4SOC report. ... 29

Table 2-2 Principal ancillary data required to accompany *in situ* observations suggested by the NASA Ocean Optics Protocols (J. L. Mueller 2004) for satellite ocean color system validation, and algorithm development and validation. The right-hand column identifies and classifies measurements as: (a) required for minimal validation match-ups; (b) highly desired and important for general algorithm development and validation; (c) specialized measurements of important, but restricted, applicability to algorithm development and validation (for the present); and (d) calculated or derived quantities. ... 30

1 Introduction

1.1 Scope of the document

1.1.1 Statement of Work

The scope of this document as defined by the ESA SOW is to:

i) Document measurement requirements for FRM OCR used to validate satellite OCR products.

ii) Design and document measurement protocols to operate instruments used for satellite OCR validation activities and maintain FRM status.

iii) Build on previous work (eg. NASA Ocean Optics Protocols series http://oceancolor.gsfc.nasa.gov/cms/techdocs).

iv) Provide a consolidated and easy to use/manage community consensus of protocols to follow when making field measurements (to FRM standards) that are used for satellite OCR validation.

v) Critically review the exact methodology used to maintain the calibration of OCR FRM field radiometers.

vi) Clearly explain how measurements used for satellite ocean colour radiometry (OCR) validation attain Fiducial Reference Measurement status.

vii)Include any other aspect considered relevant to the Task and objectives of FRM4SOC.

The FRM4SOC team, reflecting the ESA SOW more generally, considers it of prime importance to accurately estimate and validate the uncertainties of measurements used for satellite OCR validation. This total uncertainty estimate includes components arising from: a) the type of instrument used; b) the instrument calibration; c) the measurement protocol and data processing methods; and d) the spatio-temporal characteristics of the satellite-ground "matchup" measurements.

The present document considers only c) the measurement protocol and data processing methods, analyzing the Measurement Equation used to derive water-leaving radiance and reflectance from underwater and from above water radiometric measurements including the associated models/assumptions/approximations and aspects of instrument deployment; and d) the spatio-temporal characteristics of the satellite-ground "matchup" measurements.

The companion Technical Report FRM4SOC TR-2 deals with a) the type of instrument and its characterization, including thermal sensitivity, straylight/out-of-bound response, non-linearity, etc. The decomposition of measurements into "protocols" (deployment, data acquisition and processing methods) and "instruments" is adopted here in order to conveniently represent the wide diversity of possible combinations of methods and instruments in a synthetic and generic way. However, it is fully recognised that "protocol" and "instrument" are sometimes coupled and the design of the measurement protocol and the assessment of the uncertainty of any specific measurement requires a combined analysis of the protocol and the instrument together. For example, the methodology for removing of skylight reflected at the air-water interface in above water radiometric and its associated uncertainty depends on the frequency of acquisition possible with the instrument used. Radiometers based on a filter-wheel design will typically sample at high enough frequency to resolve fluctutations of upwelling radiance arising from reflection of direct sun (sunglint") and sky ("skyglint") from individual surface waves and hence allow for minimum-based filtering techniques to remove the brightest sunglint flashes (Stanford B. Hooker et al. 2002). On the other hand radiometers based on a hyperspectral spectrometer will typically sample at lower frequency (e.g. 1-4s) and hence underresolve wave effects with a consequent need to apply larger corrections for sky/sunglint with correspondingly larger uncertainty.

FRM4SOC Task 3 (LCE-1, LCE-2) deals in detail with uncertainty from SI-traceable calibration sources, through instrument calibration, controlled lab measurements by OCRs of those sources and controlled field measurements, and hence covers aspects of b) instrument calibration. The companion FRM4SOC Technical Report 7 (TR-7) will report on tracing uncertainty through all components of the measurement process.

As regards, point (v) of the SOW, the current "Protocols" review covers maintenance of the calibration of OCR FRM field radiometers in sections such as section 4.1.2.4 where measures to assess and limit bio-fouling are described, including the use of portable calibration lamps and pre/post-deployment calibration comparisons. Other aspects of radiometer calibration, and specifically absolute laboratory calibration, are covered in companion reports of the FRM4SOC project, while specific examples of portable calibration lamps are given in the FRM4SOC Technical Report 2 on "Radiometers".

1.1.2 Broad range of validation conditions

The scope of this document covers measurements made for validation of water surface radiance/reflectance data derived from calibrated satellite-borne optical sensors after atmospheric correction. This validation must be made over the full diversity of conditions where satellite optical products will be used.

It is fully recognized that the section 4.1 of this document on protocols for underwater radiometry using fixed depth measurements is strongly influenced by the MOBY and BOUSSOLE activities, which prioritise the highly accurate measurement of blue and green wavelengths in homogeneous open ocean case 1 waters for the purposes of vicarious calibration, and that this whole document is strongly influenced by the previous NASA Ocean Optics protocols (J.L. Mueller, Fargion, and McClain 2004), which have strong heritage from open ocean measurements. The accurate measurement of water radiance/reflectance for open ocean waters remains vital for assessing the contribution of phytoplankton processes to the global carbon cycle (McClain et al. 1998) and for detecting changes in oceanic ecosystems, e.g. related to anthropogenic climate change. However, satellite-borne optical sensors are also used for many other applications in coastal and inland waters, including eutrophication assessment, Harmful Algae Bloom detection, sediment transport, etc. (Mouw et al. 2015).

The scope of the current document on validation measurements is therefore quite different from previous NASA "Ocean" Optics protocol documents and from the FRM4SOC vicarious calibration activities. Whereas vicarious calibration measurements should be made in the best possible measurement conditions (horizontally and vertically homogeneous waters with low temporal variability, low and stable aerosol optical thickness, etc.), validation measurements must cover the full diversity of conditions where satellite optical products will be used, including coastal, estuarine and inland waters and suboptimal water and/or atmosphere conditions, where "suboptimal" means that conditions may not be optimal but the satellite data is still considered as usable and is not rejected by automated quality control procedures.

For example, validation is required for:

- aquatic conditions which include strong horizontal variability (onshore/offshore gradients, patchy waters, etc.), vertical variability (deep chlorophyll maxima, shallow river plumes, thermally stratified waters, etc.) and/or temporal variability (tidal waters, rapid algae blooms/declines);

• diverse aquatic constituents, including phytoplankton-dominated "case 1" waters, but also regions with high terrigenic Coloured Dissolved Organic Matter (CDOM), with non-algae particles, etc.

• diverse and difficult atmospheric conditions including low/moderate/high and rapidly varying aerosol optical thickness, different aerosol type (marine/urban/dust, etc.) including absorbing aerosols, thin clouds, including cirrus, a wide range of sun zenith angles, conditions when the satellite measurement includes significant sunglint, etc.

• water surfaces with moderate/high waves (if data is exploited in such conditions), and fetch-limited and/or developing surface wave fields, including estuarine and inland waters.

• locations and sun/viewing conditions with strong adjacency effects, where "adjacency" here refers to violation of typical atmospheric correction assumptions of a horizontally homogeneous water and atmosphere as may occur near land surfaces.

• locations where bottom reflectance may contribute to the water-leaving radiance.

• any other situations where the performance of atmospheric correction algorithms may be different.

Measurement protocols for radiometric validation therefore need to consider all such situations, and the "optimal" protocol may be highly situation- or location-specific.

In view of the broad scope necessary for validation measurements, terminology specific to "ocean" colour or "marine" reflectance or the "sea" surface is therefore avoided wherever possible in favour of "aquatic", which can include oceanic, coastal and inland waters. Unfortunately, because of the strong heritage from open ocean remote sensing the "ocean" colour terminology is often difficult to avoid and, for example, appears throughout the ESA Statement of Work where OCR represents "Ocean Colour Radiometry" although the same SOW does point out the importance of Sentinel-2 and coastal and inland waters. The importance and value of the IOCCG in structuring the aquatic optics community also reflects this strong "ocean" heritage. In the long term it could be preferable to adopt the terminology of "Water Colo(u)r Radiometry/Satellites" to fully reflect the widening of this community and these satellite sensors from the historial *ocean* colour perspective to include the coastal and inland water communities and applications.

Similarly the scope is not limited to the dedicated "ocean colour" medium-resolution multispectral polar-orbiting missions such as Sentinel-3/OLCI, MODIS/AQUA and VIIRS, but must consider all present and future satellite-borne optical sensors that are used for aquatic applications, including land-dedicated polar-orbiting missions such as Landsat-8 and Sentinel-2 (and many others), geostationary missions such as GOCI and GEO-CAPE, hyperspectral missions (HICO ... PACE), etc.

1.1.3 Approach based on uncertainty estimates

It is important to note that the current document does not try to identify a "best" protocol nor does it aim to prescribe mandatory requirements on specific aspects of a measurement protocol such as "acceptable tilt" or "minimum distance for ship shadow avoidance" or "correct azimuth and zenith angle for above water radiometry". While such prescriptions have great value in encouraging convergence of methods and in challenging scientists to make good measurements, the diversity of aquatic and atmospheric conditions where validation is required, the diversity of instruments and platforms and the corresponding diversity of measurement protocols suggests that some flexibility may be needed. This flexibility is acceptable **provided that each measurement is accompanied by a SI-traceable uncertainty budget that is a) based on a full analysis of the protocol and b) that is itself validated**, e.g. by measurement intercomparison exercises (S.B. Hooker, Zibordi, and Maritorena 2001; G. Zibordi, Ruddick, et al. 2012; Ondrusek et al. 2016).

The current document does aim to provide at least a minimal checklist of elements that should be considered in the complete uncertainty analysis of a measurement protocol and to identify key considerations and some useful references for each element.

1.2 Definition of Fiducial Reference Measurement (FRM)

Using the definition proposed by (Donlon et al. 2014) in the context of Sea Surface Temperature measurements, the defining mandatory characteristics of a "Fiducial Reference Measuement (FRM)" are:

- An uncertainty budget for all FRM instruments and derived measurements is available and maintained, traceable where appropriate to SI, ideally through a National Metrology Institute (NMI)
- FRM measurement protocols and community-wide management practices (measurement, processing, archive, documents, etc.) are defined and adhered to
- FRM measurements have documented evidence of SI traceability via intercomparison of instruments under operational-like conditions
- FRM measurements are independent from the satellite retrieval process

The FRM4SOC SOW adds the requirement that:

- FRM measurements are openly and freely available for independent scrutiny

and the proviso that FRM measurements may impact the satellite retrieval process in the specific case where they may be used for vicarious calibration of the satellite sensor.

1.3 Motivation – the needs for FRM for satellite validation

As clearly summarised in the ESA SOW, "**FRM are required to determine via independent validation activities the in-orbit uncertainty characteristics of satellite geophysical measurements**".

As stated in the ESA SOW "*The Copernicus program is a European system for monitoring the Earth. It includes earth observation satellites (notably the Sentinel series developed by ESA), ground-based measurements and services to processes data to provide users with reliable and up-to-date information through a set of Copernicus Services related to environmental and security issues. ... They will provide critical information in near-real time. Collectively they support a wide range of applications, including environment protection, management of urban areas, regional and local planning, agriculture, forestry, fisheries, health, transport, climate change, sustainable development, civil protection and tourism. Copernicus satellite missions are designed to serve all Copernicus Services by providing systematic measurements of Earth's oceans, land, ice and atmosphere to monitor and understand large-scale global dynamics.*"

The FRM4SOC project follows the terminology of the Committee for Earth Observation Satellites (CEOS 2016) which defines Calibration as “*the process of quantitatively defining a system's responses to known, controlled signal inputs*”. Validation, on the other hand, is “*the process of assessing, by independent means, the quality [uncertainty] of the data products derived from those system outputs*”.

Clearly, quoting the FRM4SOC SOW, “*Without adequate validation, the geophysical retrieval methods, algorithms, and geophysical parameters derived from satellite measurements cannot be used with confidence and the return on investment for the satellite mission is reduced. In addition, meaningful uncertainty estimates cannot be provided to users*.”

The task of providing such uncertainty estimates to end-users is both crucial – users repeatedly stress the need for “confidence” in satellite-derived products - and extremely challenging because of the long and complex chain of processes underlying a final information product. This can be illustrated by an example taken from the use of satellite-derived chlorophyll a information in the reporting of eutrophication (Kevin Ruddick et al. 2008; Gohin et al. 2008) required by the European Union Water Framework Directive (WFD) and Marine Strategy Framework Directives (MSFD). One requirement of these directives is that the EU Member States must report the chlorophyll *a* concentration for their marine, coastal and inland water bodies via the 90 percentile (P90) of measurements made during the algal growing season, e.g. March-October. This is obtained by combining “Level 2W” water constituent data, chlorophyll a concentration in this example, from the "Level 2R" radiometric data from all imagery over the growing season, March-October, for a number of years.

A sample product is illustrated in Figure 1-1 together with the processing steps required to achieve this and including: a) acquisition of calibrated “Level 1” top-of-atmosphere radiance data from a satelliteborne optical sensor; b) atmospheric correction to yield “Level 2R[1]” bottom of atmosphere radiometric data or water leaving radiance reflectance; c) bio-optical model inversion to estimate; d) multitemporal combination of the instantaneous “Level 2W” data to yield the “Level 3” multitemporal product, here chlorophyll 90 percentile (P90). Each of these processing steps contains uncertainties and must be quality controlled to ensure reliability of the final information product. In the case of water colour products the atmospheric correction step is particularly prone to large uncertainties and the validation of Level 2 Radiometric (L2R) products is both crucial and, at the time of writing, inadequate despite the best efforts of the Sentinel-3 Validation Team the NASA Ocean Color validation Team, the NOAA Ocean Color Validation Team and similar teams worldwide including the important contributions of the BOUSSOLE and MOBY teams and of the AERONET-OC network.

[1] The terminology L2R and L2W is adopted here to distinguish between Level 2 Radiometric data and Level 2 Water constituent data (K. Ruddick et al. 2010).

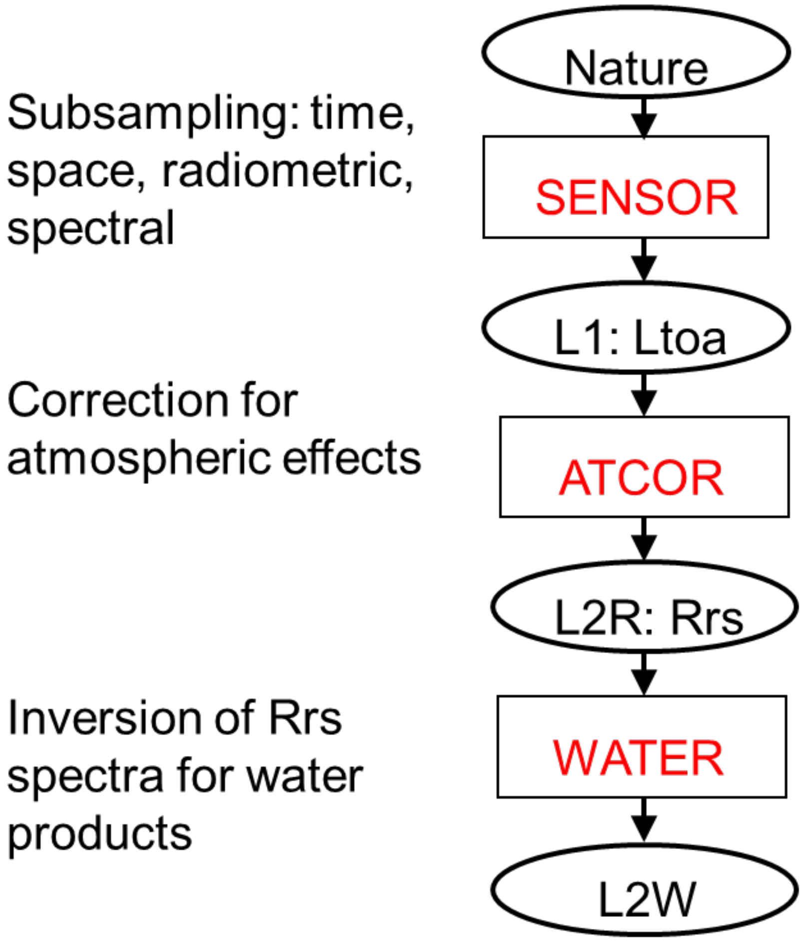

Figure 1-1 Processing steps from: a) calibrated TOA radiance ("Level 1"), which represents temporal (snapshot), spatial (image), spectral (bands) and radiometric (digitised) sampling of nature through b) Level 2 radiometric (L2R) data after atmospheric correction, to the c) Level 2 water (L2W) used as basis for applications. From (K. Ruddick et al. 2010).

It is noted that FRM4SOC deals only with radiometric validation and hence does not provide the complete validation of the final information products received by users, e.g. a multitemporal chlorophyll P90 map taking the above-mentioned example. Radiometric validation covers all upstream processes in Figure 1-1, including TOA calibration and atmospheric correction, but leaves downstream processes, such as chlorophyll a retrieval from L2R data and multitemporal compositing, unvalidated. Complete validation therefore requires further efforts, e.g. validation of chlorophyll retrieval algorithms, validation of Level 2 Water (L2W) chlorophyll products with in situ (FRM!) measurements, and consideration of temporal sampling in the derivation of L3 products (Van der Zande et al. 2011). The importance of these post-L2R validation needs is not ignored, however the L1 calibration and L2R validation steps are considered to be highest priority since if the L1 products or the L2R products cannot be trusted there is no possibility to trust the downstream L2W and L3 products.

1.4 Key protocol documents and prior references

1.4.1 NASA Ocean Optics Protocols for Satellite Ocean Color Sensor Validation

Historically, the key protocol document for aquatic radiometric measurements for satellite validation has been provided by the NASA Ocean Optics Protocols series, which grew from a 45 page document in its first appearance (James L. Mueller and Austin 1992) to a 308 page document at Revision 3 (J. Mueller et al. 2002) and a 6 Volume set at Revision 4 (J.L. Mueller, Fargion, and McClain 2003). Two of those Volumes were further revised at Revision 5, including a new Part 2 of Volume VI which includes some advances in radiometry. At the time of writing the Revision 5 made in 2004 is the latest available version of these protocols, although it is clearly recognized that there have been many improvements in methodology, instrumentation and understanding over the last 13 years.

Revision 5 of the NASA Ocean Optics Protocols is composed of the following Volumes:

- Volume I: Introduction, Background and Convetions (Rev. 4)
- Volume II: Instrument Specifications, Characterization and Calibration (Rev. 4)
- Volume III: Radiometric Measurements and Data Analysis Methods (Rev. 4)
- Volume IV: Inherent Optical Properties: Instruments, Characterization, Field Measurements and Data Analysis Protocols (Rev. 4 and Erratum 1 dated 28 Aug. 2003)
- Volume V: Biogeochemical and Bio-Optical Measurements and Data Analysis Methods (Rev. 5)
- Volume VI: Special Topics in Ocean Optics Protocols and Appendices (Rev. 4)
- Volume VI, Part 2: Special Topics in Ocean Optics Protocols, Part 2 (Rev. 5)

Since the FRM4SOC Projet is concerned only with radiometry, Volumes IV and V are not relevant here.

Volume I contains an introduction to validation measurements, a definition of terminology, and some basic optical theory. Volume I also proposes a list of minimal measurements required for satellite validation, which are further discussed here in section 2.1.3 and 2.1.4.

Volume II reviews instrumentation used for validation mesurements, focusing primarily on radiometry and is a key reference for the FRM4SOC Technical Report 2 on "A Review of Commonly used Fiducial Reference Measurement (FRM) Ocean Colour Radiometers (OCR) used for Satellite OCR Validation".

Volume III describes methods used in the field to make radiometric measurements and contains detailed chapters on in-water radiometric profile measurements and above water radiometric meaurements, which are key references for the present FRM4SOC Technical Report sections 3 and 4.

Volume VI Part 1 contains chapters on the MOBY buoy and data processing (Chapter 2) and on radiometric measurements from moored and drifting buoys (Chapter 3), which are important sources of information for sections 4.1 and 4.2 of the present FRM4SOC report.

Volume VI Part 2 contains a chapter (6) reviewing methods for correcting platform/superstructure and instrument shading, relevant for section 4.1.2.3 of the present FRM4SOC report and a chapter (7) on advances in radiometric calibration methods, which is relevant for the FRM4SOC project as a whole.

1.4.2 REVAMP/MERIS protocols

The EU/FP5-funded REVAMP Project ("Regional validation of MERIS chlorophyll products in North Sea coastal waters" (REVAMP; EVG1-CT-2001-00049) compiled a set of protocols (Tilstone et al. 2003) for measurement of apparent and inherent optical properties and optically-relevant biogeochemical parameters (chlorophyll a concentration, Total suspended matter).

The REVAMP protocols and the associated documentation of MERIS water products, validation strategies and sampling criteria (Doerffer 2002) themselves draw heavily on the NASA Ocean Optics Protocols described in section 1.4.1 and on protocols developed in the EU-funded Colors project (Coastal region long-term measurements for colour remote sensing development and validation MAS3 – CT97 – 0087; funded by the EU Marine Science and Technology Programme MAST III Startegic Marine Research).

Whereas the NASA Ocean Optics Protocols are written generically as far as possible with only few mentions on specific implementations, the REVAMP protocols are more focused on specific implementations with specific instruments, e.g. the so-called "TRIOS method" and "SIMBADA method" are described in the section on above water radiometry.

1.4.3 MERIS Optical Measurement Protocols and MERMAID database

The "MERIS MAtchup In-situ Database" (MERMAID) is supported by documentation describing the various datasets that have been archived (Barker et al. 2008). This documentation describes many radiometric measurements, broken down by Principal Investigator. The information contains a description of the dataset, e.g. details of measurement locations and deployment methods, and, to different degrees, details of or references to the measurement protocol. Contributors were encouraged to supply information and data values for measurement uncertainty, although in many cases the latter are incomplete or denoted as "not yet available".

MERMAID is specifically designed to facilitate matchup validation for MERIS data and the in situ database is integrated with a tool to allow users to automatically extract MERIS satellite data at the date/time of the in situ measurements and generate "on-the-fly" scatterplots and validation statistics.

The in situ data is supplemented by a standard set of Measurement Quality Control (MQC) flags, denoting quality control checks made by the data provider, and Processing Quality Control (PQC) flags, denoting quality control performed by the database manager as summarized in Table 1-1 and Table 1-2.

Flag ID	Flag position	String options	Conditions and criteria
MQC	1	0 1	Protocol provided by PI
	2	0 1 2	Correction of self-shading (2 = N/A as self-shading avoided).
	3	0 1 2	Correction for straylight (2 = N/A)
	4	0 1 2	Made dark measurements (and used in processing)
	5	0 1 2	Measured immersion coefficients (and used in processing)
	6	0 1	Instrument calibration history provided
	7	0 1	Data processed to MERIS band characterisation
	8	0 1	Hyperspectral integration done
	9	0 1	Error budget provision
	10	0 1 2 (L1.5)	In-situ data filtering (PI's QC checks)
	11	0 1	In-situ ρ_w already normalised or f/Q and $\Re$ corrected
	12	0 1 2	Tilt measurement made
	13	0 1 2	Calibration of tilt sensor
	14	0 1 2 3	Type of E_s: E_s or $E_d(0+)$ (0 = N/A, 1 = E_s measured in-situ, 2 = $E_d(0+)$ measured in-situ/derived in-situ, 3 = E_s computed)
	15	0 1	E_s tilt corrected
	16	0 1 2	Type of L_u: L_w or $L_u(0-)$ (and extrapolated to $L_w(0+)$). (0 = N/A, 1 = L_w, 2 = $L_u(0-)$ (and extrapolated to $L_w(0+)$.
	17	0 1	L_u tilt corrected
	18	0 1 2 (L1.5)	(AERONET-OC only) Data quality level: 0 = N/A, 1 = L1.5, 2 = 2.0 (see AERONET website http://aeronet.gsfc.nasa.gov, for more details)

Table 1-1 MERMAID database Measurement Quality Control (MQC) flag criteria definition. Flag position is counted from the first numeric character after the leading 'M'. Unless otherwise specified: 0 = No / Not done, 1 = Yes / done/ provided, 2 = Unknown / not available / not applicable (N/A). Reproduced from (Barker et al. 2008).

Flag ID	Flag position	String Options	Conditions and criteria
PQC	1	0 1	Passed in-situ ρ_w QC
	2	0 1 2	Hyperspectral integration
	3	0 1	Case 1 Normalisation by MERMAID *
	4	0 1	Case 2 Normalisation
	5	0 1	Band shifted correction [AERONET-OC data only; presently only AAOT]
	6	0 1	Nearest neighbour (refer to MERIS Optical Protocols): 0 = data at bands greater than ±5nm from MERIS 1 = data at bands less than ±5nm from MERIS **NOMAD only**: Flag is 0 when data is at 560 nm and 1 when at 555 nm
	7	0 1	AlphaNIR (1 & 2) derived from 870-675 nm
	8	0 1	AlphaNIR (1 & 2) derived from 870-665 nm

*See MQC flag #11 to check if normalisation has already been performed by PI.

Table 1-2. Processing Quality Ccontrol (PQC) flag criteria definition. Flag position is counted from the first numeric character after the leading 'P'. Unless otherwise specified: 0 = No / Not done, 1 = Yes / done/ provided, 2 = Unknown / not available. Reproduced from (Barker et al. 2008).

1.4.4 GLASS and MERIS Lake Water protocol documents

The sea-going oceanographic community has traditionally been at the forefront of radiometric protocol development and community-wide harmonization, in particular via the NASA Ocean

Optics Protocols (J.L. Mueller, Fargion, and McClain 2003), the inland water community also has significant expertise in aquatic radiometry. The advent of free and high quality data from the USGS/Landsat-8 sensor and the ESA/Sentinel-2 satellites has hugely enhanced the usage of satellite remote sensing for inland waters ... and generated a parallel need for high quality validation data and supporting protocols.

As an example, the GLASS project (Tartu Observatory et al. 2015) collected and tested protocols measurement of the Remote Sensing reflectance, including above water measurements with skyglint correction using a) a handheld 3-sensor system with integrated irradiance sensor (Hommersom et al. 2012), b) a single sensor system with reflectance panel measurement for estimation of $E_d^{0+}(\lambda)$, c) a TRiOS RAMSES 3-sensor system and also d) an underwater radiance measurement. The NASA Ocean Optics Protocols were generally used as guidelines, but the standard procedures were sometimes modified for practical reasons when using small boats. The protocols used in the GLASS project differed also on the calculation of the Rrs from above-water measurements: 1) whether Fresnel reflectance coefficient ρF was considered as a constant or dependent on the wind speed, 2) selection of the outliers, 3) whether the fingerprint method (Simis and Olsson 2013) and whether the "NIR similarity spectrum" was applied (KG Ruddick et al. 2006).

As another example, the "MERIS Lake Water algorithms" project summarises some protocols used to make validation measurements in inland waters (Kallio et al. 2007).

1.4.5 CEOS INSITU-OCR

The Committee on Earth Observation Satellites (CEOS) set up the "International Network for Sensor Inter-comparison and Uncertainty assessment for Ocean Color Radiometry (INSITU-OCR)" initiative to integrate and rationalize inter-agency efforts on satellite sensor inter-comparisons and uncertainty assessment for remote sensing products with particular emphasis on requirements addressing the generation of ocean colour Essential Climate Variables as proposed by the Global Climate Observing System (GCOS). This working group provides recommendations both on satellite measurements (calibration, development and assessment of satellite products) and on in situ measurements, with special consideration given to traceability, application and accessibility of the in situ measurements that are necessary for any ocean colour mission.

CEOS INSITU-OCR does not specify measurement protocols themselves but has provided in its White Paper (G. Zibordi, Bailey, et al. 2012) a set of recommendations that have driven to a large extent the design of the FRM4SOC Project SOW. These recommendations are reproduced verbatim in the following subsections in italic text, to denote that this text is not the original work of the FRM4SOC project and its collaborators. Specifically INSITU-OCR recommends:

- ***"R3.1 Improving traceability of in situ measurements***

Funding agencies should enforce common calibration schemes and measurement protocols, and unifying processing schemes and quality assurance criteria to ensure consistency and traceability of in situ measurements to SI standards. Inter-comparison exercises should be considered as the means to enforce traceability by promoting state-of-art on instrument calibration, measurement methods, data processing, and quality assurance. Practical implementation of inter-comparisons may entail a series of round-robins on specific topics together with training opportunities.

- **R3.2 Continuous consolidation and update of measurement protocols** *Measurement protocols should be consolidated as a result of a critical review and update of those currently documented in peer-review literature or already included in compilations produced by former programs. Consolidated protocols should then be published using modern communication methods. A possibility would be to create "living documents" (e.g. Wiki format, easily accessible and modifiable through continuous community contributions and discussions, but envisaging mechanisms for tracking successive versions). This objective could be initiated through independent and well focused workshops on protocols for the determination of in situ data from: i. water apparent optical properties; ii. water inherent optical properties; iii. water pigments; and iv. atmospheric optical properties. Expertise on standardization quality assurance should be represented in each leading activity.*

- **R3.3 Uncertainty budgets**

In situ data should be linked to uncertainty budgets determined in agreement with defined protocols and accounting for a comprehensive range of uncertainty sources. Ideally these uncertainty budgets should include contributions from calibration, processing, deployment restrictions, and environmental conditions.

- **R3.4 Quality Assurance of *in situ* data**

Define and implement quality assurance schemes for in situ data. These criteria should be specific for the different quantities and should take benefit of ancillary information provided with the data itself (e.g., cloud cover or sea state in the case of radiometric data), empirical thresholds, closure between inherent and apparent optical properties, models estimate.

- **R3.5 Archival of *in situ* data**

Centralized open access data repositories should be established, supported and maintained beyond any individual mission's life. Repositories should ideally have the capability of indexing data as a function of their fitness for specific applications (e.g., vicarious calibration, bio-optical modeling, and validation). Suitable mechanisms should be put in place to warrant data submission (e.g., requesting timely data delivery for field data produced within the framework of measurement programs funded by Space Agencies, or creating benefits like full processing and quality assurance of submitted data, or, where appropriate, convincingly recommending authors exploiting archived data to contact contributors and offer co-authorship).

- **R3.6 Community processor for *in situ* data**

Design, implement and apply community consensus processors for in situ data. This development should proceed through incremental steps, for instance by initially creating open access libraries and requesting manufacturers to adopt common (or user definable) data formats.

- **R3.7 Priority for variables to be collected**

A list of variables considered essential for satellite ocean color applications should be defined and considered with high priority by any field program.

- **R3.8 General coordination of field campaigns**

Establish a coordination mechanism to allow for a continuous exchange of information on forthcoming field activities to create opportunities for collaboration including instrument exchange, field training, inter-comparisons. The coordination should be instrumental in ensuring the collection of prioritized in situ variables for satellite ocean color applications. A web page service may efficiently support the activity."

2 Measurement Requirements

2.1 Required parameters

2.1.1 Essential geophysical radiance/reflectance product

The present chapter focuses on measurements of the standard level 2 radiometric (L2R) product from Sentinel-3, the "water-leaving radiance reflectance", ρ_w , or "directional reflectance", which is defined as:

$$\rho_w(\lambda,\theta,\varphi) = \pi \frac{L_w(\lambda,\theta,\varphi)}{E_d^{0+}(\lambda)} \tag{1}$$

where $E_d^{0+}(\lambda)$ is the above water downwelling irradiance, also called E_s or "surface/reference" irradiance in some studies, and $L_w(\lambda,\theta,\varphi)$ is the water-leaving radiance just above water in the upward direction measured by the satellite sensor and defined by zenith angle θ and azimuth angle φ. In this terminology, further detailed by (C.D. Mobley 1994), the water-leaving radiance is the component of above water directional upwelling radiance that has been transmitted across the air-water interface or, equivalently, is the above water directional upwelling radiance, L_u^{0+}, after removal of the downward sky/sun radiance reflected at the air-water interface, L_r :

$$L_w = L_u^{0+} - L_r \tag{2}$$

The latter term is called hereafter "skyglint", but may include also specularly reflected sunglint.

All radiometric quantities terms in this review are assumed to vary spectrally but for brevity the dependence on wavelength, λ, is generally not represented in the terminology unless cross-wavelength inelastic processes are important.

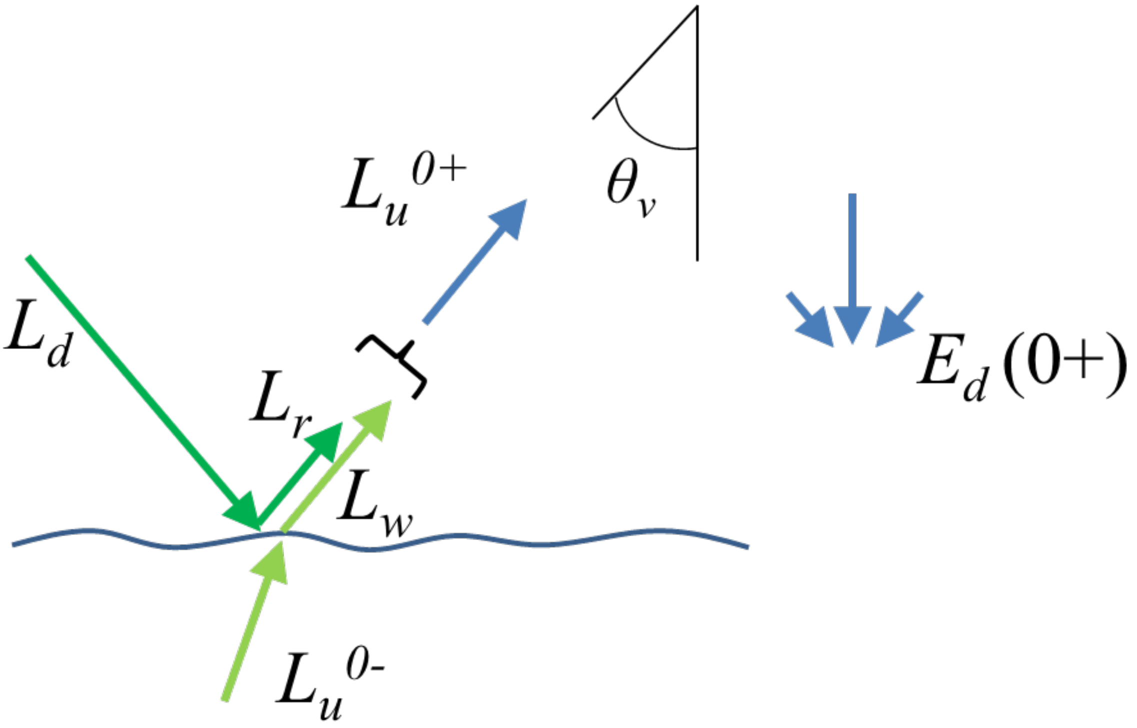

Figure 2-1 Illustration of definitions of water-leaving radiance, L_w, above water upwelling radiance, L_u^{0+} , and downwelling irradiance. See also [http://www.oceanopticsbook.info/view/overview_of_optical_oceanography/reflectances]

Other missions or processing software may generate alternative L2R products such as normalised water-leaving radiance[2] (nLw or L_{wN}) (H.R. Gordon and Clark 1981; J. L. Mueller 2004) or Remote sensing reflectance (Rrs) which can easily be related to ρ_w and/or L_w by simple relationships:

$$R_{rs}(\lambda,\theta,\phi) = \frac{L_w(\lambda,\theta,\phi)}{E_d^{0+}(\lambda)} = \frac{\rho_w(\lambda,\theta,\phi)}{\pi} \quad (3)$$

$$L_{wN}(\lambda,\theta,\phi) = \frac{L_w(\lambda,\theta,\phi)}{E_d^{0+}(\lambda)}\overline{F_0}(\lambda) = \frac{\rho_w(\lambda,\theta,\phi)}{\pi}\overline{F_0}(\lambda) \quad (4)$$

where $\overline{F_0}$ is the extraterrestrial solar irradiance (spectrum), which is assumed known to a specified uncertainty, from other studies, , e.g. (Thuillier et al. 2003), and is possibly used in the generation of the satellite products. In equation (4), following the terminology and reasoning of (Morel and Mueller 2003) the viewing zenith angle, θ, and azimuth angle ϕ dependencies are retained. Corrections can then be made to estimate from L_{wN}

[2] Notation for and definition of „normalised" water-leaving radiance may differ between references. In the current review, L_{wN}, is the (directional) normalised water-leaving radiance, as defined in equation (4), whereas the notation, L_{wn}, represents the nadir-viewing water-leaving radiance.

the water-leaving radiance that would be measured for nadir-viewing and in the case of a zenith sun. If such "bidirectional corrections" are made, the resulting parameter will be called "exact" normalised water-leaving radiance, L_{wN}^{ex} , as described in (Morel and Mueller 2003), and can be used for consistent time series.

All of these parameters require the measurement of upwelling radiance and downwelling irradiance. While there may be applications where measurement of upwelling radiance alone may be sufficient, or may be combined with satellite-derived downwelling irradiance to yield a reflectance product, an FRM L2R product clearly requires both upwelling radiance and downwelling irradiance to be based on in situ measurements.

The MERMAID database (Barker et al. 2008) does offer the possibility to calculate an alternative ρ_w product based on the in situ L_w measurement and an E_d^{0+} based on the satellite data that is being validated instead of an in situ measurement of E_d^{0+}. This alternative product avoids certain measurement uncertainties, for example relating to imperfect cosine response of E_d^{0+} sensors and fore-optics contamination of unsupervised E_d^{0+} deployments. Use of satellite E_d^{0+} also changes other measurement uncertainties, e.g. the absolute calibration of L_w sensors becomes more important because uncertainties relating to the calibration lamp output which reduce in the ratio L_w/E_d^{0+} if sensors are calibrated at the same time with the same lamp (G. Zibordi and Voss 2014) p59, no longer cancel if E_d^{0+} is derived from a satellite measurement. While this approach is interesting and does provide extra information, it clearly does not correspond to the FRM requirement that "measurements are independent from the satellite retrieval process".

2.1.2 Directionality of radiometric products

The viewing direction of the satellite-borne optical sensor will in general differ from the viewing direction of the in situ measurement instrument, typically nadir for underwater measurements, and often at a zenith angle of 40° and a azimuth angle of 90-135° relative to sun for above water measurements.

For some applications the satellite measurement may be „normalised" to yield a radiometric product corresponding to a nadir-viewing direction by use of a suitable Bidirectional Reflectance Distribution Function (BRDF) model, e.g. (Morel and Gentili 1996). BRDF models can also be used to remove the impact of sun zenith angle and give a product that depends more strongly on the Inherent Optical Properties of the water body. For some applications, e.g. climate-relevant multi-mission time series of open ocean chlorophyll *a* concentration, these normalisations may be essential. However, for some applications it is preferable to retain the radiometric product in the viewing direction of the satellite sensor as input to downstream processing, e.g. because the downstream processing will independently take into account the directional effects.

Since a BRDF model can always be applied *a posteriori* to a directional product, but a directional product cannot always be derived from a „normalised" nadir-viewing product, maximum flexibility is achieved by retaining the directional product as „standard" L2R product and providing optional extra products or tools for the BRDF normalisation.

In the present document the in situ measurement product will be considered as sufficient if it is provided in the direction of the in situ instrument (provided that this direction is clearly defined). Consideration/modelling of the different in situ and satellite viewing directions is then left as a post-FRM step in the validation process. However, provision of a nadir-viewing radiometric product is clearly encouraged as an additional product for in situ measurement systems, e.g. most above water systems, that do not measure at nadir.

Bidirectional corrections are further discussed in Chapter 5

2.1.3 Auxiliary optical parameters

2.1.3.1 Auxiliary optical and biogeochemical parameters – NASA Ocean Optics protocols

The NASA Ocean Optics Protocols Volume I (J. L. Mueller 2004) specified a minimum set of optical and geophysical parameters required for validation purposes – see Table 2-1 - with the following considered as mandatory:

- Downwelling irradiance in water, $E_d\ (\lambda, z)$
- Upwelling radiance in water at nadir, $L_{un}(\lambda, z)$
- Downwelling irradiance in air, $E_d^{0+}(\lambda)$
- Normal solar irradiance in air[3], $E_N(\lambda, \vartheta_0, \phi_0)$
- Aerosol optical depth, τ_a
- Phytoplankton pigment composition (HPLC Method)
- Chlorophyll a and Phaeopigments concentration (Fluorimetric Method)

While this "minimal" list seems appropriate for ship-based campaigns using underwater radiometry and water sampling, it clearly needs to be revisited. For example:

- Reflectance mesurements that are relevant for validation can be made by unsupervised above water radiometry, e.g. from AERONET-OC (G. Zibordi et al. 2009), where no in-water measurements are available.
- Phytoplankton pigment composition measurements can only practically be made by (supervised) shipborne campaigns. Considering this to be a mandatory parameter would exclude all autonomous measurements, yet these are the primary source of validation matchups.
- Normal solar irradiance and aerosol optical depth measurements can be made by handheld or automated sunphotometers, but are typically not made from moored buoys because accurate sun-pointing is generally not possible from a tilting buoy. In general, such information is available only from „nearby" land-based sunphotometers. In practice these parameters have not be found to be very useful in validation analyses because the most relevant aerosol parameter used in atmospheric correction, the aerosol reflectance in the sun-satellite (backscattering) geometry, is not dependent only on aerosol optical depth.

2.1.3.2 Auxiliary optical and biogeochemical parameters – MERMAID database

The MERMAID database (Barker et al. 2008) lists the following as minimum data requirements, including ancillary data and documentation:

- "Water reflectances, ρw (visible and NIR, at MERIS bands if possible); either multi or hyperspectral. Or, hyperspectral convolved to the last definition of the 15 MERIS spectral filters;

[3] This is the direct solar irradiance on a plane normal to the solar beam, transmitted downward through the atmosphere, as typically measured by a sunphotometer – see *ref* equation (2.59).

- The associated water-leaving radiances, Lw (λ) and downwelling surface irradiance, Es (λ), or Ed (λ ,0+), from which ρw were computed (or relevant CIMEL or TriOS parameters);
- Associated Chl-a measurements (if available), with a description of the method to derive it;

In the FRM4SOC context, elements of this can be revisited as follows:

- In situ measurements should not be provided only for the spectral bands of an individual satellite sensor since there is great value in multi-mission re-use of measurements. While data providers could provide radiometric parameters band-shifted/interpolated to specific satellite spectral bands, the radiometric parameters should always be provided at least for the spectral bands of the in situ instruments (with the understanding that very minor band shifts may be needed to account for small variations in spectral reponse function over the in situ instrument set).
- Chl-a measurements are generally not available from autonomous above water systems

2.1.3.3 Auxiliary optical parameters – FRM4SOC suggestion

While, data providers are obviously encouraged to measure many more apparent and inherent optical properties and optically-relevant biogeochemical parameters, it is suggested that the absolute minimum requirements would be measurements of:

- Downwelling irradiance in air, $E_d^{0+}(\lambda)$
- Water-leaving radiance (in air) at nadir, $L_w(\lambda)$ or in the in situ measurement direction for above water systems, $L_w(\lambda, \vartheta_v, \phi_v)$

together with ancillary metadata as defined in section 2.1.4.

For above water systems the following parameters should also be supplied:

- Upwelling radiance in air, $L_u^{0+}(\lambda, \vartheta_v, \phi_v)$
- Sky downwelling radiance in air, $L_d^{0+}(\lambda, -\vartheta_v, -\phi_v)$
- Fresnel reflectance coefficient used for skyglint removal, ρ_F (possibly wavelength-dependent)

For underwater systems the following parameters should also be supplied:

- Upwelling radiance in water at surface, $L_{un}(\lambda, 0-)$
- Diffuse attenuation coefficient for upwelling nadir radiance, $K_{Lu}(\lambda)$, if constant, or information on the effective $K_{Lu}(\lambda)$ or the extrapolation method, if $K_{Lu}(\lambda)$ is not assumed constant (see section 4.1.2.1).

According to the FRM principle of traceability, it is necessary to archive and be prepared to produce and/or reprocess all data and software that has been used to generate the abovementioned key radiometric parameters. This includes potentially: raw binary data as originally stored during data acquisition, a time history of calibration coefficients for all instruments, ancillary measurements needed in processing and/or quality control (tilt, , ϑ_v, ϕ_v, etc.), processing algorithm coefficients or models (Fresnel reflectance, etc.), intermediate radiometric parameters (e.g. time-averaged means and standard deviations), etc.

In practice, it is probably most appropriate that most of this supporting data and software be retained by the data provider rather than being submitted to a public database, although there is a clear advantage in pushing transparency further upstream of the abovementioned minimal parameters, eg. to better harmonise measurements by the use of open source community-approved software for elements of in situ data processing, and faciltate reprocessing with improved or alternative algorithms.

According to the FRM principle (section 1.2), all data values should be accompanied by a (spectrally-varying) uncertainty estimate. In practice, at the time of writing, these uncertainty estimates are usually provided as %uncertainty for each wavelength, but for an entire dataset, although it is clear that the uncertainty of each individual reflectance measurement will usually be different because of variation in illumination and/or deployment conditions.

	Required	Highly Desired	Specialized Measurement	Derived
Radiometric Quantities				
Downwelled Irradiance $E_d(z,\lambda)$	✓			
Upwelled Radiance $L_u(z,\lambda) = L(z, \lambda,0,0)$	✓			
Upwelled Irradiance $E_u(z,\lambda)$			✓	
Radiance Distribution in water $L(z, \lambda,\theta',\phi')$			✓	
Water Surface Radiance in air $L_{sfc}(\lambda,\theta,\phi)$		✓		
Incident Irradiance in air $E_s(\lambda) = E_d(0^+,\lambda)$	✓			
Normal Solar Irradiance $E_N(\lambda, \theta_o,\phi_o)$	✓			
Sky Radiance $L_{sky}(\lambda,\theta,\phi)$		✓		
Diffuse Sky Irradiance $E_{sky}(\lambda)$		✓		
Direct Sun Irradiance $E_{sun}(\lambda) = E_s(\lambda) - E_{sky}(\lambda)$				✓
Water-Leaving Radiance $L_w(\lambda,\theta,\phi,\theta_o,\phi_o)$				✓
Remote Sensing Reflectance $R_{RS}(\lambda,\theta,\phi,\theta_o,\phi_o)$				✓
Attenuation Coefficient $K(z,\lambda)$ for $E_d(z,\lambda)$ and $L_u(z,\lambda)$				✓
Ocean Bidirectional Reflectance Distribution Function BRDF				✓
Aerosol Optical Depth $\tau_a(\lambda)$	✓			
Aerosol Phase Function $P_a(\lambda,\Psi)$				✓
Absorbing Aerosol Height Profiles (LIDAR Profilometer)			✓	
Inherent Optical Properties				
Beam Attenuation Coefficient $c(z,\lambda)$		✓		
Absorption Coefficient $a(z,\lambda)$		✓		
Backscattering Coefficient $b_b(z,\lambda)$		✓		
Scattering Coefficient $b(z,\lambda) = c(z,\lambda) - a(z,\lambda)$				✓
Volume Scattering Function $\beta(z, \lambda,\Psi)$			✓	
Particle Absorption Coefficient $a_p(z,\lambda)$		✓		✓
Dissolved Material (CDOM) Absorption Coefficient $a_g(z,\lambda)$		✓		
Non-Pigmented Particle Absorption Coefficient $a_d(z,\lambda)$		✓		
Phytoplankton Absorption Coefficient $a_\phi(z,\lambda)$		✓		
Biogeochemical and Bio-Optical Quantities				
Phytoplankton Pigment Composition (HPLC method)	✓			
Chlorophyll *a* and Phaeopigments Conc. (Fluorometric method)	✓			
Phycobiliprotein Concentrations			✓	
Coccolith Concentrations			✓	
Total Suspended Particulate Material (SPM)			✓	
Particle Size Distribution			✓	
Particulate Organic Carbon (POC)			✓	
Particulate Organic Nitrogen			✓	
Fluorescence Intensity, *in situ* profile $F(z)$		✓		

Table 2-1 Principal optical and biogeochemical *in situ* observations suggested by the NASA Ocean Optics Protocols (J. L. Mueller 2004) for satellite ocean color system validation, and algorithm development and validation. The right-hand column identifies and classifies measurements as: (a) required for minimal validation match-ups; (b) highly desired and important for general algorithm development and validation; (c) specialized measurements of important, but restricted, applicability to algorithm development and validation (for the present); and (d) calculated or derived quantities. Notation used in this Table is defined is detail in (Morel and Mueller 2003) but does not include all notation used in the present FRM4SOC report.

2.1.4 Other auxiliary parameters and information

The in situ radiometric measurement must clearly be accompanied by sufficient ancillary data and information for it to be usable.

2.1.4.1 Ancillary data – NASA Ocean Optics protocols and MERMAID database

An example of such ancillary data considered to be essential for supervised underwater radiometry in the NASA Ocean Optics Protocols is given in Table 2-2. However, it is clear that this list needs to be revisited, e.g. for unsupervised radiometry (where no Secchi depth information will be available)

	Required	Highly Desired	Specialized Measurement	Derived
Ancillary Data and Metadata				
Latitude and Longitude	✓			
Date and Time (UTC)	✓			
Wave Height	✓			
Whitecap Conditions (fractional amount of surface)		✓		
Wind Speed, W, and Direction	✓			
Surface Barometric Pressure	✓			
Cloud Cover (amount, and sun obscuration information)	✓			
Cloud Type		✓		
Secchi Depth	✓			
Water Depth	✓			
Conductivity and Temperature over Depth (CTD) $T(z)$, $S(z)$		✓		

Table 2-2 Principal ancillary data required to accompany *in situ* observations suggested by the NASA Ocean Optics Protocols (J. L. Mueller 2004) for satellite ocean color system validation, and algorithm development and validation. The right-hand column identifies and classifies measurements as: (a) required for minimal validation match-ups; (b) highly desired and important for general algorithm development and validation; (c) specialized measurements of important, but restricted, applicability to algorithm development and validation (for the present); and (d) calculated or derived quantities.

The MERMAID database (Barker et al. 2008) requires the following metadata and documentation

- Sun zenith angles if available;
- Associated meta data (latitude, long, date, time in UTC);
- A written protocol to be included in the MERIS Optical Measurement Protocols document; it is a requirement of potential usage in matchups that adherence to an accepted protocol is confirmed."

In the FRM context, metadata and a written protocol are clearly required. However, sun zenith angle seems superfluous if position and date/time information are accurately supplied

2.1.4.2 Ancillary data – FRM4SOC suggestion

For the purposes of L2R FRM it is suggested to consider the following ancillary parameters as essential:

- Geographical position, preferably defined as latitude and longitude according to the WGS84 horizontal datum used by the Global Positioning System (GPS), and associated uncertainty (including variation during the measurement)
- Altitude of the air-water interface and hence the water-leaving radiance (and vertical datum, e.g. WGS84 used by GPS),. This will often be 0m for ocean measurements, but may be at very different altitude for inland waters.
- UTC date and time, expressed as center time for the measurement, as well as start and finish times when appropriate

The following ancillary parameters are also highly desirable:

- Total water depth

- Significant wave height
- Wind speed
- Wind direction
- Surface atmospheric pressure
- Water salinity
- Water temperature (especially if measurements are being made in-water using a radiometer which does not measure internal or ambient temperature for the purposes of correcting/quantifying any thermal sensitivities)
- Air temperature (especially if measurements are being made in-air using a radiometer which does not measure internal or ambient temperature for the purposes of correcting/quantifying any thermal sensitivities)
- Cloud cover, e.g. in oktas following the World Meteorological code 2700
- Cloud type ("genus"), e.g. following the World Meteorological code 0508

In some cases it may be preferable or more practical to obtain information from extraneous sources (e.g. meteorological models, other satellite data, bathymetric maps accompanied by tidal models, etc.), particularly for unsupervised measurements.

It is also highly recommended that each measurement be associated with a photograph of:

- Water state showing qualitatively the water colour as well as waves and any floating material
- Sky conditions preferably full sky, e.g. fisheye lens
- Instruments showing any fouling or unusual obstructions

These can be made with simple uncalibrated RGB cameras, e.g. (Garaba et al. 2015), and are intended mainly to identify any unusual conditions that will contaminate but cannot be identified by the radiometric point measurements.

2.2 Uncertainty estimation

Clearly FRM data should be associated with uncertainty estimates based on documented methodology and taking account of all possible sources of uncertainty (as far as they are imaginable).

A generic framework for uncertainty estimation, for all fields of metrology, has been established by the "Guide to the Expression of Uncertainty in Measurement (GUM) (GUM 2008). A discussion of uncertainty estimation for ocean colour radiometery is provided by (Johnson et al. 2014) and an example of application of the GUM to a specific ocean colour protocol is provided by (Gergely and Zibordi 2014). General methodology for uncertainty estimation is dealt with in other FRM4SOC Technical Reports, especially TR-7 on "Uncertainty Budgets of FRM4SOC Fiducial Reference Measurement (FRM) Ocean Colour Radiometer (OCR) systems used to Validate Satellite OCR products".

Uncertainty estimation is discussed in detail for each class of measurement protocol in Chapter 4.

2.3 Traceability

FRM data should be traceable to SI standards (See R3.1 of INSITU-OCR in section 1.4.4) , meaning that the essential parameters, ρ_w , L_w , and E_d^{0+} have been derived from raw measurements according to a documented process including instrument calibration to an SI reference, instrument deployment, reproducible data processing and quality control. As regards traceability of the radiometers, the principal instruments should be calibrated against SI-traceable standards just before and after the end of a field campaign. In addition, during the field campaign portable calibration devices can be used.

2.4 Protocol and Measurement Documentation

One element of traceability is the use of published protocols for instrument calibration, instrument deployment and data acquisition, and data processing and quality control. Each FRM measurement should be linked to such protocol documentation, including versioning control where protocols evolve in time.

One element of measurement documentation is the calibration history of each instrument that is used. Further calibration/characterisation documentation including reports of special test for nonlinearity, thermal effects, stray light effects as described in more detail in the companion FRM4SOC Technical Report 2 on "Radiometers".

2.5 Quality Control and associated measurement and processing flags

Quality control checks that have been applied to the data should be documented, either in the measure protocol, or as flags in the dataset itself – see for example the example flags suggested by MERMAID (Table 1-1 and Table 1-2).

2.6 Data Processing software

It is assumed in this document, and particularly in the detailed Chapters 3 and 4 describing measurement uncertainties for the various protocols, that the software used to process the measurements is a correct implementation of the mathematical equations and that no rounding error is introduced by the use of finite precision calculations. Uncertainties relating to, for example, time-averaging of measurements, vertical extrapolation of underwater data, skyglint correction of above water data, etc. are considered to be dealt with under the corresponding elements of the protocol/instrument uncertainty budget and not "software-related".

Open publication of data processing software allows full traceability of this component of the measurement process.

2.7 Data archiving and distribution

See INSITU-OCR recommendation R3.5 in section 1.4.4.

2.8 Data exploitation

The exploitation of in situ measurements for optical satellite validation is largely out of the scope of this document and may include use of different statistical metrics. An example of validation analysis is provided by (Bailey and Werdell 2006).

However, match-up considerations relating to space/time differences are discussed in section 5.

2.9 Document structuration with separate chapters for Lw and Ed

In the NASA Ocean Optics Protocols (J. L. Mueller 2004) methods were structured according to whether measurements were made underwater or above water. Above water radiometric methods were further grouped into 3 broad classes:

- Method 1 "Calibrated radiance and irradiance measurements" – one calibrated irradiance radiometer (with a cosine collector head) measures directly E_d^{0+}, and one or two calibrated radiometers measure directly upwelling radiance, L_u^{0+}, and downwelling sky radiance,L_d^{+} (see Figure 2-1 for definitions). This straightforward method has been implemented by many scientists, e.g. (Morel 1980; Joseph Rhea and Davis 1997) etc.
- Method 2 "Uncalibrated radiance and reflectance plaque measurements" – in this variant on Method 1, the direct measurement of E_d^{0+} by an irradiance radiometer is replaced by a measurement of the radiance diffused from a calibrated reflectance plaque deployed horizontally. This method is typical of the earliest water reflectance measurements, e.g. (Carder and Steward 1985), because of the obvious economy of using the same instrument for all 3 measurements, and is still typical of land surface reflectance measurements, e.g. (Milton et al. 2009), which are generally supervised.
- Method 3 "Calibrated surface polarized radiance measurements with modelled irradiance and sky radiance" – in this method the upwelling radiance measurement, $L_{up}(0^+, \theta_v, \Delta\varphi)$, is made by a radiometer equipped with a polarizing filter set to pass only the vertically polarized component of viewed radiance. By viewing at a zenith angle close to the Brewster angle the skylight reflected at the air-water interface is significantly reduced. The measurement of E_d^{0+} is achieved by a direct sun measurement from a sunphotometer and use of a radiative transfer model to estimate E_d^{0+} from the aerosol optical thickness and potentially other auxiliary parameters (atmospheric pressure, cloud cover, etc.). This method was the basis of the specially-designed SIMBAD radiometer (Fougnie et al. 1999; Deschamps et al. 2004), and was subsequently upgraded to the SIMBADA radiometer.

A number of developments since the writing of this Chapter of the NASA Ocean Optics Protocols (J.L. Mueller et al. 2003), suggests that these classes of above water radiometric methods need to be revised, particularly in the Fiducial Reference Measurement context:

- In the FRM context there is really no justification for using uncalibrated instruments and the inclusion of this method with uncalibrated instruments in the NASA Protocols contradicts the requirements of the same Protocols series that E_d^{0+}, i.e. not just reflectance, is a required radiometric quantity (cf NASA Protocols 2003 Volume I, Table 3-1, reproduced here as Table 2-1) and that instruments should be adequately calibrated and characterised (NASA Protocols 2003Vulume II). Method 2 should therefore be at least renamed to reflect that instruments should be radiometrically calibrated, even if the use of a reflectance plaque does effectively reduce uncertainties associated with potential inter-instrument calibration and/or sensitivity differences in Method 1.
- The original Method 3 introduces new ways of measuring both L_w and E_d^{0+} specifically tailored to the hand-held SIMBAD instrument. However, it is quite resonable to adopt variant or hybrid methodologies with different instrumentation. e.g. direct measurements of E_d^{0+} could be made with an irradiance radiometer, alongside measurements of polarized upwelling radiance, $L_{up}(0^+, \theta_v, \Delta\varphi)$. Measurements could be made of both unpolarized, $L_u(0^+, \theta_v, \Delta\varphi)$, and polarized upwelling radiance, $L_{up}(0^+, \theta_v, \Delta\varphi)$ to better characterise the reflectance of skyglint at the air-water interface. Sunphotometrically derived E_d^{0+} could be combined with unpolarized measurements of $L_u(0^+, \theta_v, \Delta\varphi)$ and $L_d(0^+, -\theta_v, \Delta\varphi)$ as in the AERONET-OC methodology (G. Zibordi et al. 2009).

- To overcome the uncertainties associated with estimation of the skylight reflected at the air-water interface, (Z. Lee et al. 2010, 2013), proposed a "Skylight Blocked Approach (SBA)" whereby the water-viewing radiometer is deployed in air, very close to the air-water interface, viewing at nadir, and is supplemented with a "skylight-blocking cone" – see later Figure 4-8 and section 4.4.
- Further variants on approaches for above water radiometry render the former Method 1/2/3 structure inappropriate. e.g. the AERONET-OC protocol (G. Zibordi et al. 2009) combines the sunphotometric estimation of E_d^{0+} suggested in the NASA2003 Method 3, but with an unpolarised measurement of L_u .

Moreover for underwater radiometry it is now generally accepted (G. Zibordi and Voss 2014) that E_d^{0+} as used in the computation of R_{rs} should always be measured above water[4].

Because of this standardisation of using above water measurements of E_d^{0+} in all cases, it is suggested here to structure the current document with one chapter for measurement of L_w, with sections for underwater and above water methods, and one chapter for measurement of E_d^{0+}, relevant for all L_w methods. This restructuring of the NASA Ocean Optics Protocols is illustrated in Figure 2-2

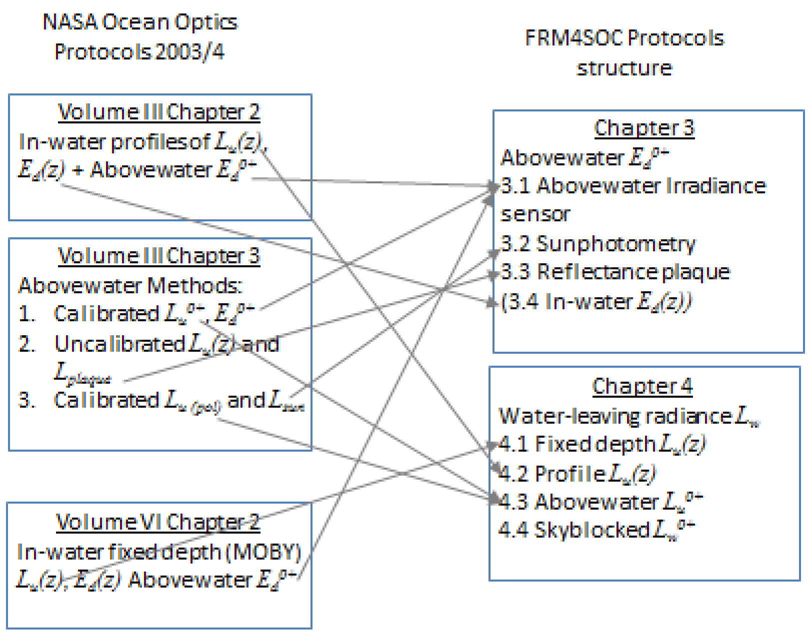

Figure 2-2 Illustration of restructuring of NASA Ocean Optics Protocols into these FRM4SOC Protocols with separate Chapters for E_d^{0+} and L_w.

---

[4] There are still good reasons to perform underwater measurements of $E_d(z)$, e.g. for determination of parameters such as the biologically important diffuse attenuation coefficient of downwelling irradiance, K_d . However, the above water measurement of E_d^{0+} is now always considered the reference for use in computation of R_{rs}.

3 Measurement Protocols for above water downwelling irradiance

In the current section the fundamental Measurement Equation and approach is summarised for measurement protocols that are currently used to measure above water downwelling irradiance, E_d^{0+}, for satellite radiometric validation. This parameter may also, in some references, be called "surface irradiance" typically with notation E_s , or more ambiguously "reference irradiance". The parameter is most completely described as "above water spectral downward planar[5] irradiance" and is defined[6] e.g. (C.D. Mobley 1994)'s equation (1.23), as the integral of radiance weighted by cosine of the incident angle for all downward directions.

Protocols for measurement of E_d^{0+} are grouped into three broad families of method:

- Direct above water measurement of E_d^{0+} with an upward pointing irradiance sensor
- Estimation of E_d^{0+} from direct sunphotometry and a clear sky atmospheric model
- Estimation of E_d^{0+} using a downward pointing radiance sensor and a reflective plaque

For each family of method, the Measurement Equation is defined and the measurement parameters are briefly described. The elements that should be included for estimation of total protocol-related measurement uncertainty are discussed with some considerations and references for further reading. Owing to the diversity of approaches and instrumentation and water types possible within each family and taking account of the FRM concept (section 1.2), no attempt is made to prescribe specific thresholds (e.g. for “acceptable” tilt, sea state, cloud conditions, etc.) that should be observed when making measurements. Such decisions are left as the responsibility of the measurement scientists. The approach here is rather to provide a list of elements that need to be considered in the measurement uncertainty analysis, as well as associated deployment recomendations.

3.1 Direct above water measurement of E_d^{0+} with an upward pointing irradiance sensor

3.1.1 Measurement equation

Except for the Measurement Equation relating electrical output of an instrument to calibrated irradiance (which is within the scope of the FRM4SOC Technical Report 2 on instuments), no additional "Measurement Equation" is required here for the deployment technique since E_d^{0+} can be measured directly using instruments that are designed to measure planar irradiance. Imperfections in such instruments contribute, of course, to the uncertainty budget of the measurement and imperfect cosine response is one of the specific aspects that must be considered. Since this is essentially related to instrument design and performance rather than the deployment protocol it is treated in the FRM4SOC Technical Report TR-2 on Ocean Colour Radiometers.

Direct measurement of E_d^{0+}, sketched in Figure 3-1, can be made from various platforms including ships, buoys, fixed offshore structures and underwater profiling platforms that contain a floating element or the ability to surface. These measurements can be either supervised or unsupervised. Some examples are shown in Figure 3-2. In all cases it is

[5] Also sometimes called "plane irradiance"

[6] The term "plane irradiance" distinguishes this parameter from the "scalar irradiance", which is also an angular integral of radiance but without the cosine weighting. Scalar irradiance is typically measured using a spherical collector whereas plane irradiance is measured with a flat collector, also called "cosine collector" – see (C.D. Mobley 1994) section 1.5 for full definitions and discussions.

recommended to mount the E_d^{0+} radiometer as high as possible, above any superstructure elements, to avoid optical contamination of the measurement e.g. by use of a fixed or telescopic mast, e.g. (Hlaing et al. 2010).

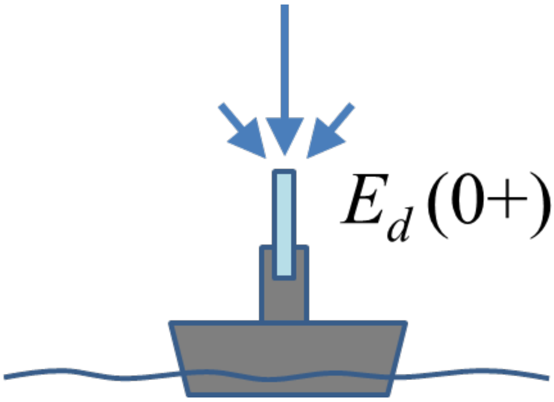

Figure 3-1 Schematic of direct above water measurement of E_d^{0+} with an irradiance sensor (not drawn to scale).

Figure 3-2 Typical deployment of above water irradiance sensors (top) Combined with a sunphotometer system on a mast, taken from (Hlaing et al. 2010) (bottom) combined with sea- and sky-viewing radiance sensors at the prow of a ship, as in (KG Ruddick et al. 2006)

3.1.2 Protocol-dependent sources of uncertainty

In addition to the instrument-related sources of uncertainty which arise from imperfections in the radiometers themselves, as dealt with in FRM4SOC Technical Report TR-2, the measurement of above water downwelling irradiance has a number of sources of uncertainty relating to the deployment conditions. These protocol-related sources of uncertainty are described here.

3.1.2.1 Tilt effects

Non-verticality of the E_d^{0+} instrument, e.g. caused by imprecise installation, wave-tilting of floating structures (buoys, ships), wind-tilting of offshore structures, including masts, and even ballast changes for ships (fuel, water, large equipment), will give uncertainty in the measurement of E_d^{0+}. It is, therefore, necessary to measure the tilt of radiometers at sufficiently high frequency and perform appropriate filtering of non-vertical data and/or averaging of data to reduce tilt effects.

For E_d^{0+} the effect of tilt may be particularly strong in sunny (satellite validation) conditions because of the highly anistropic light field and the effect of tilt is similar to a change in solar zenith angle[7]. Passive gimballing of an E_d^{0+} sensor, if sufficiently well-designed, may help to reduce tilt, as implemented in the DALEC system (Brando et al. 2016; Slivkoff 2014). Active gimballing of an E_d^{0+} sensor, using electric motors to correct for tilt, may now be feasible, although at the time of writing no information is available on use of such hardware for E_d^{0+} measurement.

The impact of tilt on measurement uncertainty can be estimated if the two angles of tilt with respect to sun are measured and approximate angular variation of sky radiance, e.g. from imaging cameras, or estimated from atmospheric properties, is known.

Obviously, minimisation of tilt can be a consideration in the design (D. Antoine et al. 2008) or in the location (e.g. low waves) of validation measurement structures. Floating buoys and small ships may be particularly subject to high tilt.

3.1.2.2 Shading from superstructure

The light field that is being measured may itself be perturbed by the presence of solid objects such as the superstructure of the platform used to mount them. This may be especially problematic on ships where practical considerations may prevent mounting of the E_d^{0+} sensor above all other structures, particularly if regular inspection by humans of the fore-optics is required.

The process of sky shading can be easily understood from fish-eye photographs taken vertically upwards at the location of an E_d^{0+} sensor as illustrated in Figure 3-3 and Figure 3-4. Any part of the upward hemisphere that is not sky represents optical contamination of the measurement and this contamination will be related to the solid angle of sky that is replaced by the object with near-zenith objects contributing more than near-horizontal objects to the cosine integral of radiances. Of course, it is best to make such photos with a calibrated fully hemispherical sky radiance camera (Kenneth J. Voss and Chapin 2005). However, even photos from simple cameras with less than a full hemispherical field of view and without any calibration can

[7] At high tilt a E_d^{0+} sensor may also measure some light from water instead of the sky, although grazing angle incident light has a low contribution to the cosine-weighted intergral for E_d^{0+}.

rapidly identify major contamination of measurements from superstructure and/or other objects.

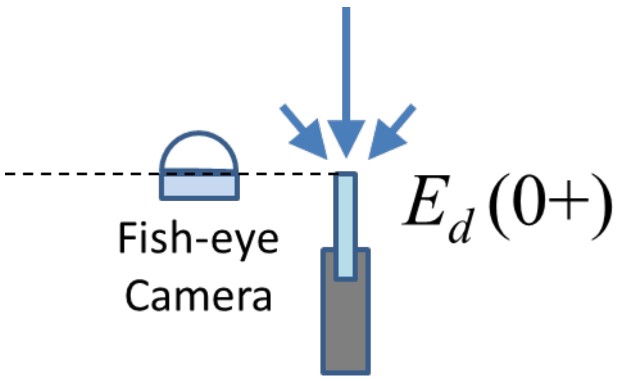

Figure 3-3 Schematic showing how a fish-eye camera, preferably fully hemispherical, can be used to qualitatively check for superstructure contamination of E_d^{0+} measurements.

Figure 3-4 Example fish-eye photos taken to check for contamination of E_d^{0+} measurements. (top) Contamination of field of view by other instuments, (middle) Contamination of field of view by a scientist in bottom of photo, (top) No

obvious contamination of field of view by nearby obstructions. Radiance from the trees does contribute to E_d^{0+} (and this may be deemed inappropriate for satellite validation in some contexts) but since these objects are distant the E_d^{0+} measurement is representative of the E_d^{0+} field illuminating the water target. In none of these cases are the sky/cloud conditions suitable for satellite validation.

While direct sun shadowing of the E_d^{0+} sensor is generally avoided by design of the deployment method and can easily be identified and removed from data, the impact of more subtle optical contaminations of sky radiance can be more difficult to identify and estimate.

It is obvious that humans should remain fully below the level of a E_d^{0+} sensor at all times during measurements. It is not unknown for resting birds to contaminate unsupervised E_d^{0+} measurements and measures may be taken to avoid this, e.g. use of spikes below the field of view. Unusual contaminations may be identified by video camera monitoring of unsupervised installations.

On some platforms optical contamination may also arise from atmospheric steam or smoke emissions from ship engine funnels, and other exhaust gases (airconditioning, etc.).

Fixed offshore structures with limited access (e.g. oil and gas platforms, wind farm structures, navigational structures) as well as large ships with tall masts may be particularly subject to superstructure shading. Improvements in the stability of telescopic masts (S.B. Hooker 2010), which allowing high mounting but easy inspection of fore-optics, and reductions in the price of such equipment should facilitate the adoption of deployment techniques with greatly reduced or zero superstructure shading.

For shipborne E_d^{0+} measurements the use of a floating platform to carry the E_d^{0+} instrument away from the ship will clearly minimise, possibly to negligible, the superstructure-related perturbations. This may be conveniently combined in a floating/profiling platform used for underwater profiling of $L_{un}(z)$ – see section 4.2.2.3.

Measures to reduce and/or estimate the uncertainties associated with superstructure shading may include redundant measurement by multiple sensors located in different positions and hence subject to different shading effects, or experiments with sensors at different heights/locations, etc. 3D radiative transfer modelling may also be used to estimate uncertainties in E_d^{0+} measurements associated with superstructure effects.

3.1.2.3 Fouling

In constrast with downward-facing sensors, the upward-facing sensors needed for measurement of E_d^{0+} are particularly prone to fouling of the fore-optics, particularly for long-term unsupervised deployments.

Fouling may occur because of sea spray, atmospheric deposition of particles (which may even embed within the stucture of some diffuser materials used as fore-optics), rain droplets, spiders and other insects, etc. This can be mitigated by cleaning of fore-optics and can be monitored by frequent calibration checks, e.g. with portable relative calibration devices (Stanford B. Hooker and Maritorena 2000) – see FRM4SOC TR-2.

Fouling is generally kept negligible for supervised deployments by regular inspection and, when necessary cleaning, of fore-optics and protection by lens caps when not measuring (e.g. at night and between "stations" for discrete measurements).

For unsupervised deployments fouling could be minimised by protection of fore-optics when not measuring by use of external mechanical shutters or rotation of sensors to point downwards (similar to the "parking" function of the CIMEL CE-318 sunphotometer when not measuring).

Major fouling events can be identified by time series analysis of data and/or video camera imagery.

The uncertainty estimate related to fouling can be validated by comparing post-deployment calibrations before and after cleaning.

3.1.2.4 High frequency natural fluctuations

In clear sky conditions the natural variability of E_d^{0+} over a typical measurement time scale (~1-10 minutes) is low and may be easily estimated from a clear sky irradiance model, e.g. (Gregg and Carder 1990), using as input the temporal variation of sun zenith angle and an estimate/measurement of aerosol optical thickness.

If measurements are made during partially cloudy conditions, in addition to the tilt-induced fluctuations described in section 3.1.2.1, natural variability of E_d^{0+} may be non-negligible, particularly if there are clouds or haze near the sun. In such cases careful quality control of data is necessary to remove individual measurements or complete sets of measurements that cannot be used for satellite validation. Quality control will typically include tests on temporal variability including second derivative "spike/jump" analysis and min/max/standard deviation analysis and may also include comparison of data with a clear sky model.

A full sky imager can be used to provide detailed information on sky conditions for quality control (Kalisch and Macke 2008)

It is suggested here that Fiducial Reference Measurements for satellite validation should not be made during during fully cloudy conditions or when the sun is obscured by clouds or haze. In situ measurements can be made at a slightly different time from the satellite overpass, e.g. 1-6 hours depending on natural variability (see also Chapter 6), and so a cloud-free satellite image could theoretically correspond with an in situ reflectance measurement made during cloudy conditions within an acceptable time window. However, many factors, including the very different bidirectional reflectance of water under a sunny or a cloudy sky suggest that this should be avoided in the satellite validation context[8].

Uncertainties associated with high frequency natural fluctuations can be estimated from the standard deviation of measurements made over a certain interval of time. High uncertainty may lead to simple rejection of the measurement.

[8] In other contexts, such as simultaneous reflectance and chlorophyll a measurements used for algorithm calibration/validation it may be acceptable to use measurements made in cloudy conditions, particularly fully overcast conditions, provided that the corresponding measurement uncertainties are sufficiently quantified and limited.

3.1.3 Variants on the method of Direct above water measurement of E_d^{0+} with an upward pointing irradiance sensor

Underwater drifting floats used for satellite radiometry validation (Claustre et al. 2011) may lack a permanently above water E_d^{0+} sensor and make only occasional E_d^{0+} measurements, when surfacing. This precludes monitoring of illumination during the upwelling radiance measurements, which is of relevance for the L_w measurement itself – see Chapter 4. As regards the E_d^{0+} measurement required for reflectance normalisation in equation (1), there is no fundamental difference between the "surfacing" E_d^{0+} sensor and the permanently above water E_d^{0+} sensors considered in the bulk of this section, except that time and horizontal space differences between E_d^{0+} and L_w measurements must be considered and the presence of water, already mentioned in section 4.1.2.4, and aquatic algae on the fore-optics may be more problematic.

3.2 Estimation of E_d^{0+} from direct sunphotometry and a clear sky atmospheric model

As an alternative to direct measurement of $\boldsymbol{E_d^{0+}}$ using a vertically-pointing irradiance sensor described in section 3.1, it is possible to estimate aerosol optical thickness by measuring the direct sun radiance with a sunphotometer and estimating total atmospheric transmittance with this and other inputs – see Figure 3-5 and Figure 3-6. This method was originally developed for satellite validation measurement using the hand-held SIMBAD radiometer (Deschamps et al. 2004) and has the interesting feature for satellite validation studies of providing more information on atmospheric parameters than the direct $\boldsymbol{E_d^{0+}}$ measurement described in section 3.1. In the handheld SIMBAD protocol only aerosol optical thickness is measured, but for automated sun/sky radiometers, such as those of the AERONET-OC network (G. Zibordi et al. 2009), with many other pointing scenarios many extra atmospheric parameters including aerosol size distribution and phase function can be estimated (Holben and al 1998).

The method was described in the NASA Ocean Optics Protocols (J.L. Mueller et al. 2003) as above water radiometry "Method 3", in combination with measurements of water-leaving radiance using a vertical polariser, as implemented for the SIMBAD instrument. However, this method for estimating $\boldsymbol{E_d^{0+}}$ may be combined with different methods for estimating L_w, e.g. above water methods without a vertical polariser, and so is described here as a generic method for estimating $\boldsymbol{E_d^{0+}}$ - see also the discussion of section 2.9.

The pointing accuracy required for direct sun measurements generally requires a very stable platform, such as a fixed offshore structure as in the AERONET-OC protocol (G. Zibordi et al. 2009), for unsupervised measurements, or can be achieved by a handheld sunphotometer, e.g. SIMBAD radiometer (Deschamps et al. 2004). However, the feasibility of making direct sun maesurements from a moving platform has been demonstrated for an airborne instrument (Segal-Rosenheimer et al. 2014).

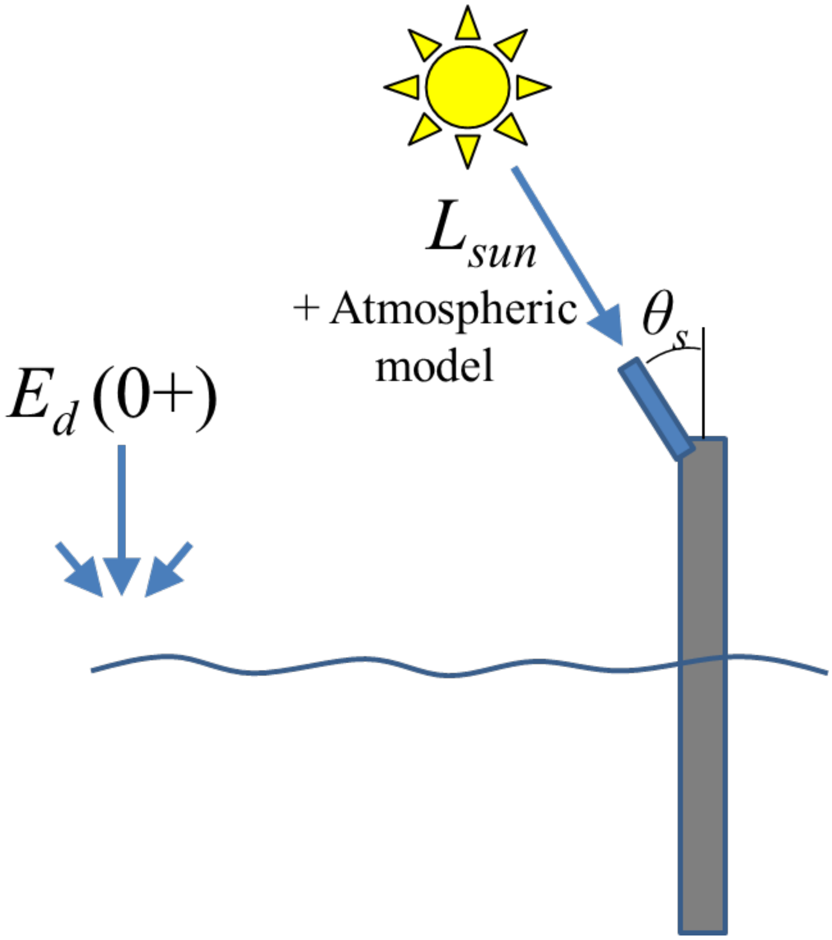

Figure 3-5 Schematic of direct sun measurement for estimation of E_d^{0+}.

Figure 3-6 Typical deployment of instrumentation for estimation of E_d^{0+} by sunphotometry. (left) SeaPRISM instrument [photo courtesy: Dimitry Van Der Zande], (right) handheld SIMBADA instrument.

3.2.1 Measurement equation

The full measurement equations for this method are described in (Deschamps et al. 2004) using a notation typical for atmospheric radiative transfer studies and which does not explicitly mention $\boldsymbol{E_d^{0+}}$. For compatibility with the rest of the current document, these equations are rewritten here in a form which facilitates identification of $\boldsymbol{E_d^{0+}}$ itself.

Thus, the total (direct and diffuse) downward (sun to water) atmospheric transmittance, T_0, is defined by

$$T_0 = \frac{E_d^{0+}}{E_d^{TOA}} \quad (5)$$

and the downwelling irradiance at Top of Atmosphere, E_d^{TOA}, is given by

$$E_d^{TOA} \quad = F_0 \ Cos\vartheta_0 \left(\frac{d}{d_0}\right)^2 \quad (6)$$

where F_0 is the extraterrestrial solar irradiance for mean sun-earth distance d_0, e.g. tabulated by (Thuillier et al. 2003), ϑ_0 is the sun zenith angle and d is the sun-earth distance at the time of the measurement, which can be easily calculated from position and date/time using earth orbital models.

Combining these gives:

$$E_d^{0+} = T_0 * F_0 \ Cos\vartheta_0 \left(\frac{d}{d_0}\right)^2 \tag{7}$$

T_0 is estimated using a clear sky radiative transfer model, e.g. (Deuzé, Herman, and Santer 1989), which takes as input ϑ_0, vertically integrated ozone amount (obtained from extraneous data such as Total Ozone Mapping Scanner satellite data and/or meteorological models or climatologies), surface atmospheric pressure (which influences Rayleigh optical thickness and may be obtained from simultaneous surface measurements or from appropriate meteorological models), and aerosol optical thickness, $\tau_a(\lambda)$ – see equation (7) of (Deschamps et al. 2004). The impact of other absorbing gases may be included in the atmospheric radiative transfer model, if necessary.

The aerosol thickness $\tau_a(\lambda)$ is deduced from direct sun measurements taking account of sunphotometer calibration, earth-sun distance variation d/d_0, sun zenith angle ϑ_0, and including corrections for molecular scattering and gaseous absorption, considered mainly due to ozone – see section 4.1 of (Deschamps et al. 2004) including their equations (5) and (6).

The Angström exponent for spectral variation of $\tau_a(\lambda)$ can also be computed and in the SIMBADA protocol is used in the skyglint correction for L_w, but is not needed for computation of E_d^{0+}.

The calculation of T_0 required for this $\boldsymbol{E_d^{0+}}$ measurement protocol is quite comparable to the computation of $\boldsymbol{E_d^{0+}}$ made in satellite data processing software , e.g. SeaDAS.

3.2.2 Protocol-dependent sources of uncertainty

In addition to the instrument-related sources of uncertainty which arise from imperfections in the radiometers themselves, as dealt with in FRM4SOC Technical Report TR-2, including the Bouger-Langley calibration, the measurement of above water downwelling irradiance from direct sun radiometry and atmospheric modelling has a number of sources of uncertainty relating to the measurement equation and deployment conditions. These protocol-related sources of uncertainty are described here.

3.2.2.1 Atmospheric radiative transfer model

The atmospheric radiative transfer model used to estimate T_0 has both intrinsic uncertainties, associated with models and simplifications of many complex atmospheric optical processes, as well as uncertainties which arise from uncertainties in the various input parameters (absorbing gas amounts, atmospheric pressure, sun zenith angle, etc.) and which propagate through the model. The extraterrestrial solar irradiance also includes some uncertainty – ideally the same solar irradiance data will be used for the in situ and the satelltie data processing.

The estimation of uncertainty from all these sources is complex and is described in detail in section 5 of (Deschamps et al. 2004).

3.2.2.2 Sky conditions

The atmospheric radiative transfer model used to estimate T_0 assumes that the sky is horizontally homogeneous and , in particular, contains no clouds. This assumption is valid for the design conditions of clear sky satellite validation, but significant and difficult to estimate uncertainties will arise if this assumption is violated, e.g. for a partially cloudy sky. In the SIMBAD and AERONET-OC protocols automated quality control steps identify when the direct sun measurement is affected by clouds or haze near the sun and remove such data from processing. In the SIMBAD protocol the human observer can also identify suboptimal conditions, such as clouds somewhere else in the sky, and quality flag such data accordingly.

3.2.2.3 Pointing effects

While high pointing accuracy is crucial for direct sun measurements, this can be well achieved by both robotic and handheld systems allowing for fine pointing adjustments. The field of view of sunphotometer instruments is by design small, e.g. 1.5-3°, typically not much larger than the sun's linear angle of about 0.53°, to minimise the contribution of atmospheric scattering yet completely cover the sun disk.

Inadequate pointing accuracy can be identified from replicate measurements and/or very high apparent optical thickness and corresponding measurements removed during quality control steps.

Uncertainties associated with direct sun pointing may be grouped with other uncertainties in the measurement of aerosol optical thickness.

3.2.2.4 Shading

Shading of the direct sun measurement by the presence of solid objects is generally not a problem because, in contrast to direct measurement of E_d^{0+} with an irradiance sensor where the whole upward hemisphere should be free of obstructions, for direct sun measurement only the direct sun path must be free of obstructions. For unsupervised measurements, most structure shading will be very obvious in direct sun measurements and can be automatically removed either a priori, by defining a range of acceptable viewing azimuth angles, or a posteriori, by eliminating very low radiance values. Minor obstructions, such as wires and cables potentially in the field of view should be eliminated during deployment and other occasional obstructions (birds, humans) can be monitored by video camera. For supervised measurements, any structural shading can easily be identified and avoided.

On some platforms there may be a risk of optical contamination from atmospheric steam or smoke emissions and other exhaust gases (airconditioning, etc.).

3.2.2.5 Fouling

Sunphotometers are always associated with a pointing mechanism, either robotic or human, and so are generally protected from most fouling mechanisms when not measuring.

Nevertheless some fouling of the fore-optics may occur for long-term unsupervised deployments because of sea spray, rain droplets, and/or spiders and other insects, etc.

Major fouling events can be identified by time series analysis of data and/or video camera imagery.

The uncertainty estimate related to fouling can be validated by comparing post-deployment calibrations before and after cleaning.

3.2.2.6 High frequency natural fluctuations

This method for E_d^{0+} can only be used in ideal clear sky conditions, where high frequency natural fluctuations of E_d^{0+} do not occur. The latter can easily be detected by replicate measurements and the corresponding measurement sequence can be eliminated.

3.2.3 Variants on the method of measurement of E_d^{0+} from direct sunphotometry and a clear sky atmospheric model

As mentioned previously, this protocol can be used with human or robotic pointing systems and measurements can be made with or without a vertical polariser. Because this protocol has very different assumptions and very different sources of uncertainty from the protocol using a vertically-pointing irradiance sensor (section 3.1) there is signficant added value to combine sunphotometric estimation of $\boldsymbol{E_d^{0+}}$ with direct measurement of $\boldsymbol{E_d^{0+}}$ using an irradiance sensor, as proposed in the OSPREY system (Stanford B. Hooker et al. 2012).

3.3 Estimation of E_d^{0+} using a downward pointing radiance sensor and a reflective plaque

3.3.1 Measurement equation

The downwelling irradiance, $\boldsymbol{E_d^{0+}}$, can also be measured indirectly by measuring the upwelling radiance, L_P, from a horizontally deployed Lambertian reflectance plaque of known reflectance, ρ_P – see Figure 3-7. The Measurement Equation is given by:

$$E_d^{0+} = \frac{\pi * L_P}{\rho_P} \tag{8}$$

where all terms may vary with wavelength.

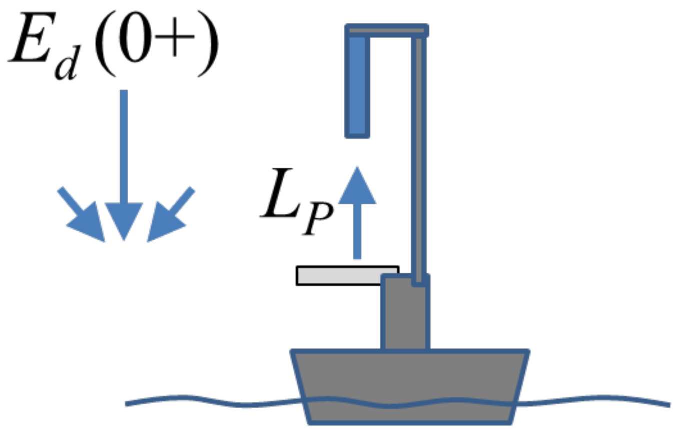

Figure 3-7 Schematic showing indirect measurement of E_d^{0+} using a downward pointing radiance sensor and a reflective plaque (sensor, plaque and holder not to scale).

Figure 3-8 Typical measurement equpment and deployment for measurement of E_d^{0+} using a downward pointing radiance sensor and a reflective plaque. Photo courtesy A. Ruiz-Verdu.

A common material for such plaques is Spectralon™, which can be manufactured to give near 100% reflectance ($\rho_P \approx 1.0$) for "white" plaques, or lower reflectance, e.g. $\rho_P \approx 0.1$, for "grey" plaques, with low spectral variation of reflectance, low departure from the perfect Lambertian angular response (Early et al. 2000), low spatial heterogeneity and reasonable temporal stability. Other diffusive materials have been used in this method, including grey "cards" used traditionally in photography. All materials used in the FRM context need to be adequately characterised as regards bidirectional, spectral, spatial variability and degradation.

Historically, measurement of E_d^{0+} using a downward pointing radiance sensor and a Lambertian reflective plaque was adopted for cost considerations, allowing all measurements to be made with a single radiance sensor. This method also allows reduction of some calibration-related uncertainties, since only one sensor is used. The method was even suggested in the NASA Ocean Optics protocols 2003 version "Method 2" (J.L. Mueller et al. 2003) as being appropriate for measurement of reflectance using an *uncalibrated* sensor, although it is now inconceivable, particularly in the FRM context, to use an uncalibrated radiometer. **Although relevant at the time (2003) because of difficulties to maintain regular absolute radiometric calibration, the use of an uncalibrated sensor is now inconceivable, particularly in the FRM context.** While the water reflectance is the primary parameter that is needed for validation of satellite data, it is important to have also the contributing L_w and contributing E_d^{0+} measurements since the latter enables validation of atmospheric transmittances calculated during the satellite data processing (and were indeed considered as mandatory in the NASA Ocean Optics Protocols – see Table 2-1). Moreover the interpretation of in situ measurement intercomparison exercises (G. Zibordi, Ruddick, et al. 2012), as required by the FRM process, necessitates a separation of uncertainties arising from Lw and E_d^{0+} measurements, e.g. comparing E_d^{0+} measurements from a vertically-mounted irradiance sensor (impacted by cosine angle uncertainties, etc.) with E_d^{0+} measurements deduced from a radiance sensor viewing a reflectance plaque (impacted by BRDF uncertainties, etc.). This can only be achieved when using a calibrated radiance sensor in the latter protocol. Use of a calibrated radiance sensor also enables better quality control of E_d^{0+} measurements made using this protocol, e.g. comparison of absolute E_d^{0+} with a clear sky model (Gregg and Carder 1990).

The reflectance plaque method is popular in the land remote sensing community, possibly because for land applications, measurement for Short Wave Infrared wavelenths (1-3µm) is important, which very significantly raises the cost of an instrument, and perhaps also because of less focus on highly accurate radiometric measurements for validation of satellite-derived land reflectances.

Use of the reflectance plaque protocol for measurement of E_d^{0+} has stimulated considerable discussion during the drafting of this review and it has been difficult to reach a consensus with the first author suggesting that the method be "strongly discouraged" and other co-authors considering that the method is acceptable. **Referring strictly to the definition of Fiducial Reference Measurements provided in section 1.2 and including the requirement that an uncertainty budget be provided, it seems reasonable to consider this method as acceptable provided that it meets at least the standards expected from measurements made with a vertically-mounted irradiance sensor (section 3.1),** including the requirements that:

1. There be no humans above the level of the reflectance plaque (and thereby affecting the sky radiance contributing to downwelling irradiance illuminating the plaque in a way that is highly variable and essentially not quantifiable in an uncertainty estimate),

2. The reflectance plaque be mounted as high as possible on the ship/platform, typically higher than any superstructure elements with significant solid angle as viewed from the plaque

3. The reflectance plaque be mounted on a fixed structure, not hand-held, and associated with an inclinometer allowing estimation of uncertainties associated with non-horizontal measurements (comparable to non-vertical measurements using an irradiance sensor),

4. The E_d^{0+} measurements made using a reflective plaque be supported by experiments and/or simulations to estimate the measurement uncertainties and validate these estimations, e.g. (Doxaran et al. 2004), as detailed in the following section (and including instrument and superstructure shading of the plaque).

Outside the FRM satellite validation context, the educational value of measurements made using this protocol, e.g. with very simple optical instruments (Leeuw 2014), are clearly recognised.

Measurements with a reflective plaque are generally not suitable for unsupervised systems because of the need to protect the plaque from fouling when not measuring. Measurements with a reflectance plaque can be made from fixed structures. However, because of the need for supervision, the method is generally used from ships despite the associated problems of tilt and superstructure shading.

The NASA 2003 Protocols (Volume III, section 3.3) recommended that measurements of $\boldsymbol{E_d^{0+}}$ with a reflective plaque should be made with a vertical downward (nadir) pointing radiance sensor and a plaque with BRDF calibration for varying downwelling light distributions (typically characterised by sun zenith angle) and vertical upwelling reflected radiance. However, off-nadir viewing with the same zenith angle as water-viewing mesurements (see section 4.3 for abovewater $\boldsymbol{L_w}$ **)** has often been adopted for practical reasons, e.g. for easy switching between plaque and water-viewing modes for certain deployments. It is noted that (C.D. Mobley 1999) provides the scientific basis for a water-viewing zenith angle of 40° (and relative azimuth to sun of 135°) as a good geometry for sunglint avoidance, but does not give a scientific basis for a plaque-viewing zenith angle of 40° - the latter is merely suggested as practically convenient. On the other hand, an off-nadir plaque-viewing geometry may indeed be desirable for other scientific reasons, such as minimisation of instrument shading (Ken Voss, Private Communication). Optimal plaque-viewing geometry is thus an open question, although this question does not have to be answered here. In contrast with the more prescriptive approach of the NASA Ocean Optics Protocols of 2003, the FRM4SOC approach is not to prescribe a single viewing geometry (or any other specific aspect of a measurement protocol), but is more generic and "simply" requires that for whatever plaque-viewing geometry that is adopted, the related uncertainties (instrument and superstructure shading of plaque, plaque BRDF) be quantified.

3.3.2 Protocol-dependent sources of uncertainty

In addition to the instrument-related sources of uncertainty which arise from imperfections in the radiometers themselves, as dealt with in FRM4SOC Technical Report TR-2, the measurement of above water downwelling irradiance using a reflectance plaque has a number of sources of uncertainty relating to the deployment conditions. These protocol-related sources of uncertainty are described here.

3.3.2.1 Plaque calibration

Clearly the reflectance of the plaque used for this measurement must be calibrated with traceability to an SI standard and an uncertainty associated with this calibration – this is dealt with in detail in the accompanying FRM4SOC Project Technical Report 3 on "Protocols and Procedures to Verify the Performance of Reference Irradiance and Radiance Sources used to by Fiducial Reference Measurement (FRM) Ocean Colour Radiometers (OCR) for Satellite Validation". Optical contamination/degradation of the plaque and bidirectional effects are further considered in subsections 3.3.2.5 and 3.3.2.7.

3.3.2.2 Plaque homogeneity and sensor field of view

It is known that plaques do have spatial inhomogeneities and so it is assumed that the measurement area on the plaque corresponds sufficiently well to the area on the plaque used during plaque calibration, taking account of the surface average of any inhomogeneities.

Clearly the plaque must fully fill the sensor field of view (FOV) so that the measurement of E_d^{0+} will not be contaminated by the background around the reflectance plaque. This can be facilitated by small FOV instruments. In any case the angular response of the radiance sensor should be checked for any residual reponse outside the manufacturer-specified FOV – see also the FRM4SOC Technical Report 2 (currently in preparation) on radiometer characterisation.

Uncertainties associated with sensor field of view and plaque inhomogeneity can be assessed by experiments deploying the instruments at different heights above the reflectance plaque and by changing the background around the reflectance plaque (since instrument shading effects will also vary with instrument height – see section 3.3.2.4).

3.3.2.3 Tilt effects

Non-horizontality of the reflectance plaque used for measurements of E_d^{0+} will give uncertainty in the measurement of E_d^{0+} in the same way as non-verticality of an irradiance instrument used to directly measure E_d^{0+}, discussed previously in section 3.1.2.1. Tilting of the plaque can be caused by a number of factors, including imprecise levelling and, if measuring from a ship, wave-tilting during measurements if measuring from a ship. It is, therefore, necessary to measure the tilt of the plaque (not just the ship) at sufficiently high frequency and perform appropriate filtering of non-vertical data and/or averaging of data to reduce tilt effects.

Although digital inclinometers are now readily available for integration with radiometric data streams they seem not to be used for shipborne measurement of E_d^{0+} using a reflectance plaque.

For E_d^{0+} the effect of tilt may be particularly strong in sunny (satellite validation) conditions because of the highly anistropic light field and the effect of a non-horizontal plaque is similar to a change in solar zenith angle[9].

The impact of tilt on measurement uncertainty can be estimated if the two angles of tilt with respect to sun and approximate angular variation of sky radiance (from imaging cameras or estimated from atmospheric properties) are known – see section 3.1.2.1.

Obviously, minimisation of tilt should be a consideration in the choice of measurement platform. Small ships may be particularly subject to high tilt.

3.3.2.4 Shading from superstructure and instruments and mounting equipment

The light field that is being measured is itself perturbed by the presence of solid objects anywhere above the level of the reflectance plaque. This includes, necessarily, the radiometer itself used for measurements, but also any superstructure elements of the ship/platform as well as any equipment related to fixing the radiometer above the reflectance plaque.

The shading problems associated with this method are conceptually similar to those already described for direct measurement of E_d^{0+} (section 3.1.2.2), but are significantly worse:

- Firstly, there will always be some shading of sky radiance onto the plaque from the radiometer itself. The radiometer must be held above the plaque at a height that is sufficiently small that the plaque fills the whole field of view of the instrument. The exact height depends on the instrument and the size of the plaque. Shading from the radiometer (and any associated fixations) will be related to the solid angle of sky filled by the radiometer as seen from any point on the reflectance plaque and will be worse for instruments held close to the plaque or having a large diameter.
- Secondly, while it is typical to mount irradiance sensors high on poles/masts (section 3.1.2.2) and certainly above head height, measurements with a reflectance plaque are nearly always made much lower on a ship/platform for practical reasons – it is

[9] At high tilt a E_d^{0+} sensor may also measure some light from water instead of the sky, although grazing angle incident light has a low contribution to the cosine-weighted integral for E_d^{0+}.

generally necessary to manipulate the radiometer (e.g. to then point to water and sky) and the plaque (e.g. to protect it when not measuring). Optical contamination from ship/platform sides, upper decks, masts and even humans (often including those making the measurement!) can be very significant and difficult to quantify.

The process of sky shading can be easily understood from fish-eye photographs taken vertically upwards at the location of a reflectance plaque. Any part of the upward hemisphere that is not sky represents optical contamination of the measurement and this contamination will be related to the solid angle of sky that is replaced by the object with near-zenith objects contributing more than near-horizontal objects to the cosine integral of radiances.

Measures to estimate the uncertainties associated with shading could include experiments made with irradiance sensors located a) alongside the plaque and, b) on a mast above possible optical contamination and/or experiments combining optimal and non-optimal locations (Doxaran et al. 2004).

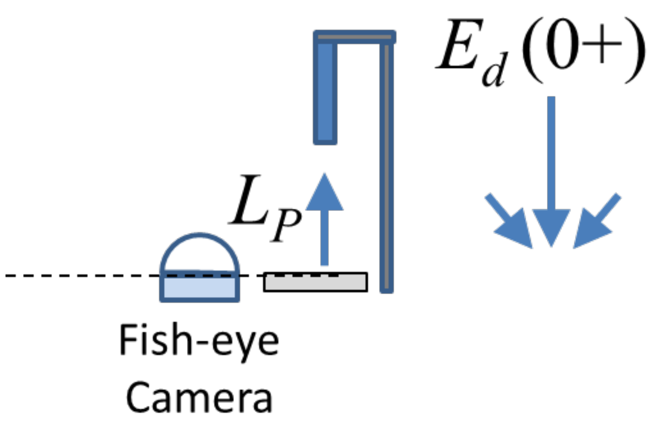

Figure 3-9 Location of fish-eye camera used for qualitative checking of shading of reflectance plaque, for comparison with Figure 3-3 for the direct measurement of E_d^{0+} using an irradiance sensor, described in section 3.1.

3.3.2.5 Fouling

Since measurements made with a reflectance plaque are supervised, there should be no significant contamination of the radiance sensor fore-optics, which should be cleaned whenever necessary following manufacturers' recommendations.

Optical contamination of the plaque itself may be a significant problem because of atmospheric deposition of particles (which may embed within the stucture of some diffuser materials) of both natural and ship-related origin, marks from contact with any objects including materials used to protect the plaque during storage, etc. For example, it is recommended to keep plaques away from plastics and hydrocarbons (diesel fumes) and to build a storage box that holds the plaque fixed in a way it cannot touch the inner top surface. Obviously humans should not touch the diffusive surface itself. The cleaning of dirty plaques is, of course, recommended but should be accompanied by recalibration.

In addition to optical contamination, plaques may change naturally from photodegradation processes related to ultraviolet exposure. For example, the reflectivity of Spectralon™, a proprietary form of polytetrafluoroethane produced by Labsphere and used for both spaceborne calibration diffusers and the ground-based measurements described here, may change at short wavelengths because of absorption from organic impurities (Stiegman, Bruegge, and Springsteen 1993; Georgiev and Butler 2007), which can only be removed by vacuum baking. Careful handling and storage of plaques is required to limit such degradation.

The uncertainty estimate related to fouling can be validated by comparing post-deployment calibrations before and after cleaning of a plaque.

3.3.2.6 High frequency natural fluctuations

Considerations and uncertainties associated with high frequency natural fluctuations of E_d^{0+} over a typical measurement time scale (~1-10 minutes) are identical to those already discussed in section 3.1.2.4, except that asynchronicity of E_d^{0+} and L_w^{+} measurements is inevitable for this method.

3.3.2.7 Bidirectional reflectance of plaques

In general, a plaque calibration is made for unidirectional illumination (typically 8°) and with hemispherical collection, using an integrating sphere – termed "8/h" or "8/d" calibration. Whereas the cosine response of irradiance sensors must be considered for the direct measurement of E_d^{0+}, the bidirectional reflectance of a plaque (from all illuminating directions to the single nadir-viewing direction) must be considered in the uncertainty estimate for the reflectance plaque method. This data is reported in some cases for typical white Spectralon™ plaques (Georgiev and Butler 2007) but may be unknown for other materials, including grey cards. A full characterisation of the optical properties of a plaque will include polarisation sensitivity in the calibration process(Georgiev and Butler 2004). The uncertainty associated with imperfect Lambertian response of a plaque can be validated by comparison with a zenith-pointing irradiance sensor, if the latter has a sufficiently characterised cosine response.

3.3.3 Variants on the method for measurement of E_d^{0+} using a downward pointing radiance sensor and a reflectance plaque

Multiple measurements can be made with different plaques (Ondrusek et al. 2016), e.g. of different reflectivity, to reduce/validate uncertainties associated with individual plaques (calibration, optical contamination/degradation, bidirectionality, etc.). An interesting idea here was the use of a "blue tile" reported by B.C. Johnson in section 7.10 of (Ondrusek et al. 2016). This specially-manufactured reflectance plaque has spectral properties similar to that of blue water and so provides an intercomparison target which allows testing of both some aspects of abovewater L_w protocols (section 4.3) with some aspects of radiometer instrument characterisation, such as straylight (covered more fully in the FRM4SOC "Insrtuments" Technical Report 2).

3.4 Estimation of E_d^{0+} from underwater measurements

It is common for underwater radiometric measurements of $L_{un}(z)$ to be accompanied by underwater measurements of downwelling irradiance, $E_d(z)$. Historically, E_d^{0+} was often estimated from these underwater measurements, by extrapolation to just beneath the surface and transmission across the air-water interface, as described in Sections 4.1 and 4.2 for $L_{un}(z)$. However, the high frequency variability of $E_d(z)$ associated with wave focussing/defocussing is particularly difficult to remove and this method for estimating E_d^{0+} has been replaced by the direct above water E_d^{0+} measurement. **Estimation of E_d^{0+} from underwater measurements is thus considered outside the scope of the current document, which is focussed on satellite radiometric validation measurements.**

Outside the satellite validation context, underwater measurements of $E_d(z)$ are still relevant for estimation of optically and biologically important parameters such as the spectral diffuse attenuation coefficient of downwelling irradiance, $K_d(\lambda, z)$, and related parameters such as euphotic depth.

A detailed description of protocols for measuring $E_d(z)$, $K_d(\lambda, z)$ and, if considered useful, E_d^{0+} can be found in the NASA Ocean Optics protocols (J. L. Mueller 2003).

4 Measurement Protocols for water-leaving radiance

In the current section the fundamental Measurement Equation and approach for measurement of L_w is summarised for measurement protocols that are currently used for satellite radiometric validation. These protocols are grouped into four broad families of method:

- Underwater radiometry using fixed depth measurements
- Underwater radiometry using vertical profiles
- Above water radiometry with sky radiance measurement and skyglint removal
- Above water radiometry with optical blocking of skyglint

For each family of method, the Measurement Equation is defined and the measurement parameters are briefly described. The elements that should be included for estimation of total protocol-related measurement uncertainty are discussed with some considerations and references for further reading. Owing to the diversity of approaches and instrumentation and water types possible within each family and taking account of the FRM concept (section 1.2), no attempt is made to prescribe specific thresholds (e.g. for "acceptable" tilt, sea state, cloud conditions, etc.) that should be observed when making measurements. Such decisions are left as the responsibility of the measurement scientists. The approach here is rather to provide a list of elements that need to be considered in the measurement uncertainty analysis as well as associated considerations.

4.1 Underwater radiometry – fixed depth measurements

4.1.1 Measurement equation

In fixed depth underwater radiometry, as typified by BOUSSOLE (D. Antoine et al. 2008; David Antoine et al. 2008) and MOBY (Clark et al. 1997, 2003; Brown et al. 2007), radiometers are deployed underwater and attached to permanent structures, to measure nadir upwelling radiance, $L_{un}(z)$, at two or more depths, $z = z_1, z_2, \ldots$ – see Figure 4-1 and Figure 4-2. A further measurement is made above water of downwelling irradiance, E_d^{0+}, to allow for calculation of ρ_w (Chapter 3) and to monitor for possible variation of illumination conditions during the measurement. In the case of MOBY these measurements are made with $z_1 = 1m$, $z_2 = 5m$ and $z_3 = 9m$, while the BOUSSOLE system makes measurements at $z_1 = 4m$, $z_2 = 9$.

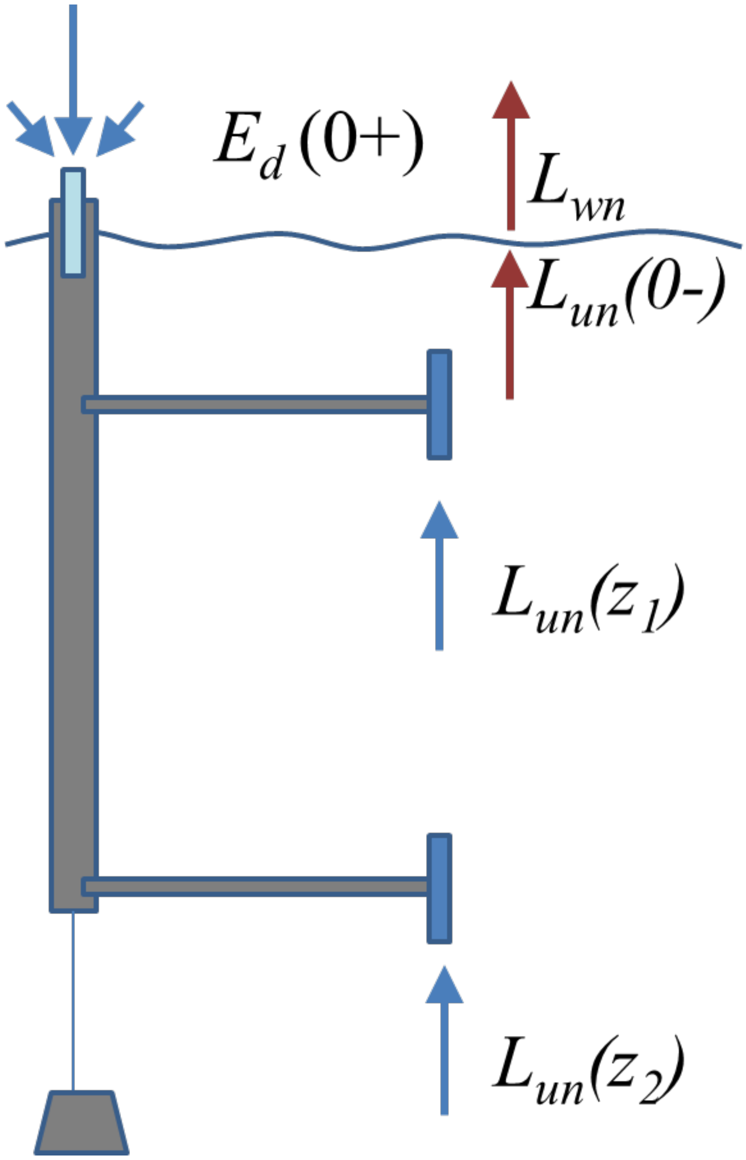

Figure 4-1 Schematic of fixed depth underwater measurements.

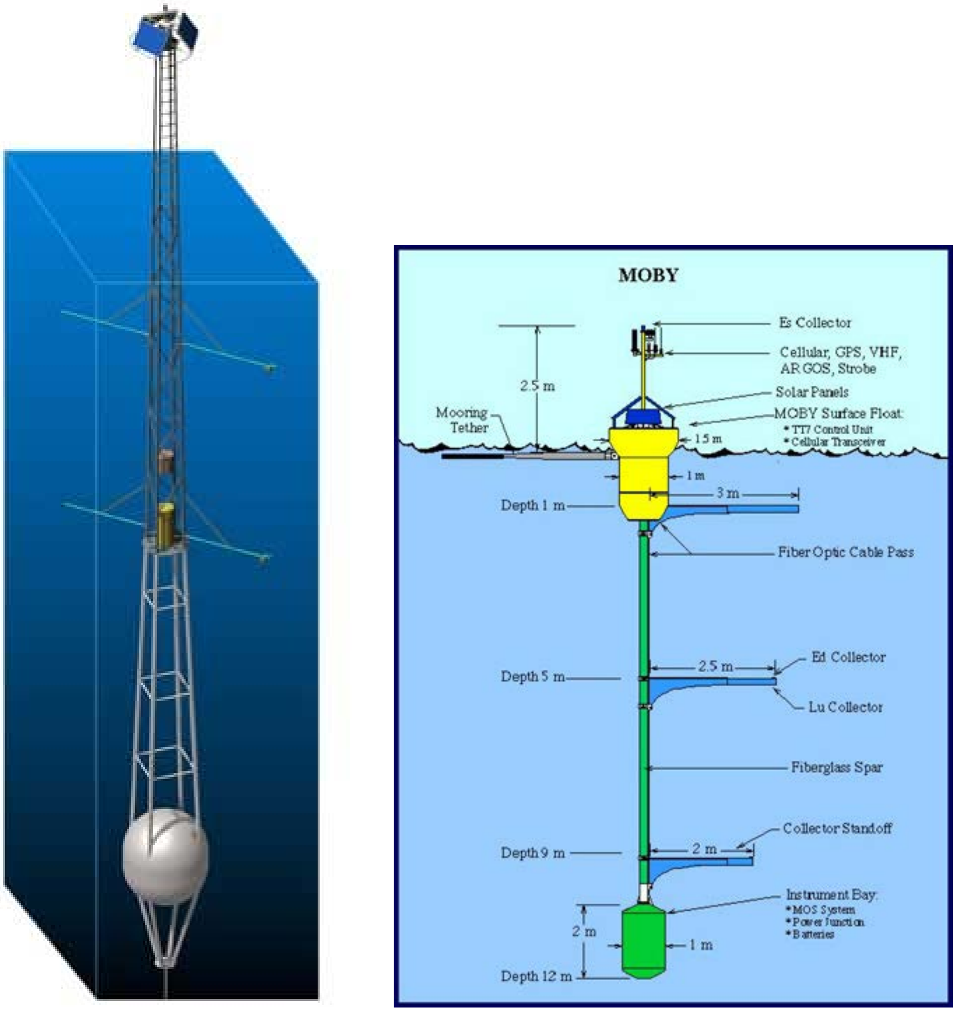

Figure 4-2 Typical deployments of fixed depth underwater measurements. (left) BOUSSOLE buoy (D. Antoine et al. 2008); (right) MOBY buoy [https://moby.mlml.calstate.edu/photo-gallery/]

The nadir water-leaving radiance, L_{wn}, is then calculated by first estimating the nadir upwelling radiance just beneath the water surface, $L_{un}(0-)$, by extrapolating from, for example, the two shallowest depth measurements z_1 and z_2 assuming that the depth variation of $L_{un}(z)$ between the surface, $z = 0$, and , $z = z_2$, is exponential with constant diffuse attenuation coefficient for upwelling radiance, K_{Lu}. Thus, using the convention that depths beneath the water surface are considered as positive (but retaining the notation 0^- for radiance just beneath the water surface),

$$L_{un}(0-) = L_{un}(z_1)exp[K_{Lu}z_1] \tag{9}$$

where,

$$K_{Lu} = \frac{1}{z_2 - z_1} ln\left[\frac{L_{un}(z_1)}{L_{un}(z_2)}\frac{E_d^{0+}(t_2)}{E_d^{0+}(t_1)}\right] \tag{10}$$

where $E_d^{0+}(t_1)$ and $E_d^{0+}(t_2)$ represent the downwelling irradiance measured at times t_1 and t_2, corresponding to the times of measurement of $L_{un}(z_1)$ and $L_{un}(z_2)$. If these radiances are measured at precisely the same time then obviously $E_d^{0+}(t_1) = E_d^{0+}(t_2)$ and equation (10) simplifies accordingly to:

$$K_{Lu} = \frac{1}{z_2 - z_1} ln \left[\frac{L_{un}(z_1)}{L_{un}(z_2)}\right] \tag{11}$$

Finally the water-leaving radiance is obtained from $L_{un}(0-)$ by propagating the latter across the water-air interface using,

$$L_{wn} = \frac{T_F}{{n_w}^2} L_{un}(0-) \tag{12}$$

where T_F is the Fresnel transmittance of radiance from water to air and n_w is the refractive index of water. The refractive index of air, n_{air}, is here assumed equal to unity . T_F, which depends also on n_w , can be easily calculated from Fresnel's equations in the case of a flat water-air interface, e.g. (C.D. Mobley 1994) chapter 4.2, and has a typical value of 0.975 for oceanic water. T_F/n_w^2 takes a typical value of 0.543 for ocaenic water (Austin and Halikas 1976). In the case of a wave-roughened interface, combination of the reciprocity condition between radiance reflectance and transmittance coefficients (Howard R. Gordon 2005) and the simulations of Figure 18 of (Preisendorfer and Mobley 1986), it is established (K. J. Voss and Flora 2017) that there is negligible (much less than 1%) difference for T_F between a flat interface and a wave-roughened interface for wind speeds up to 20 ms-1 (neglecting whitecaps and breaking waves). However for a more precise calculation of T_F/n_w^2 it is necessary to take account of salinity and temperature variations of the refractive index, n_w both for oceanic waters (K. J. Voss and Flora 2017) and for inland waters.

In addition to the time variation of illumination conditions due to time-varying solar zenith angle and diffuse atmospheric transmission (aerosols, clouds) which is accounted for in $E_d^{0+}(t_1)$ and $E_d^{0+}(t_2)$, it is necessary to account for the high frequency variation of underwater radiances $L_{un}(z_1)$ and $L_{un}(z_2)$ associated with waves at the air-water interface. Wave focusing and defocusing effects (J. R. Zaneveld, Boss, and Hwang 2001; D'Alimonte et al. 2010; Darecki, Stramski, and Sokólski 2011; M. Hieronymi and Macke 2012) and wave shadowing (Martin Hieronymi 2016) may have very fast time scales, less than 1s, and very short length scales, less than 1cm, giving a time-varying 3D light field. These effects are reduced by averaging for $L_{un}(z_1)$ and $L_{un}(z_2)$ over a large number of measurements and making the extrapolation to depth 0^- with the time-averaged values $\overline{L_{un}}(z_1)$ and $\overline{L_{un}}(z_2)$ or $\overline{L_{un}(z_1)}/\overline{E_d^{0+}(t_1)}$ and $\overline{L_{un}(z_2)}/\overline{E_d^{0+}(t_2)}$ (performing time-averaging on each parameter before taking the ratio), when taking account of possible time variation of illumination conditions. The probability density functions for $E_d^{0+}(t_1)$ and $L_{un}(z\ \ ,t)$ are skewed near the surface and approach normal distributions with depth (Gernez, Stramski, and Darecki 2011; M. Hieronymi and Macke 2012). For BOUSSOLE data, median averaging is used (David Antoine et al. 2008). For MOBY mean averaging is used, e.g. p21 of (Clark et al. 2003).

4.1.2 Protocol-dependent sources of uncertainty

In addition to the instrument-related sources of uncertainty which arise from imperfections in the radiometers themselves[10], as dealt with in FRM4SOC deliverable TR-2, the measurement of water reflectance by fixed depth underwater radiometry has a number of sources of uncertainty relating to the basic measurement equation and deployment conditions. These protocol-related sources of uncertainty are described here.

4.1.2.1 Non-exponential variation of upwelling radiance with depth

The essential assumption of exponential variation of $L_{un}(z)$ used to extrapolate measurements from two fixed depths to just beneath the sea surface is only an approximation of reality. Firstly, the water inherent optical properties themselves may vary with depth (Giuseppe Zibordi, Berthon, and D'Alimonte 2009), for example because of a vertical gradient in phytoplankton-related pigments or non-algae particles e.g., vertical variability related to thermal stratification including a "Deep Chlorophyll Maximum", resuspended or river plume particles in coastal waters, etc. Secondly, inelastic processes such as Raman scattering and/or fluorescence (Li, Stramski, and Reynolds 2016) may lead to departures from exponential variation of radiance. Thirdly, while for a homogeneous aquatic medium the attenuation with distance of a collimated beam of light can indeed be expected to be exponential the same does not hold for a diffuse light field. The angular distribution of upwelling light varies with depth, e.g. (Kenneth J. Voss 1988), and K_{Lu} depends on the angular distribution of light and so may be expected to vary slightly with depth even for a homogeneous water column and without inelastic scattering – see Figures 9.5 and 9.6 of (C.D. Mobley 1994).

If a more appropriate non-exponential functional form can be found to represent the vertical variation of radiance with depth, e.g. by characterising vertical variability from profile measurements or from radiative transfer modelling (D'Alimonte et al. 2013), it is possible to modify equation (9) to improve accuracy of the extrapolation, as suggested using Case 1 models in (David Antoine et al. 2008) Appendix A and (K. J. Voss et al. 2017).

The difficulties of non-exponential variation of upwelling radiance with depth become greater in waters or at wavelengths where the diffuse attenuation coefficient is high compared to the reciprocal of the measurement depths, e.g. in turbid waters and/or at red and near infrared wavelengths.

The uncertainty estimate associated with K_{Lu} can be validated by comparing K_{Lu} at different depths for systems where measurements are made at more than 2 depths (Brown et al. 2007), or by measuring K_{Lu} at high vertical resolution, e.g. from occasional shipborne campaigns.

4.1.2.2 Tilt effects

Non-verticality of instruments, e.g. caused by wave-tilting of floating structures, will give uncertainty in the measurements of both E_d^{0+} and $L_{un}(z)$ because of the anisotropic nature of the down- and up-welling light fields respectively. It is, therefore, necessary to measure the tilt

[10] The decomposition of measurements into "protocols" (deployment, data acquisition and processing methods) and "instruments" is adopted here in order to conveniently represent the wide diversity of possible combinations of methods and instruments in a synthetic and generic way. However, it is fully recognised that "protocol" and "instrument" are coupled and the assessment of the uncertainty of any specific measurement requires a combined analysis of the protocol and the instrument together. For example, the impact of thermal sensitivity of the instruments will depend on the ambient temperature range, which depends itself on location and depth of deployment.

of radiometers at high frequency using fast response inclinometers and perform appropriate filtering of non-vertical data and/or averaging of data to reduce tilt effects.

The impact of tilt on E_d^{0+} mesurements is discussed in section 3.1.2.1.

Tilt can also affect the effective underwater radiance measurement depths, z_i, which should therefore be measured continuously, e.g. using pressure sensors close to the optical sensors.

Obviously, minimisation of tilt can be a consideration in the design (D. Antoine et al. 2008) or in the location of validation measurement structures.

4.1.2.3 Self-shading from instruments and/or superstructure

The light field that is being measured is itself perturbed by the presence of solid objects such as the radiometers and the superstructure used to mount them. These perturbations are most pronounced when the water volume being measured (roughly defined by instrument field of view and diffuse attenuation coefficient, K_{Lu}) is in some way shadowed from direct sun, although shadowing of downwelling skylight and reflection of down/upwelling light also contribute to optical perturbations.

As regards the radiometers, self-shading can be minimised by using a sensor with fore-optics of small diameter compared to the mean free path of photons. This requirement becomes more challenging at longer wavelengths, such as in the near-infrared where water absorption coefficient is high. A partial correction for self-shading effects for a radiometer with idealised geometry was proposed by (Howard R. Gordon and Ding 1992) for a concentric sensor and tested experimentally by (G. Zibordi and Ferrari 1995).

As regards the superstructure, self-shading can be minimised by limiting the cross-section of the structure above the radiometers, e.g. by a subsurface buoy (D. Antoine et al. 2008) rather than surface buoy, and by increasing the distance between structure and radiometer, e.g. by the use of horizontal arms. The use of multiple redundant radiometers at the same depth but differently affected by superstructure and/or the measurement of superstructure azimuth and the identification/correction (J. L. Mueller 2004) of possible superstructure effects can also reduce superstructure shading uncertainty and/or be used to validate uncertainty estimates.

4.1.2.4 Bio-fouling

In addition to sensitivity changes inherent to the radiometer, modification of the transmissivity of the fore-optics can occur because of growth of algal films, particularly for long-term underwater deployments. Such bio-fouling can be mitigated: a) by the use of shutters and/or wipers (provided the latter do not themselves scratch optical surfaces), b) by use of copper surfaces and/or release of anti-fouling compounds close to the optical surface, e.g. p15 of (Clark et al. 2003), c) by limiting the duration of deployments between maintenance (David Antoine et al. 2008), d) by monitoring optical surfaces in some way, e.g. occasional diver-operated underwater calibration lamps, e.g. p15 of (Clark et al. 2003), e) regular diver cleaning of optics during the deployment.

In general, downward facing-sensors used to measure L_u are not particularly prone to bio-fouling [D. Antoine, Private Communication].

The accumulation of bubbles on the horizontal surface of the L_u fore-optics would also affect data.

Fouling of the above water upward-facing E_d^{0+} sensor is described in section 3.1.2.3.

The uncertainty estimate related to bio-fouling can be validated by comparing post-deployment calibrations before and after cleaning.

4.1.2.5 Depth measurement

The measurement equation implies that the depth of measurement is accurately known. For large and permanent structures such as MOBY and BOUSSOLE measurement of depth can be achieved quite precisely using pressure sensors and does not vary in time, except because of tilt and wave effects. If fixed depth measurements are used at shorter length scales, e.g. in shallow lakes or for measurement in high attenuation waters or wavelengths, depth measurements should be made sufficiently accurate so as to not contribute to overall measurement uncertainty.

4.1.2.6 Fresnel transmittance

The Fresnel transmittance, T_F, used to propagate upwelling nadir radiance across the water surface in (12), is often assumed to have a constant value of 0.543 in sea water, but does vary with wavelength, salinity and temperature via the index of refraction of water. Improvements on use of a constant value and uncertainties associated with T_F are discussed by (K. J. Voss and Flora 2017) – see also section 4.1.1

4.1.2.7 High frequency fluctuations

Measurements are averaged over a certain interval of time (see 4.1.1) to remove as far as possible the high frequency variations associated with wave focussing/defocussing effects. Simulations can be performed (Gernez, Stramski, and Darecki 2011; M. Hieronymi and Macke 2012)to assess the effectiveness of different averaging approaches/time intervals and any associated residual uncertainty.

If measurements from all sensors are not simultaneous the corresponding time corrections should be made and residual uncertainty estimated.

4.1.3 Variants on the fixed depth underwater radiometric method

Section 4.1 has been written primarily for MOBY/BOUSSOLE-style systems where instruments are deployed at fixed underwater depths attached to a structure fixed to the sea bottom in an approximately constant geographical location (notwithstanding possible small horizontal movements associated with currents). Variants on this method, which are based on the same essential Measurement Equation, are briefly discussed here.

While the MOBY/BOUSSOLE superstructures are designed with small optical cross-section to minimise optical perturbations, buoys/platforms designed for other purposes, e.g. hydrographic measurements or navigation-related structures, may also be used for underwater radiometric measurements. The essential Measurement Equation and checklist of elements to be included in the uncertainty budget remain the same, although measurement uncertainties associated with superstructure shading will need to be very carefully assessed and will generally be much more significant.

Fixed depth measurements may also be made from ships, e.g. when using instruments with too slow a response time for fast vertical profiling. The essential Measurement Equation and checklist of elements to be included in the uncertainty budget remain the same, although measurement uncertainties associated with ship shading/reflection will need to be very carefully assessed and will generally be much more significant unless the instruments are somehow deployed at a sufficient distance from the ship.

At the time of writing, there are no known cases of multiple fixed depth radiometric validation measurements being made from a horizontally moving platform. In general, such platforms (Claustre et al. 2011) (BioArgo, PROVAL, HARPOONS/Waveglider) can also move vertically and so use a measurement technique based on high vertical resolution profiling, as described in section 4.2.

The Tethered Attenuation Chain Colour Sensors (TACCS), e.g. documented by (Beltrán-Abaunza, Kratzer, and Brockmann 2014), is a variant on the fixed depth measurement, where a single underwater L_{un} measurement, made at 0.5m depth, is supplemented by a vertical chain of four downwelling irradiance sensors measuring $E_d(z)$ at multiple depths, in addition to the usual above water E_d^{0+}measurement. The diffuse attenuation coefficient, K_{Ed}, that is derived from these $E_d(z)$ measurements is then used as an approximation of the K_{Lu}, that is needed to extrapolate $L_{un}(-0.5m)$ to $L_{un}(0-)$. In the implementation described in (G. Zibordi, Ruddick, et al. 2012) the $E_d(z)$ measurements are made at a lower spectral resolution that the L_{un} measurements, and K_{Ed} must therefore be interpolated/extrapolated spectrally. In other respects this variant on the fixed depth underwater radiometry method has the same sources of uncertainty as listed in sections 4.1.2, except that further uncertainties must be assessed relating to the modelling of K_{Lu} from K_{Ed}, and the spectral interpolation/extrapolation of K_{Ed} in section 4.1.2.1.

The HYPERspectral Tethered Spectral Radiometer Buoy (Hyper-TSRB) makes a single measurement of spectral upwelling radiance at 65cm beneath the sea surface. The K_{Lu} required to extrapolate to the surface is thus not measured but is estimated using a model which takes the L_{un} spectrum as input.

4.2 Underwater radiometery – vertical profiles

Water-leaving radiance reflectance can also be validated using underwater radiometry based on vertical profiling – see Figure 4-3 and Figure 4-4. This method has frequently been used for supervised deployments from ships (Stanford B. Hooker and Maritorena 2000) and can also be made from fixed platforms (Giuseppe Zibordi, Berthon, and D'Alimonte 2009). Theoretically, vertical profiling from a fixed platform could also be automated and unsupervised, although in practice long-term deployments of instruments with moving underwater parts are vulnerable to mechanical failures. As an alternative unsupervised vertical profiles can be carried out from horizontally drifting platforms, as further described in section 4.2.3.

The first vertical profile radiometric measurements were generally made from winches attached to ships (Smith, Booth, and Star 1984). However, it is clearly important to avoid as far as possible optical (shadow/reflection) (K.J. Voss, Nolten, and Edwards 1986) as well as hydrographic perturbations (ship wake, ship hull and propellor-induced mixing, bow wave, etc.) from the ship. (J. L. Mueller 2003) p8 recommended making measurements from the stern of a ship with the sun's relative bearing aft of the beam at a minimum distance of $1.5/K_{Lu}$ from the ship or at greater minimum distance when deploying off the beam of a large vessel.

A popular method for getting instruments away from ship perturbations is to float instruments away a few tens of metres and then profile vertically using a specially-designed rocket-shaped „free-fall" platform (Waters, Smith, and Lewis 1990). More recently a new „kite" free-fall design allows slower profiling, closer to the water surface (S. B. Hooker, Morrow, and Matsuoka 2013).

In view of such improvements in deployment hardware that have become commercially available over the last 15 years **it is suggested that Fiducial Reference Measurements**

should not be made from shipborne winch deployments unless the measurement is supported by a careful uncertainty analysis covering all ship perturbations specific to the ship/deployment method/water type combination, including, for example, measurements made at different distances from the ship and/or 3D optical model studies.

Vertical profiles can also be made from fixed offshore structures, e.g. WISPER system on Aqua Alta Oceanographic Tower (AAOT) (Giuseppe Zibordi, Berthon, and D'Alimonte 2009). These structures have the advantage over shipborne winches of reduced tilt of instruments and reduced hydrodynamic pertubrations. However, it is again **suggested that underwater profiling Fiducial Reference Measurements should not be made from fixed offshore structures unless the measurement is supported by a careful uncertainty analysis covering optical perturbations (shadow/reflection) caused by the structure,** including, for example, measurements made at different distances from the platform (Giuseppe Zibordi, Doyle, and Hooker 1999) and/or 3D optical model studies (Doyle and Zibordi 2002).

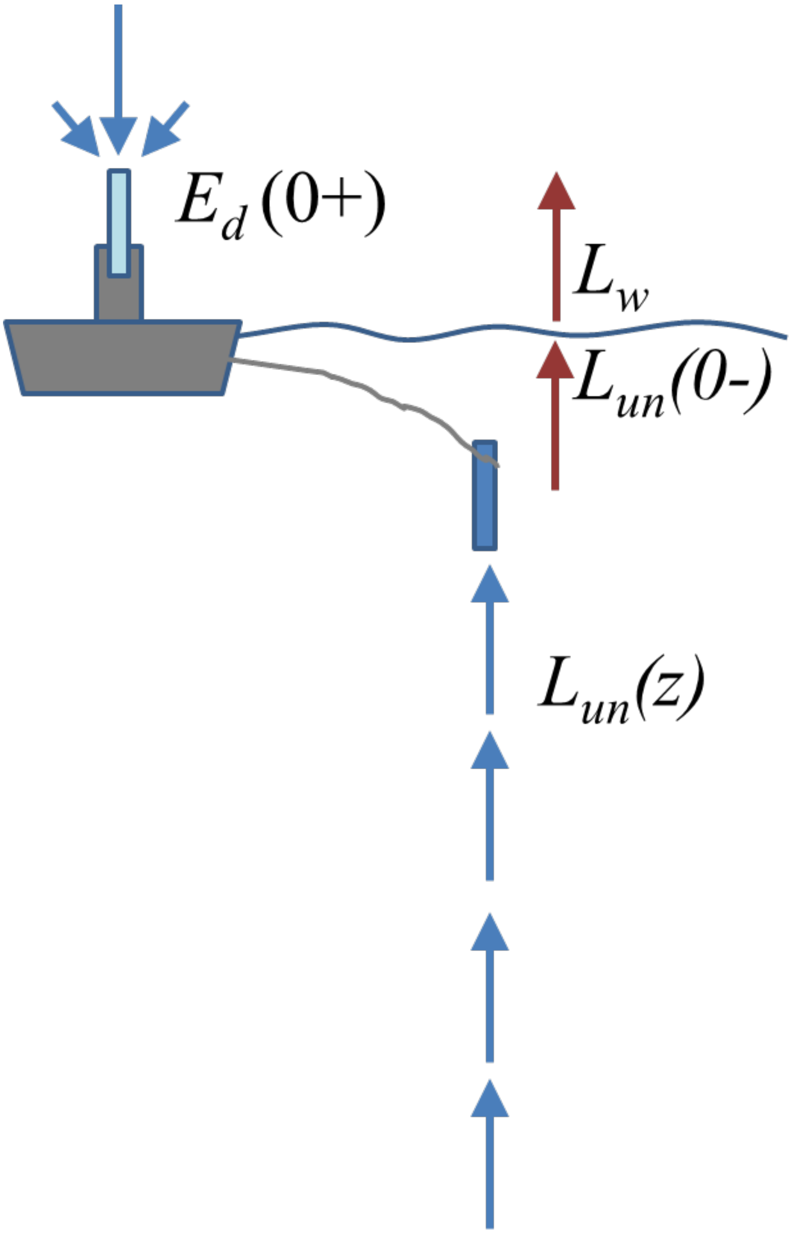

Figure 4-3 Schematic of underwater vertical profile measurements

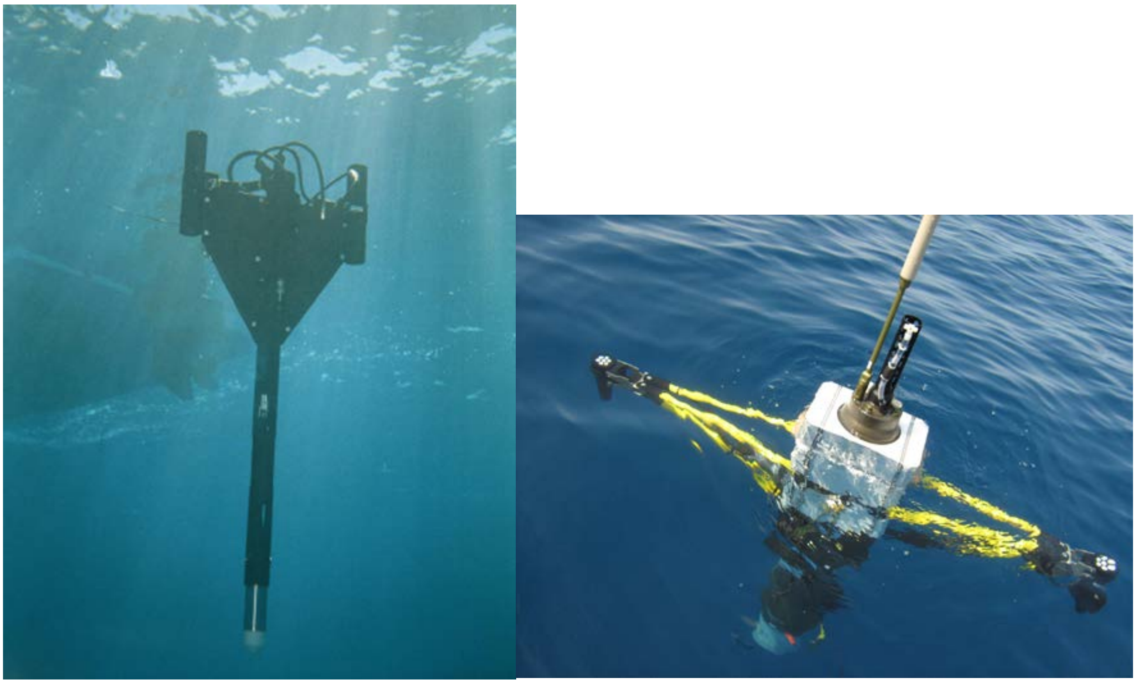

Figure 4-4 Typical deployments of underwater profiling radiometers (left) Ship-tethered free-fall profiler measuring upwelling radiance and downwelling radiance [Photo courtesy Satlantic]; (right) Freely-drifting vertically profiling radiometr platform [Photo courtesy: Laboratoire Océnographique de Villefranche].

4.2.1 Measurement equation

The fundamental Measurement Equation is similar to that used for fixed depth measurements, except that measurements are now available for a range of depths $z_1 \le z \le z_2$ for estimation of the vertical variation of $L_{un}(z)$.

By definition of K_{Lu}, the diffuse attenuation coefficient for L_{un},:

$$L_{un}(z, t_0) = L_{un}(0-, t_0)e^{-\int_0^z K_{Lu}(z\prime)dz\prime} \quad (13)$$

where z is positive underwater and increases with depth beneath the surface (but retaining the notation 0^- for radiance just beneath the water surface) and t_0 is the time to which measurements are referred. This gives, after natural logarithm transformation and reorganisation:

$$\ln[L_{un}(z, t_0)] = ln[L_{un}(0-, t_0)] - \int_0^z K_{Lu}(z')dz' \quad (14)$$

If it is assumed that K_{Lu} is constant with depth over the depth range of measurements and up to the water surface, then this simplifies to:

$$\ln[L_{un}(z, t_0)] = ln[L_{un}(0-, t_0)] - K_{Lu}z \quad (15)$$

$L_{un}(0-, t_0)$ is then obtained from vertical profile measurements as the exponential of the intercept of a linear regression of $\ln[L_{un}(z, t_0)]$ against z over a specified depth range.

Since measurements at different depths are made at slightly different times, t, the radiance measurements are first corrected for any variations in above water downwelling irradiance by:

$$L_{un}(z,t_0) = L_{un}(z,t)\frac{E_d^{0+}(t_0)}{E_d^{0+}(t)} \tag{16}$$

Finally the water-leaving radiance is obtained from $L_{un}(0-,t_0)$ by propagating the latter across the water-air interface as in equation (12).

A number of deployment and data processing factors influence the quality of $L_{un}(0-,t_0)$ derived from measurements of $L_{un}(z,t)$:

- Measurements should be made as close as possible to the air-water interface to minimise the uncertainties associated with extrapolation from depth, particularly if there are vertical gradients of inherent optical properties or for wavelengths/waters with high vertical attenuation. Very near-surface measurements are complicated by waves, which affect instrument tilt and vertical positioning as well as the radiance field itself (focussing/defocussing). To deal with this, new profiling platforms have been designed for very slow and stable sampling close to the surface, e.g. within 1cm (S. B. Hooker, Morrow, and Matsuoka 2013).
- Sufficient measurements are needed for each depth (interval) to ensure that wave focussing and defocussing effects can be removed, implying that profiling speed should be sufficiently slow, adding to the time required to make a cast, a practical consideration, and the possibility of temporal variation of illumination conditions, a data quality consideration.
- The vertical profiling speed should be matched to the acquisition rate of the instruments to ensure that the depth z of each measurement can be sufficiently accurately determined.
- According to (D. D'Alimonte, Zibordi, and Berthon 2001) the depth range $z_1 \le z \le z_2$ chosen for data processing is "the key element in extracting accurate subsurface data from in-water profiles". z_1 should be chosen suffcently large to avoid problems of near-surface tilt, wave focussing/defocussing and bubbles, but sufficiently small to limit uncertainties associated with extrapolation to the surface, particularly for high attenuation waters/wavelengths. Any depth interval with significant ship/superstructure shadowing must also be avoided. In practice, the choice of depth range is generally made subjectively (S.B. Hooker, Zibordi, and Maritorena 2001) because of the difficulty to automate such thinking.
- Different mathematical methods used to perform the regression analysis for (15) and different methods for filtering outliers (Maritorena and Hooker 2001) may give quite different results. Such considerations were analysed in detail in the Round Robin experiments documented by (S.B. Hooker, Zibordi, and Maritorena 2001).
- For measurements with significant temporal variability of $E_d^{0+}(t)$, some time filtering of $E_d^{0+}(t)$ may be needed before application of (16). For example, $E_d^{0+}(t_0)$ may be chosen as the median of $E_d^{0+}(t)$ over the measurement interval or, for ship-induced periodic variability, $E_d^{0+}(t)$ may be first linearly fitted as function of t.

For profiling systems where the upcast is made by applying tension to a wire, only downcast ("free-fall") data is used to avoid irregular motion and high tilt.

4.2.2 Protocol-dependent sources of uncertainty

In addition to the instrument-related sources of uncertainty which arise from imperfections in the radiometers themselves, as dealt with in FRM4SOC TR-2, the measurement of water reflectance by vertical profiling underwater radiometry has a number of sources of uncertainty relating to the basic measurement equation and deployment conditions. These protocol-related sources of uncertainty are described here for the case of a profiling system that is supposed to be fixed, or almost fixed, in horizontal space, e.g. tethered to a ship or an offshore platform. Additional considerations to account for significant horizontal movements, e.g. from glider platforms, are summarise in section 4.2.3.

4.2.2.1 Non-exponential variation of upwelling radiance with depth

The essential assumption of exponential variation of $L_{un}(z)$ from the measurement depth range $z_1 \leq z \leq z_2$ to just beneath the air-water interface is clearly an approximation of reality. This assumption will cause uncertainties in conditions of near-surface optical stratification, inelastic scattering (Raman, Fluorescence) and variability of the angular distribution of upwelling radiance, as already described in section 4.1.2.1 for fixed depth radiometry.

The uncertainty associated with non-exponential variation of $L_{un}(z)$ can be assessed for the measurement range $z_1 \leq z \leq z_2$ by considering the goodness-of-fit of (14), after suitable filtering of high frequency variability. For $0 \leq z \leq z_1$, between the measurement range and the surface, potential non-exponential variation of $L_{un}(z)$ can be assessed by model studies (D’Alimonte et al. 2013).

Clearly z_1 should be kept as small as possible, within constraints of deployment, tilt contamination and high frequency variability, particularly if there may be near-surface stratification of the water column.

4.2.2.2 Tilt effects

Non-verticality of instruments, e.g. caused by wave-tilting of free-fall platforms or ship winch-deployed frames, gives uncertainty in the measurements of $L_{un}(z,t)$ because of the anisotropic nature of upwelling light fields. It is, therefore, necessary to measure the tilt of radiometers at high frequency using fast response inclinometers and perform appropriate filtering of non-vertical data and/or averaging of data to reduce tilt effects (Maritorena and Hooker 2001).

The uncertainty associated with tilt effects can be estimated by reprocessing of oversampled vertical profile measurements with different thresholds for removal of non-vertical data and by 3D optical model simulations.

The impact of tilt on E_d^{0+} mesurements is discussed in section 3.1.2.1.

Obviously, minimisation of tilt should be a consideration in the design of deployment hardware. Vertical profiles carried out from fixed platforms suffer less from such tilt effects. The „rocket-shaped“ free fall platforms may suffer from high tilt, particularly in near-surface waters and high wave conditions. A new design of „kite-shaped“ profilers (Morrow et al. 2010) has significantly reduced tilt.

4.2.2.3 Self-shading from instruments and/or superstructure

The light field that is being measured is itself perturbed by the presence of solid objects such as the radiometers and the superstructure used to mount them, as discussed previously in section 4.1.2.3 for fixed depth underwater radiometry. For free-fall radiometer platforms, the considerations and corrections discussed in section 4.1.2.3 as regards self-shading from the instrument collector and from the mounting frame are relevant also for vertical profiling.

For ship- or fixed platform-deployed vertical profiling radiometers, superstructure shading/reflection effects may be considerable and should be carefully limited, by maximising horizontal distance from the structure. Uncertainties should be estimated, e.g. by radiative transfer modelling (Howard R. Gordon 1985; Doyle and Zibordi 2002) and/or by in situ measurements at different distances from the structure.

4.2.2.4 Bio-fouling

Supervised underwater radiometric measurements generally do not suffer from bio-fouling provided that fore-optics are kept clean between deployments.

Fouling of the above water upward-facing E_d^{0+} sensor is described in section 3.1.2.3.

Unsupervised fixed location vertical profiling measurements are rare but would suffer from similar problems to those described in section 4.1.2.4 for fixed depth measurments.

Horizontally drifting vertical profiling systems (section 4.2.3) may arrange to spend most time at great depth to minimise bio-fouling (Claustre et al. 2011). Bio-fouling uncertainties can be assessed by comparing pre- and post-deployment calibrations, although recovery of horizontally drifting systems is not always possible.

4.2.2.5 Depth measurement

The measurement equation implies that the depth of measurement is precisely known by a fast response and appropriately calibrated[11] pressure sensor located close to the optical sensor. Any permanent vertical shift between depth sensor and optical sensor must be corrected and any tilt-induced vertical difference between depth and optical mesurments must be included in the uncertainty estimate. Accurate measurement of depth and associated uncertainties, including referencing to surface atmospheric pressure at the moment of profiling (pressure „taring“) and temperature-sensitivity of pressure transducers, are discussed in section 5.2. of (S. B. Hooker, Morrow, and Matsuoka 2013).

4.2.2.6 Fresnel transmittance

As 4.1.2.6.

4.2.2.7 High frequency fluctuations

The removal of high frequency fluctuations in $L_{un}(z,t)$, e.g. from wave focussing/defocussing and from variation in illumination conditions, $E_d^{0+}(t)$, is complicated for vertical profile measurements because both the light field and the measurement depth, z, vary with t, and because both $L_{un}(z,t)$ and $E_d^{0+}(t)$ measurements may be affected by both natural variability (wave effects, cloud/haze effects, water variability) and by deployment-related variability (e.g. tilt).

If all other factors (above water illumination, water optical properties) are assumed invariant in time during the measurements, or suitably corrected, and $L_{un}(z,t)$ is assumed tilt-free after filtering, then natural variability caused by wave effects (J. R. V. Zaneveld, Boss, and Barnard

[11] Calibration is not limited to an absolute factory calibration, but includes also referencing to surface atmospheric pressure during deployments – see section 5.2 of (S. B. Hooker, Morrow, and Matsuoka 2013).

2001) can be minimised by performing sufficient measurements to allow adequate averaging. This can be achieved by slow profiling (Giuseppe Zibordi, D'Alimonte, and Berthon 2004; S. B. Hooker, Morrow, and Matsuoka 2013) or, if this is not possible, by multicasting (D. D'Alimonte, Zibordi, and Berthon 2001).

The uncertainty associated with all sources of high frequency fluctuations must be estimated, e.g. by testing alternative data processing options on oversampled measurements and by 4D optical simulations (D'Alimonte et al. 2013). Uncertainty estimates should be validated, e.g. by measurement intercomparison exercises, (G. Zibordi, Ruddick, et al. 2012).

4.2.3 Variants on the vertical profiling underwater radiometric method

Following on from the success of the Argo float network designed for physical oceaonography, a number of horizontally-drifting vertical-profiling instrument platforms have been designed for long-term unsupervised measurement of optical properties (Claustre et al. 2011; Gerbi et al. 2016). Such floats, when suitably networked, allow for much better spatial coverage of the oceans (but not shallow seas or inland waters). Typically the instrument will park at great depth during most of the day and night (to reduce bio-fouling) and perform one or more vertical profiles per day, potentially timed to match the acquisiton times of specific ocean colour sensors.

The essential Measurement Equation and sources of uncertainty for such measurements are the same as for other vertically profiling instruments. As for all unsupervised measurements, biofouling, particularly for the E_d^{0+} measurement, may be a significant source of uncertainty, especially if the instrument cannot be recovered for post-deployment calibration. On the other hand, the possibility of diving deep limits exposure to biofouling.

In contrast to vertical profile measurements made from ships or fixed offshore structures, drifting floats generally do not have a permanent above water instrument for $E_d^{0+}(t)$ and so there will be an additional uncertainty associated with possible time variation of illumination conditions during the vertical profile.

4.3 Above water radiometry with sky radiance measurement and skyglint removal

4.3.1 Measurement equation

In above water radiometry one or two radiometers are deployed above water from a ship or fixed structure to measure a) upwelling radiance, $L_u(0^+, \theta_v, \Delta\varphi)$, at a suitable zenith angle, θ_v, and azimuth angle relative to sun, $\Delta\varphi$, and b) downward (sky) radiance, $L_d(0^+, -\theta_v, \Delta\varphi)$, in the direction which reflects at the air-water interface into the water-viewing direction.

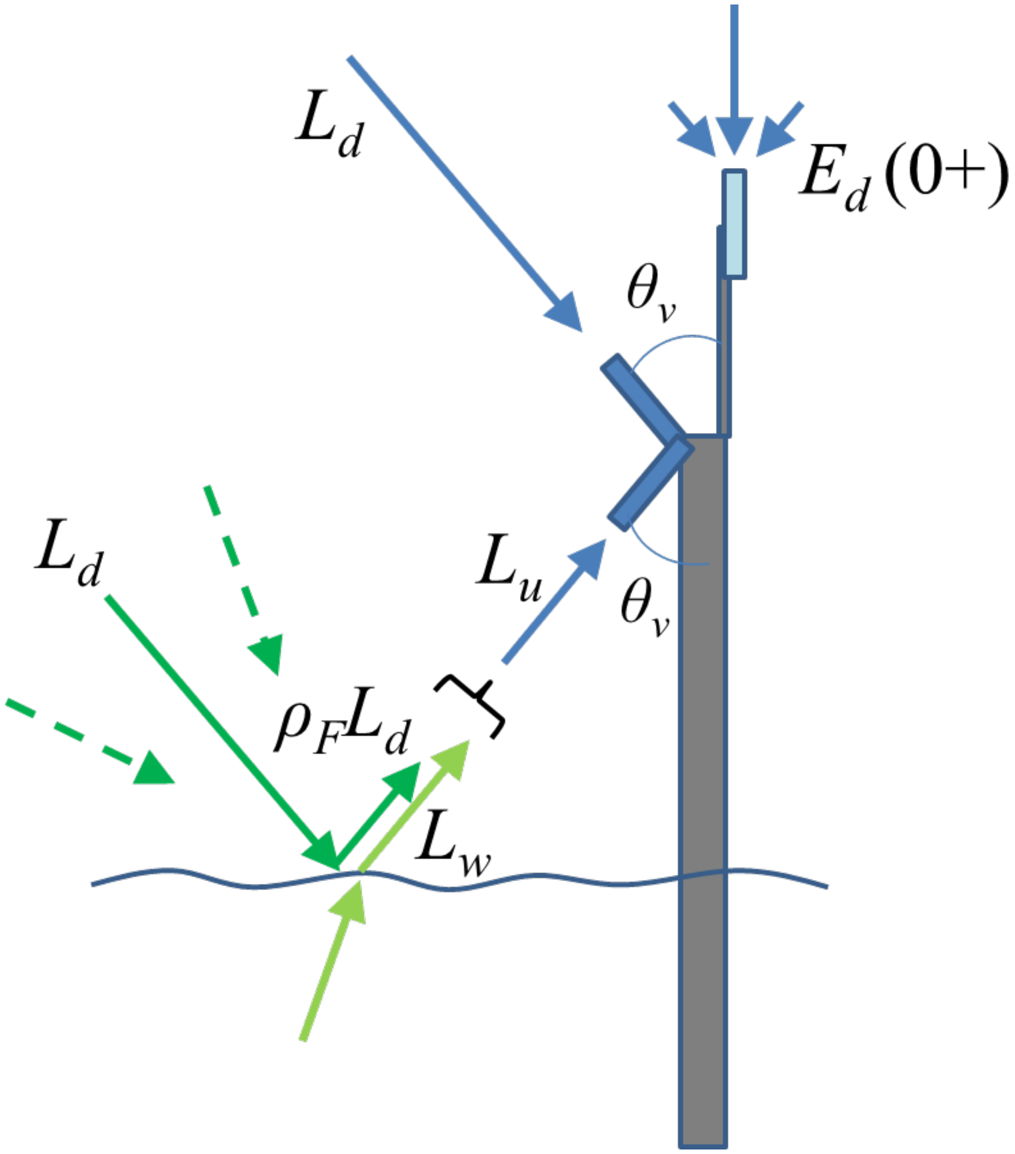

Figure 4-5 Schematic of above water radiometry with sky radiance measurement and skyglint removal. Dashed arrows indicate that contributions to the skylight reflected at the air-water interface come from directions that are not directly measured by the L_d radiance sensor, including possible contributions from the direct sunglint direction.

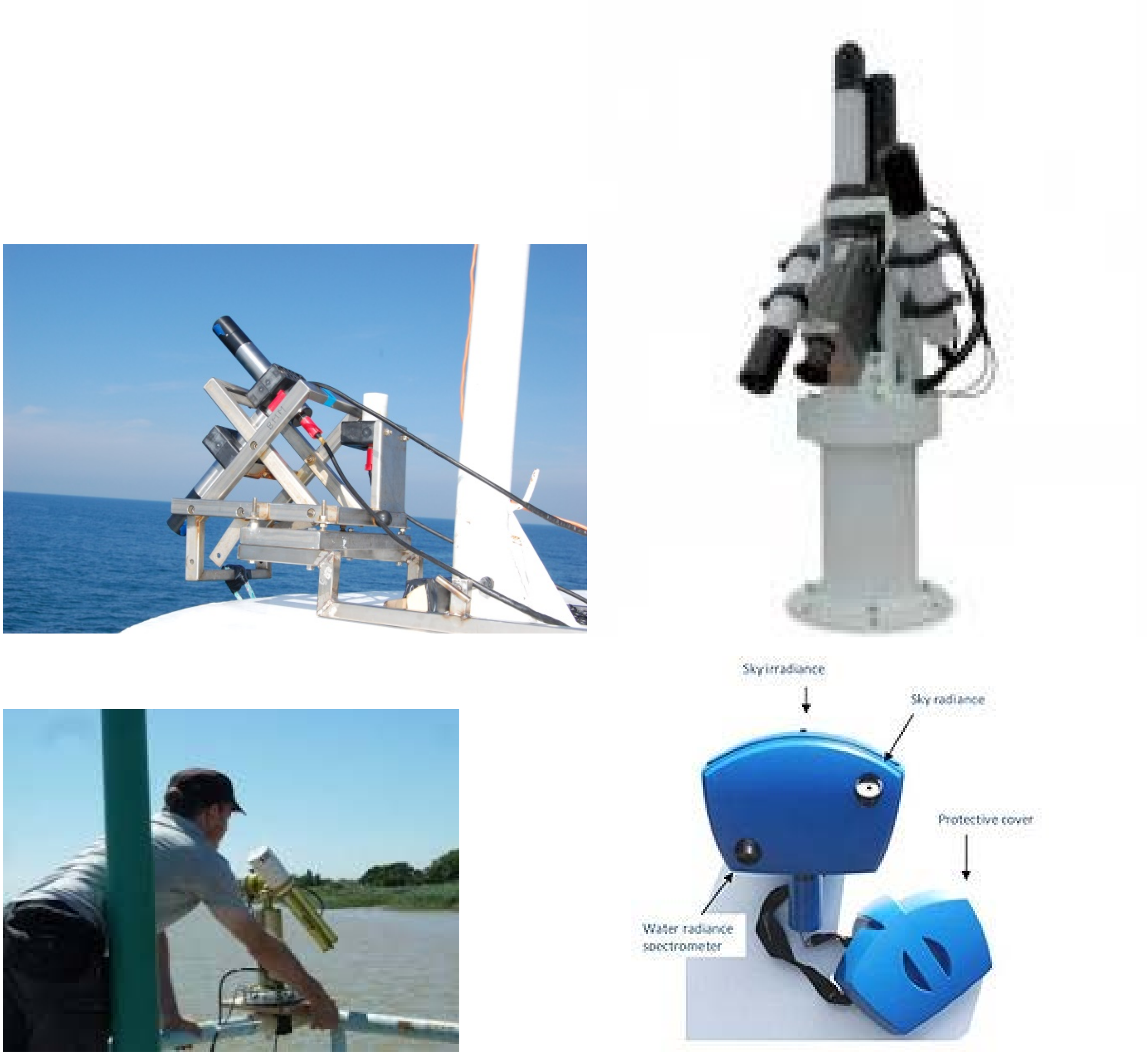

Figure 4-6 Typical deployments of above water radiometry systems: (top-left) TRIOS/RAMSES; (top-right) Satlantic Suntracker system with rotating mount; (middle-left) CIMEL SeaPRISM system with robotic pointing (bottom right) WISP 3-radiometer handheld system.

Then the water-leaving radiance in the water-viewing direction is estimated from the Measurement Equation:

$$L_w(\theta_v, \Delta\varphi) = L_u^{0+}(0^+, \theta_v, \Delta\varphi) - \rho_F L_d(0^+, -\theta_v, \Delta\varphi) \quad (17)$$

where ρ_F is a coefficient that represents the fraction of incident skylight that is reflected back towards the water-viewing sensor at the air-water interface.

The second term of this Measurement Equation, which is the basis of this protocol, is adopted as a pragmatic way of estimating and removing the upwelling radiance that originates from reflection at the air-water interface. However, it is well understood that such radiance may originate from portions of the sky dome other than the portion that is actually measured, as defined by $(-\theta_v, \Delta\varphi)$ and the field of view of the L_d instrument, and may include reflection of direct sun glint – see Figures 1 and 2 of (C.D. Mobley 1999) and equation (1) of (Z. Lee et al. 2010). This is discussed further in section 4.3.2.1.

In the case of a flat water surface with only specular reflection processes (i.e. no whitecaps or other diffuse reflection processes) and with unpolarised downwelling light, and for an infinitesimally small sensor field of view, ρ_F is simply given by the Fresnel reflectance equation:

$$\rho_F(\theta_v) = \frac{1}{2}\left\{\left[\frac{sin(\theta_v - \theta_t)}{sin(\theta_v + \theta_t)}\right]^2 + \left[\frac{tan(\theta_v - \theta_t)}{tan(\theta_v + \theta_t)}\right]^2\right\} \tag{18}$$

where θ_v is the viewing zenith angle ("above water incidence angle") and θ_t is the zenith angle of light transmitted to below water after refraction:

$$\theta_t = sin^{-1}(sin\theta_v / n_w) \tag{19}$$

where n_w is the index of refraction of water with respect to air and is often approximated by the value 1.34 but does also vary with salinity, temperature and wavelength (C.D. Mobley 1994).

For zenith viewing, $\theta_v = 0$, and equation (18) is replaced by:

$$\rho_F(0) = \left(\frac{n_w - 1}{n_w + 1}\right)^2 \tag{20}$$

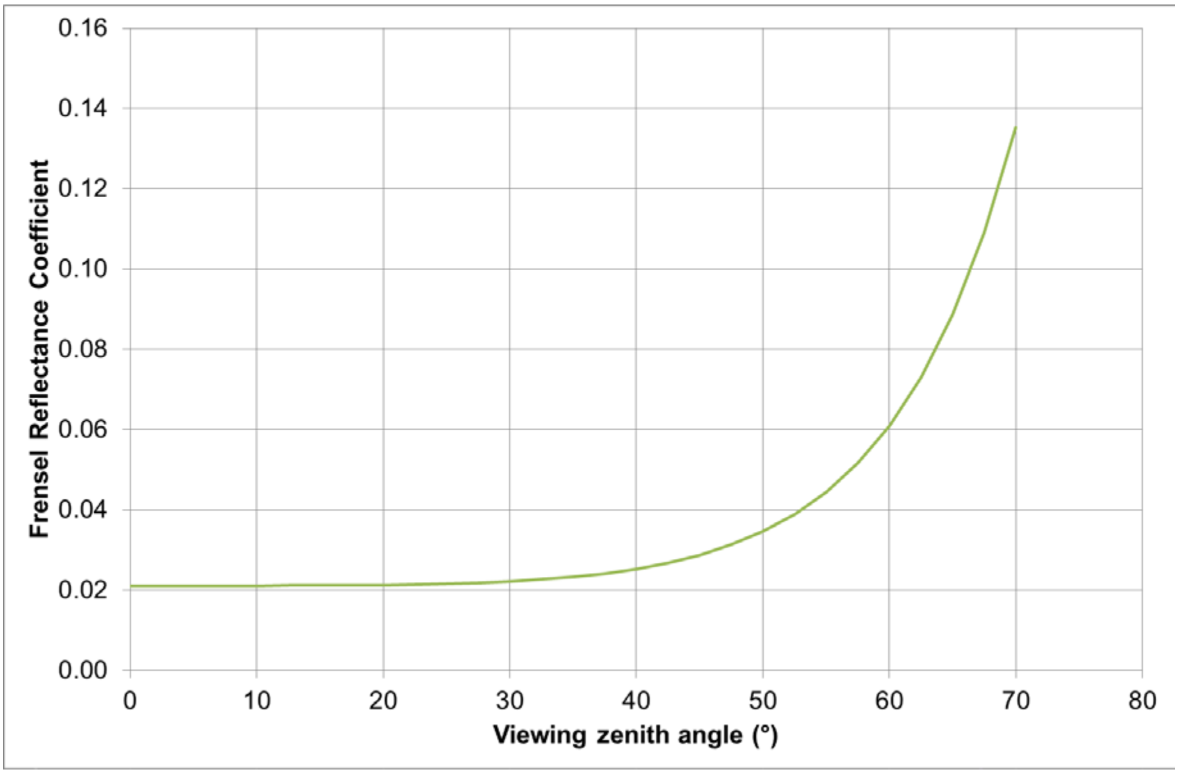

Figure 4-7 Fresnel reflectance coefficient, ρ_F, for a flat air-water interface with refractive index n_w=1.34 for light incident on the interface from air, e.g. skylight reflection.

In reality:

- the water surface is not flat but is a wavy surface (Preisendorfer and Mobley 1986) implying that a) the portion of sky reflected into the water-viewing direction may come from a zenith/azimuth angle different from that measured via $L_d(0^+, -\theta_v, \Delta\varphi)$ (C.D. Mobley 1999), and that b) the incidence angle required for calculation of the Fresnel coefficient is different from θ_v, with spatial variation of the incidence angle within the sensor field of view that increases with wave inclination.
- the downwelling light is not unpolarised, but, particularly for the molecularly scattered "Rayleigh" component at 90° scattering angle from sun, may be strongly polarised (Santer et al. 2012).
- some radiometers have field of view which can be quite significant, e.g. >10°, meaning that the measurements $L_u^{0+}(0^+, \theta_v, \Delta\varphi)$ and $L_d(0^+, -\theta_v, \Delta\varphi)$ are weighted averages over a range of viewing angles $(\theta_v, \Delta\varphi)$ and the model for ρ_F may need to account for different incidence angles even for a flat water surface.

These considerations are dealt with in detail in the following sections and their references.

As regards the classification of methods for measuring L_w, it is suggested here, and in the discussion of section 2.9, to drop the Method1/2/3 above water radiometry classification used in the NASA Ocean Optics 2003 protocols (J.L. Mueller et al. 2003) mainly for the E_d^{0+} measurement and instead classify the L_w measurement according to viewing geometry:

- Zenith viewing angle, e.g. nadir or $\theta_v = 30°$ or $\theta_v = 40°$ or "other".
- Relative azimuth angle to sun for off-nadir measurements, e.g. $\Delta\varphi = 90°$ or . $\Delta\varphi = 135°$ or "other".

and

- The method used to estimate skylight reflected at the air-water interface.

In general nadir-viewing is avoided because of the high uncertainties associated with skyglint removal in geometries close to sunglint (C.D. Mobley 1999) and because of difficulties in avoiding optical pertubation from the ship/platform. However, there may be situations where nadir-viewing can be acceptable (e.g. mirror-flat lakes, sensors deployed well above water surface from an optically small structure, high sun zenith angle) provided that uncertainties are careful assessed and validated.

The measurement of polarized upwelling radiance is considered as a variant of the above water L_w method.

In view of the quite different measurement uncertainties the Skylight Blocked Approach (SBA) approach (Z. Lee et al. 2010, 2013) is treated in the separate section 4.4.

4.3.1.1 Temporal processing of radiance measurements

Measurement of both sky radiance and water radiance involves time integration for each individual measurement and replicate measurements which are subsequently processed to yield a single value for $\overline{L_u^{0+}}(0^+, \theta_v, \Delta\varphi)$ and $\overline{L_d}(0^+, -\theta_v, \Delta\varphi)$ where the overbar denotes the multitemporal measurement, typically called "time-average", although the temporal precessing may be different from a mean average and will generally involve prior outlier removal or time series based quality control.

The integration time depends on the instrument concept and the brightness of the target – see also FRM4SOC Technical Report TR-2 on "A Review of Commonly used Fiducial Reference

Measurement (FRM) Ocean Colour Radiometers (OCR)". Filter-wheel radiometers generally measure fast, typically at many Hz, whereas spectrometer based systems may be fast, e.g. 8-32ms, for bright targets such as the sky, but much slower, e.g. integration time of 1-4s, for darker targets such as water.

For the sky radiance measurement, $\overline{L_d}(0^+, -\theta_v, \Delta\varphi)$, a small number of replicate measurements should be sufficient. If the sky conditions are good (clear blue sky) then 3-5 replicates should be sufficient to establish this and provide a mean average and standard deviation for this parameter. If the sky conditions are not good (e.g. scattered clouds and/or partially obscured sun) then this will also be immediately apparent from a low, e.g. 3-5, number of replicates either in the standard deviation or in the magnitude of $\overline{L_d}/E_d^{0+}$, which will be much higher than that of an ideal sky model, see Web Appendix 1 of (KG Ruddick et al. 2006).

For the water radiance measurement, $\overline{L_u^{0+}}(0^+, \theta_v, \Delta\varphi)$, a much larger number of replicate measurements is needed because of the rapid and large temporal variations associated with surface gravity waves. These variations include the darkening/brightening effect of large surface gravity waves oriented towards/away from the sensor (because of air-water interface reflectance differences and/or reflection of brighter/darker portions of the sky) as well as the very bright, small and fast sunglint "flashes" from specular reflectance of direct sun at suitably oriented capillary wave facets, particularly when viewing at low $\theta_v - \theta_0$, low $\Delta\varphi$ and for high wave amplitudes. The temporal processing of $L_u^{0+}(0^+, \theta_v, \Delta\varphi)$ measurements should also depend on the integration time of each measurement and may be linked to the method for estimation of ρ_F. For example, (Stanford B. Hooker et al. 2002) proposed a temporal processing method for a rapidly sampling, small field of view radiometer that retains the minimal values of $L_u^{0+}(0^+, \theta_v, \Delta\varphi)$ over a number of replicates and uses a flat sea model for ρ_F using the principle that sunglint flashes and brighter waves can be resolved and eliminated by the minimum filter. On the contrary (C.D. Mobley 1999) analyses the case effectively for a slowly sampling radiometer where the contributions of different wave facets cannot be isolated but are effectively averaged in time (and possibly space, depending on the field of view and distance from the water surface) for each individual $L_u^{0+}(0^+, \theta_v, \Delta\varphi)$ measurement. In the latter case a much higher value of ρ_F is required than that of the flat water surface model of equation (18).

4.3.2 Protocol-dependent sources of uncertainty

In addition to the instrument-related sources of uncertainty which arise from imperfections in the radiometers themselves, as dealt with in FRM4SOC TR-2, the measurement of water-leaving radiance by above water radiometry has a number of sources of uncertainty relating to the basic measurement equation and deployment conditions. These protocol-related sources of uncertainty are described here.

4.3.2.1 Estimation of reflected skylight

The most critical aspect of above water measurements of L_w lies in the removal of skylight reflected at the air-sea interface, represented by the coefficient ρ_F in equation (17) and called the "Fresnel reflectance coefficient" in the case of a flat surface. For waters or wavelengths where water reflectance, $\pi L_w/E_d^{0+}$ is low, the right hand side of (17) can be the difference of two values which are much larger than the left hand side. For example, in clear waters in the near infrared, L_w may be negligibly small whereas $L_u^{0+}(0^+, \theta_v, \Delta\varphi)$ and $\rho_F L_d(0^+, -\theta_v, \Delta\varphi)$ are not. Any uncertainty in ρ_F is then greatly amplified when taking the difference. It is important to note that the uncertainty on $\rho_F L_d(0^+, -\theta_v, \Delta\varphi)$ is an absolute uncertainty for L_w (KG

Ruddick et al. 2006) that is unrelated to the value of L_w itself and so becomes more important in relative terms as L_w decreases . This is in contrast to most radiometric uncertainties (calibration, E_d^{0+} cosine response, radiometer thermal sensitivity, etc.) which are relative uncertainties that can be expressed as a % of the desired parameter, L_w or R_{rs}.

In view of the importance of estimating ρ_F or the product $\rho_F L_d(0^+,-\theta_v,\Delta\varphi)$ there is quite some diversity of approaches. In the crudest approach, ρ_F is simply taken from the flat sea equation (18) and therefore generates large uncertainties which may be strongly positively biased for L_w. For waters with low red or near infrared reflectance, a further "residual" correction may be applied (Morel 1980), assuming that $L_w = 0$ for a suitable wavelength, λ_0 , and that $\rho_F L_d(0^+,-\theta_v,\Delta\varphi)$ has spectral variation given by $L_d(0^+,-\theta_v,\Delta\varphi)$.

Such an approach may also be used in ultraviolet wavelengths in highly absorbing waters (Kutser et al. 2013) or could conceivably be used at both ultraviolet and near infrared wavelengths to provide two fixed points at each extreme of the spectrum for a full spectrum construction of $\rho_F L_d(0^+,-\theta_v,\Delta\varphi)$.

For brighter waters such a wavelength λ_0 with negligible L_w may not exist and, in an approach analagous to turbid water aerosol correction algorithms, (Gould, Arnone, and Sydor 2001) proposes a suitable "turbid water" residual correction based on measurements at 715nm and 735 nm. This approach was generalised by (K. Ruddick, Cauwer, and Van Mol 2005) for any pair of near infrared wavelength, but was there suggested for use in qualiy control/uncertainty estimation rather than data correction.

(C.D. Mobley 1999) carried out scalar radiative transfer simulations to establish ρ_F as function of sun and viewing geometry $(\theta_0,\theta_v,\Delta\varphi)$ and wind speed at a height of 10m[12] above the water, W, assuming a Cox-Munk relationship (Cox and Munk 1954) between surface wave field and wind speed. In the case of fetch-limited inland waters W will typically be set to zero or a small value, since the Cox-Munk relationship will not apply. Similarly in overcast conditions (not very relevant for satellite validation) the dependance on surface wave field and/or W is also less strong and (C.D. Mobley 1999) proposes a constant value of $\rho_F = 0.028$.

(Z. Lee et al. 2010) notes that, since contributions to $\rho_F L_d(0^+,-\theta_v,\Delta\varphi)$ arise from different portions of the sky (including direct sun) when the surface is not perfectly flat, these will have different spectral shapes from the $L_d(0^+,-\theta_v,\Delta\varphi)$ that is measured. This effect is not accounted for in the simulatons of (C.D. Mobley 1999) where the model assumes the same colour of the sky in all directions.

(Harmel et al. 2012) pointed out that ρ_F is, in reality, significantly lower than in the (C.D. Mobley 1999) simulations because the downward radiance is not unpolarised. This effect is particularly strong when viewing near the Brewster angle of about 53°. The simulations of (Curtis D. Mobley 2015) and (Davide D'Alimonte and Kajiyama 2016) take account of such polarisation effects. The simulations of (Foster and Gilerson 2016) take account of polarisation effects and the impact of aerosols, showing the further dependency of ρ_F on aerosol optical thickness. The simulations of (Martin Hieronymi 2016) take account of polarisation effects and also demonstrate that quite different mean surface slopes and hence quite different surface reflectance factors can arise from a single wind speed.

---

[12] The height at wind speed is measured for use of these models is unclear. (Cox and Munk 1954) measure wind at 12.5m. Some references mention 10m.

(Zhang et al. 2017) model separately the sunglint and skyglint components of light reflected at the air-water interface, taking account of polarisation. In their formulation, the reflected light is still modelled as a multiple of the measured incident skylight in the sky-viewing direction, $L_d(0^+, -\theta_v, \Delta\varphi)$, but the air-water interface reflection coefficient, ρ_F, is split into two reflection coefficients, $\rho_{sun}(\lambda)$, and $\rho_{sky}(\lambda)$ representing respectively the sunglint and skyglint contributions. Although these coefficients are considered as "spectrally varying" in that paper it is noted that this "spectral variation" is a model to correct for the fact that the $L_d(0^+, -\theta_v, \Delta\varphi)$ measurement is not representative of the spectral variation of sky radiances from all portions of sky (including direct sun) that are reflected towards the water-viewing sensor. The true spectral variation of the flat sea Fresnel coefficient, because of salinity and temperature related variation of the refractive index of water, is less significant (but also accounted for in that paper).

In a way that is analgous with the development of full spectrum coupled ocean-atmosphere modelling in atmospheric correction algorithms, more complex schemes have been proposed for taking account of the expected spectral shapes of L_w and $\rho_F L_d(0^+, -\theta_v, \Delta\varphi)$. e.g. (Groetsch et al. 2017).

For hyperspectral measurements (Simis and Olsson 2013) proposes to use the fact that ρ_w can be expected to be spectrally quite smooth whereas both $L_u^{0+}(0^+, \theta_v, \Delta\varphi)$ and $\rho_F L_d(0^+, -\theta_v, \Delta\varphi)$ are affected by atmospheric absorption features. Thus ρ_F can be constrained or estimated as the value which will yield a spectrally smooth ρ_w.

In view of the wide diversity of approaches for estimation of ρ_F and continued research into methodological improvements, the present document does not intend to prescribe a single protocol for estimating ρ_F or $L_d(0^+, -\theta_v, \Delta\varphi)$ in FRM measurements. In fact, for most data acquisition protocols, different methods for estimating ρ_F or $L_d(0^+, -\theta_v, \Delta\varphi)$ can be applied in post-processing and could be applied to historical data. Rather **the approach of the current document is merely to insist that the uncertainties of any approach be thoroughly estimated and validated**.

One method for estimation of uncertainties associated with $\rho_F L_d(0^+, -\theta_v, \Delta\varphi)$ removal is to consider the spectral consistency of $R_{rs}(\theta_v, \Delta\varphi)$ in the near infrared. For clear waters and at sufficiently long wavelength R_{rs} can be assumed zero and any offset in measurements can be used as an estimator of total measurement uncertainty, provided this information has not already been used to perform a "residual correction" of data – this approach was suggested by (S.B. Hooker and Morel 2003), although in their study the uncertainty was expected to come more from ship perturbations (section 4.3.2.3) than from $\rho_F L_d(0^+, -\theta_v, \Delta\varphi)$ removal. The approach was extended by (K. Ruddick, Cauwer, and Van Mol 2005) for moderately turbid waters, where R_{rs} is non-zero but adopts a spectral shape determined primarily by the pure water absorption coefficient (KG Ruddick et al. 2006).

4.3.2.2 Tilt and roll effects

The uncertainty in the pointing angle of instruments used for measuring both $L_u^{0+}(0^+, \theta_v, \Delta\varphi)$ and $L_d(0^+, -\theta_v, \Delta\varphi)$ must be propagated through to give an uncertainty for $L_w(\theta_v, \Delta\varphi)$.

When operating from ships inaccuracies in pointing angle may arise from a) the initial setup and levelling of instruments for the "at rest" balancing of the ship, and any resetting that is required during a campaign, e.g. because of changes in ship balance (ballasting, fuel and water tanks, deployment of equipment overboard by crane, etc.) and; b) high frequency pitch and roll, which may easily reach 10° or more in heavy sea states or for small ships. Above water radiometry from most fixed platforms is not significantly affected by wave- or wind-induced tilt and angular accuracy of <1° is easily achieved.

The impact of tilt and roll can be estimated and reduced by: a) measuring the inclination of the radiometers or the mounting platform/ship with a fast response well-calibrated inclinometer and removing all data where tilt exceeds a user-defined threshold; b) calculating the mean average and standard deviation of a time series of replicate measurements.

For the $L_u^{0+}(0^+, \theta_v, \Delta\varphi)$ measurement, tilt and roll, particularly any low frequency or setup angle error, will affect the effective angle of data $L_w(\theta_v, \Delta\varphi)$ and hence any bidirectional corrections that may subsequently be applied to reproject data to nadir-viewing or to the satellite-viewing geometry. However, the related uncertainties will generally be low provided that data are sufficiently tilt-thresholded before processing. Tilt and roll will also affect the effective incidence angle for calculation of (wave-modulated) Fresnel reflectance, particularly for high wave conditions and when viewing at high zenith angle such as >40°.

For the $L_d(0^+, -\theta_v, \Delta\varphi)$ measurement, tilt and roll will result in a different portion of the sky being measured from the sky that is effectively reflected by the air-water interface into the water-viewing sensor.

4.3.2.3 Self-shading from instruments and/or superstructure

Measurements from ship- and platform-mounted water-viewing radiometers may be contaminated by optical perturbations from the ship/platform. These perturbations are most pronounced when the water volume being measured (roughly defined by instrument field of view projected onto the water surface and downwards into the water column with length scale given by the diffuse attenuation coefficients, K_{Lu} and/or K_{Ed}) is in some way shadowed from direct sun, although shadowing of downwelling skylight and reflection of downwelling light also contribute to optical perturbations.

For the above water optical perturbations to E_d, one can imagine operating a fish eye camera pointing vertically upwards from the water surface at the centre of the instrument field of view (see Figure 3-3 and Figure 3-4 except that in the context of the measurement the location for such photos is the water surface target). Anything in the hemispherical picture that is not the sun/sky represents an optical perturbation, e.g. blue sky replaced by part of the ship. This effect is most important for objects close to zenith because of their greater contribution to E_d and for objects which occupy a large solid angle of the sky.

The ship/platform may also throw a shadow (or reflections) that affect the underwater light field and hence $L_w(\theta_v, \Delta\varphi)$, particularly in clear waters and/or for wavelengths with low diffuse attenuation coefficient.

Optical perturbations from the ship/platform are generally reduced in the system design by:

1. Mounting the water-viewing radiometer as high as possible, e.g. on a telescopic mast (Hlaing et al. 2010; S.B. Hooker 2010).

2. Choosing the radiometer mounting position to limit optical pertubations, e.g. at the prow of a ship, facing forward (S.B. Hooker and Lazin 2000; KG Ruddick et al. 2006) or at a corner of a fixed offshore platform (G. Zibordi et al. 2002).

3. Viewing at a moderate zenth angle, because low zenith angle viewing generally implies that the ship/platform will be closer to the water target and will occupy a larger solid angle of the

sky as seen from the water surface (but too large zenith angle will increase uncertainties associated with Fresnel reflectance calculation)

4. Considering the viewing azimuth angle as a compromise between avoiding sunglint (need high $\Delta\varphi$ – see section 4.3.2.1) and avoiding direct shadow (need not too high $\Delta\varphi$).

Optical pertubrations caused by the radiometers themselves are generally not a problem unless the instruments are operated very close to the water surface, e.g. within 1m.

Uncertainties associated with optical perturbations can be assessed by 3D optical simulations (Doyle and Zibordi 2002), by making measurements at different distances from the ship/platform and/or by very high resolution satellite/aircraft/drone measurements.

4.3.2.4 Bio-fouling and other fore-optics contamination

In addition to sensitivity changes inherent to the radiometer, modification of the transmissivity of the fore-optics can occur because of deposition of atmospheric particles and/or water (rain, salty sea spray) and/or bio-fouling from animals (spiders, insects, birds, etc.) on the fore-optics or associated collimator tubes.

Such contamination can be easily avoided by regular checking and cleaning of the fore-optics in supervised deployments, but may be problematic for long-term unsupervised deployments, particularly for the upward facing $L_u^{0+}(0^+, \theta_v, \Delta\varphi)$ sensor. Sea spray can leave a salty deposit on fore-optics and can be reduced by mounting sensors sufficiently high above the sea surface.

For long-term unsupervised deployments fore-optics contamination can be significantly reduced by parking the radiometer facing downwards (e.g. CIMEL/Seaprism instrument) when not measuring and during periods of rain, as detected by a humidity sensor.

The uncertainty estimate related to bio-fouling and other foreoptics contamination can be validated by comparing post-deployment calibrations before and after cleaning.

4.3.2.5 High frequency fluctuations

Measurements are averaged over a certain interval of time (see 4.1.1) to remove as far as possible the high frequency variations associated with surface gravity waves – see section 4.3.2.1. Variations in illumination conditions, e.g. clouds/haze passing near the sun, or in cloudiness of the portion of sky which reflects into the water-viewing sensor, can be detected in time series of replicates and the associated data can be rejected if a user-defined threshold of variation is reached.

Uncertainties associated with any high frequency fluctuations of illumination conditions (both the direct sun and the sky in the sky-viewing direction) that pass the time series quality control can be quantified by simple model simulations.

4.3.2.6 Bidirectional effects

The difference between satellite and in situ viewing directions is considered more generally in Chapter 5 for all L_w measurements, although it is noted here that off-nadir angles, e.g. $\theta_v = 40°$, are generally used in above water radiometry.

4.3.3 Variants on the above water radiometric method

In addition to the various viewing geometries that have been used for above water radiometry, one important protocol variant was introduced by (Fougnie et al. 1999) and further developed in (Deschamps et al. 2004), who designed the SIMBAD/SIMBADA instruments with a vertically polarising filter placed as fore-optics and a measurement protocol with $\theta_v = 45°$ and

$\Delta\varphi = 135$. This design allows dramatic reduction of the magnitude of $\rho_F L_d(0^+, -\theta_v, \Delta\varphi)$ and hence associated uncertainties, provided that the polarising filter can be adequately calibrated and the polarised component of reflected skyglint can be adequately modelled.

In theory, above water measurements could also be made for multiple zenith and azimuth angles, e.g. from a robotic pointing system. However there is no study yet to show advantages that could be achieved, e.g for reducing skyglint removal uncertainties, from such measurements.

It is entirely feasible to combine both polarised and unpolarised measurements of $L_u(0^+, \theta_v, \Delta\varphi)$, e.g. in a filter-wheel instrument or by mounting in parallel radiometers with and without polarising filters (Stanford B. Hooker et al. 2012).

Theroretically above water radiometric measurements could be made for satellite validation from low altitude airborne platforms such as tethered balloons or drones, which would have advantages in terms of reducing optical perturbation by increasing distance from the water surface. However, in practice, the control of viewing geometry (platform stability) and logistical considerations (power supply, cleaning maintenance) seems to preclude significant use of such platforms for unsupervised measurements.

4.4 Above water radiometry with Skylight-Blocked Approach

4.4.1 Measurement equation

In view of the potentially large uncertainties which may arise from the skyglint correction of above water radiometry (section 4.3.2.1), the "Skylight-Blocked Approach (SBA)" was suggested by (Tanaka, Sasaki, and Ishizaka 2006; Z. Lee et al. 2010) and further developed by (Z. Lee et al. 2013) . In this approach the upwelling radiance mesurement is made with a radiance sensor to which an extension cone or cylinder is added so that the tip of the cone/cylinder lies fully beneath the air-water interface but the sensor fore-optics remains in air – see Figure 4-8 and Figure 4-9.

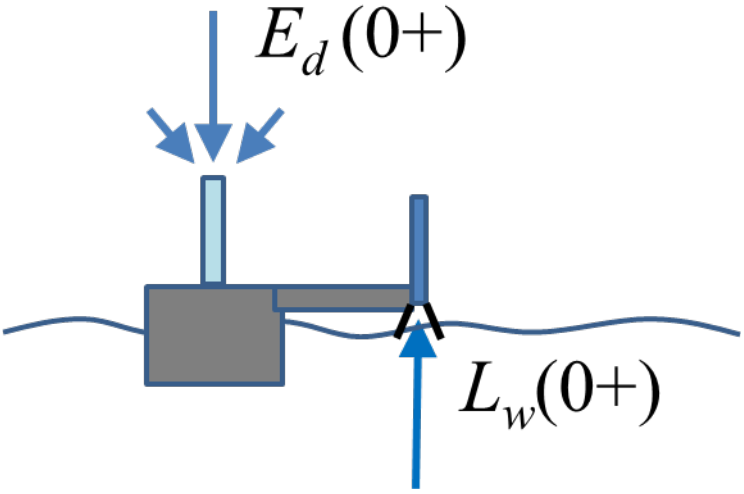

Figure 4-8 Schematic of above water radiometry with Skylight-Blocked Approach. Note that the radiometer fore-optics are in air, but the radiometer body is

extended with a cone or shield (black lines) that extends below the water surface, ensuring blocking of skylight reflection.

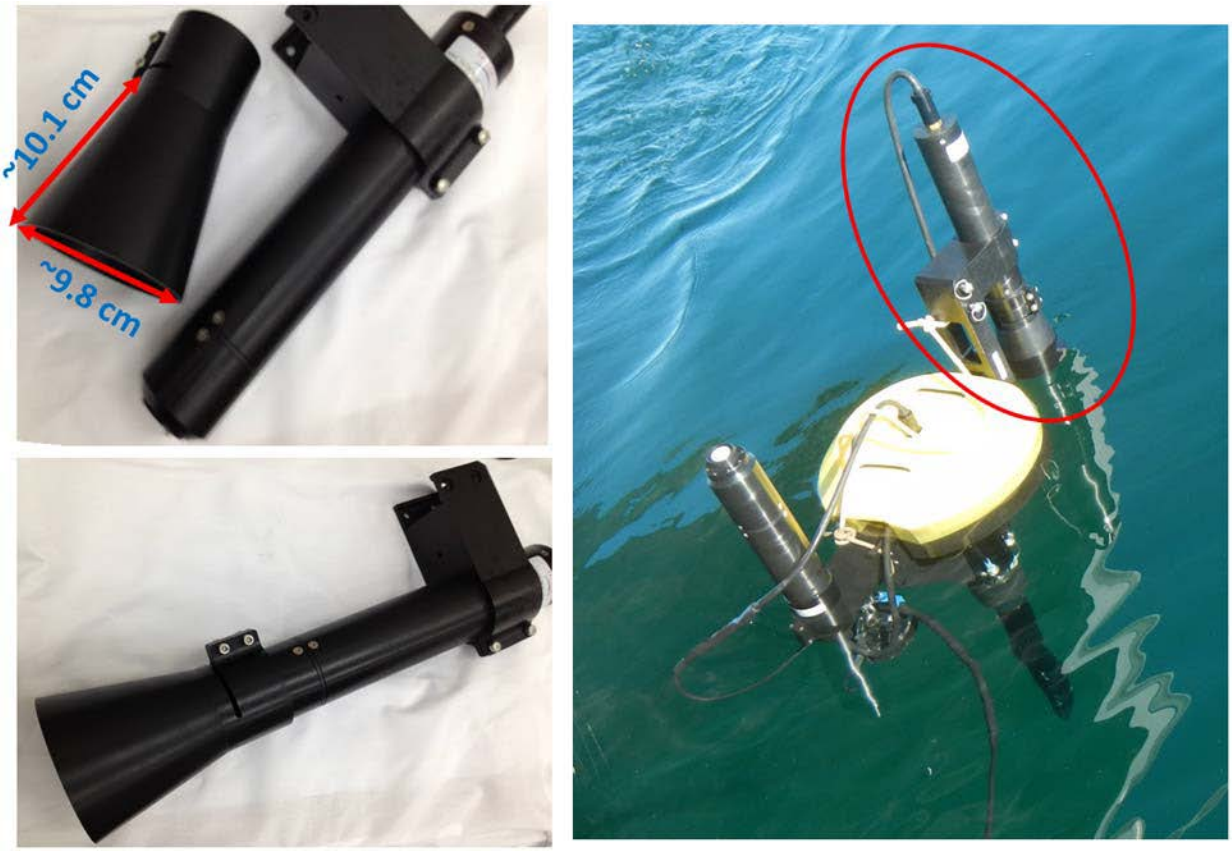

Figure 4-9 Typical deployment of radiometer using Skylight Blocked Approach, reproduced from (Z. Lee et al. 2013) (c) 2013 Optical Society of America.

With this approach there should be no skyglint reflected at the air-water interface and the Measurement Equation is simply given by:

$$L_w(\theta_v, \Delta\varphi) = L_u^{0+}(0^+, \theta_v, \Delta\varphi) \quad (21)$$

This measurement can be made for the nadir-viewing direction, $\theta_v = 0$, typically from a buoy which is floated away from a ship.

Measurement of water radiance involves time integration for each individual measurement and replicate measurements which are subsequently processed to yield a single value for $\overline{L_u^{0+}}(0^+, \theta_v, \Delta\varphi)$ where the overbar denotes the multitemporal measurement, typically called "time-average", although the temporal precessing may be different from a mean average.

The integration time depends on the instrument concept and the brightness of the target – see also FRM4SOC deliverable TR-2. Filter-wheel radiometers generally measure fast, typically at many Hz, whereas spectrometer based systems may be fast for bright targets such as the sky, but much slower, e.g. integration time of 1-4s, for darker targets such as water.

4.4.2 Protocol-dependent sources of uncertainty

In addition to the instrument-related sources of uncertainty which arise from imperfections in the radiometers themselves, as dealt with in FRM4SOC deliverable TR-2, the measurement of water-leaving radiance by above water radiometry with SBA has a number of sources of uncertainty relating to the basic measurement equation and deployment conditions. These protocol-related sources of uncertainty are described here.

4.4.2.1 Self-shading from instruments and/or superstructure

The skylight blocking cone/shield is designed to fully block all skyglint so that the reflection of skylight from the air-water interface is zero with zero uncertainty provided that there are no internal reflections within the cone and from the sensor fore-optics. However the cone/shield and instrument will also block sun and skylight illuminating the water volume which is being measured. This uncertainty, also called self-shading, needs to be evaluated and will depend on:

- Diameter of the cone/shield (preferably small)
- Angular variation of downwelling radiance (preferably high sun zenith angle)
- Distance of the cone beneath the air-water interface (preferably very small compared to a vertical attenuation length scale)

The first two parameters are similar to the process of instrument self-shading for underwater radiometry (Howard R. Gordon and Ding 1992). Minimisation of the distance of the cone beneath the air-water interface depends on surface wave height and stability of the deployment platform, e.g. buoy, and should be measured or estimated.

The uncertainties associated with self-shading using this protocol have been estimated by (Shang et al. 2017), who propose also a scheme for correcting for these effects.

Further contamination of measurements may arise from optical perturbations from the deployment platform, typically a buoy floated away from a ship to a distance sufficient to ensure no optical contamination from the ship itself. Clearly the water volume being measured should not be in the direct sun shadow of any deployment platform (buoy). This can be achieved by duplicate instruments on opposite sides of a buoy, one of which will always be outside the direct sun shadow. Measurement of the azimuthal rotation of the deployment structure with respect to sun will facilitate estimation of the uncertainty relating to optical contaminations. Figure 4 of (Shang et al. 2017) shows, from 3D Monte Carlo simulations of the structure proposed by (Z. Lee et al. 2013), that azimuthal dependence of self-shading is low provided that direct sun shadow is avoided.

Even if outside the direct sun shadow the deployment structure will to some extent modify the downwelling radiance field illuminating the water volume. Consequent uncertainties can be estimated, as for the other methods (section 4.1.2.2), by 3D optical modelling, by high resolution imagery (e.g. from drone-mounted cameras) or by experiments with instruments held at different distance from the deployment structure.

4.4.2.2 Tilt and roll effects

Any variation in the pointing angle of the instrument ("tilt") must be propagated through to give an uncertainty for L_{wn} as for other fixed depth underwater measurements – section 4.1.2.2. – but using here the above water angular variability of L_w. Typically a tilt threshold will be set for acceptable measurements and the associated uncertainty can be assessed from model simulations.

4.4.2.3 Bio-fouling and other fore-optics contamination

Since this protocol involves a downward-facing sensor with shadowed fore-optics, bio-fouling from algae is not expected to be a major problem, even for unsupervised deployment – see also section 4.1.2.4 for fixed depth underwater radiometery.

More problematic may be the possibility of water droplets reaching the fore-optics, which is supposed to be in air. In salt water water reaching the fore-optics may leave a salty deposit. This can be particularly problematic in high sea state, but can be limited by choice of a stable deployment platform (Z. Lee et al. 2013) and a sufficiently long and air-tight cone/shield (subject to instrument field of view constraints).

The uncertainty estimate related to any foreoptics contamination can be validated by comparing post-deployment calibrations before and after cleaning.

4.4.2.4 High frequency fluctuations

Measurements are averaged over a certain interval of time to remove as far as possible the high frequency variations associated with natural variability (wave focussing/defocussing (see also section 4.1.2.7), and with surface gravity waves, which may affect the depth of water in the shield/cone (section 4.4.2.1).

Variations in illumination conditions, e.g. clouds/haze passing near the sun, can be detected in time series of L_w/E_d^{0+} or E_d^{0+} and the associated data can be rejected if a user-defined threshold of variation is reached. Uncertainties associated with any high frequency fluctuations of illumination conditions (both the direct sun and the sky in the sky-viewing direction) that pass the time series quality control can be quantified by simple model simulations.

4.4.2.5 Bidirectional effects

The difference between satellite and in situ viewing directions is considered more generally in Chapter 5 for all L_w measurements.

4.4.3 Variants on the above water radiometric with Skylight Blocked Approach

The SBA protocol could be used with various instruments, shields/cones and deployment methods (buoys, etc.). The preceding subsections are thought to be sufficiently generic to cover these variants.

5 Bidirectional effects

The satellite product that is the object of this review is defined in section 2.1.1 and equation (1) as the directional water-leaving radiance reflectance. This corresponds to the viewing direction of the satellite sensor and the sun zenith angle and the sky radiance distribution at the time of the satellite measurement.

In a series of papers by Morel, (Morel and Gentili 1991, 1993, 1996), explained also in the oceanoptics web book [http://www.oceanopticsbook.info/], a number of "BRDF" corrections have been developed to obtain a product that corresponds to zenith sun and nadir viewing direction using a water optical model typical of Case 1 water with chlorophyll a concentration as the single degree of freedom, an air-water interface model with wind speed input and a typical marine atmosphere sky radiance distribution. The resulting "exact normalized water-leaving radiance" is more closely related to the inherent optical properties of the water than was ρ_w and hence is more appropriate for time series studies and for datasets merged across different satellites (International Ocean Colour Coordinating Group (IOCCG) 2007).

If such an "exact normalized water-leaving radiance" satellite product is being validated then the corresponding BRDF corrections must be applied both to the satellite measurement and to the in situ measurement. For measurements made with the in water methods described in sections 4.1 and 4.2 and the SBA approach of section 4.4, since the in situ measurement is already in the nadir viewing geometry, it is necessary to correct only for the difference between the actual sun zenith angle and sun at zenith. Chapter 4.5 of Volume III of (Morel and Mueller 2003) outlines how to do this for Case 1 waters, based on (Morel and Gentili 1996), and using as inputs to their correction equation 4.21 the following parameters: sun zenith angle, aerosol optical thickness (which influences the sky radiance distribution) and chlorophyll a concentration. In the case of above water measurements, both in situ and satellite, it is necessary to take account also of the off-nadir viewing geometry, outlined again in (Morel and Mueller 2003), with their correction equation 4.20 requiring additional inputs for viewing zenith angle, viewing azimuth angle relative to sun and wind speed (which affect water surface roughness and hence reflection and refraction effects).

These BRDF corrections based on (Morel and Gentili 1996) are relatively mature and well-accepted for Case 1 waters, but are not applicable to "Case 2" waters where inherent optical properties of the water are not determined solely by phytoplankton and its degradation products. In particular the BRDF variability is strongly dependent on the scattering phase function of the water, which depends both on the ratio of molecular to particulate scattering and on the scattering phase function of the particles, which can vary greatly between algal and non-algal particles. This has been studied in a number of papers (Loisel and Morel 2001; Albert and Mobley 2003; Park and Ruddick 2005), but there is currently no consensus approach for Case 2 waters although promising approaches are suggested by (Z. P. Lee et al. 2011; Fan et al. 2016) - see also discussion of [http://www.oceanopticsbook.info/view/atmospheric_correction/normalized_reflectances]. Indeed for the satellite data processing it is typical to either not apply BRDF corrections, leaving this task for any downstream processing, or to generate both BRDF-corrected and BRDF-uncorrected products.

For the (directional) "water-leaving radiance reflectance" parameter defined in section 2.1.1 and equation (1) as the focus of the present study the "normalisation" to zenith sun conditions is not required – both satellite and in situ measurements are made for the same sun geometry (notwithstanding possible small time differences mentioned in Chapter 6). However, there will still be differences between satellite and in situ measurements because of the different viewing geometry. For measurements made with the in water methods described in sections 4.1 and 4.2 and the SBA approach of section 4.4, this will typically be resolved by correcting the satellite measurement to a nadir-viewing geometry (and so adding the satellite viewing geometry correction to the satellite data processing that is being validated). For in situ measurements made above water, as described in section 4.3, it is theoretically possible to apply a viewing geometry correction to estimate the corresponding water-leaving radiance reflectance in the satellite-viewing direction, although this has not yet to our knowledge been implemented in validation studies. Alternatively a viewing geometry correction could be applied to both satellite and in situ measurements to reach a common nadir-viewing geometry for the validation comparison (thus again adding the nadir-viewing correction to the satellite data processing that is being validated).

Clearly, in the FRM context it is necessary to estimate the uncertainty involved in any BRDF (or viewing geometry) correction or in the full BRDF (or viewing geometry) effect if it is not at all corrected. The Case 1 BRDF correction proposed by (Morel and Gentili 1996) does of course include assumptions (water inherent optical property model as function of chlorophyll, sky radiance distribution as function of aerosol optical thickness) and inputs (aerosol optical thickness, wind speed) that are subject to some uncertainty, although the biggest problems are expected in case 2 waters where the BRDF (or viewing geometry) correction models are still a topic for research.

6 In Situ/Satellite space-time match-up considerations

The comparison of satellite data pixel values with near-simultaneous "matchup" in situ measurements is the main methodology for performing level 2 radiometric validation. Although the FRM concept applies essentially to the in situ measurement (including instrument calibration and characterisation, deployment and processing protocol) and not to the way it used in a validation matchup analysis, it is relevant to consider also the space-time characteristics of the in situ measurement and how this may impact its use for validation of satellite data with quite different space and time basis. The preceding Chapters of this report, and particularly Chapters 3 and 4, have focussed on how the in situ measurement is made including deployment protocol and data processing assumptions and associated uncertainties. In the present Chapter the different space-time coverages of satellite and in situ measurements are briefly described.

6.1 Space and time scales of natural optically-relevant processes

Satellite remote sensing is a way of sampling the oceans, seas, estuaries and lakes to provide useful information on physical or biological processes through their optical properties. These underlying processes are many and have quite diverse length and time scales of variability as illustrated in Figure 6-1 and Figure 6-2. For example, at the scale of the world's oceans, satellite imagery can show largescale features of oceanic circulation (boundary currents, trade wind induced currents, equatorial currents, etc.) and their variability, including seasonal variations, mesoscale eddies, etc. These processes may have length scales of a few km to many hundreds of km and time scales of a few months to many years (or may be quasi-permanent). Water depth is a strong constraint on hydrodynamic processes and many biological processes, including phytoplankton distributions, are in turn constrained by these hydrodynamic processes. As a result bathymetric features will strongly influence horizontal distributions of optical properties, including water reflectance. Bathymetric features have only slow time scales of variability (typically between years to many thousands of years or may be quasi-permanent) but may have very short length scales of variability (from a few metres to a few km), particularly near continental shelf breaks, near the coast and for estuaries and inland waters of small dimension. Further time scales of variability include diurnal heating/lighting (and associated processes of vertical stratification, phytoplankton physiology, vertical migration, etc.) and tidal forcing (resuspension, horizontal advection). The physical forcings of heat, light, wind stress, tide, etc. also interact with bathymetry to give diverse length scales of variability. At shorter time scales, wind and swell waves and turbulence[13] may give variability down to sub-second time scales and sub-metre or even sub-centimetre length scales.

These natural processes are sampled in quite different ways in space and time by a) instruments mounted on satellites and b) instruments deployed for field validation measurements, as described in the following sections.

[13] Here the word "turbulence" is used loosely to group diverse chaotic flow fluctuations. For a more complete description of turbulent processes the reader is referred to the vast body of fluid dynamics literature, e.g. (Thorpe 2007).

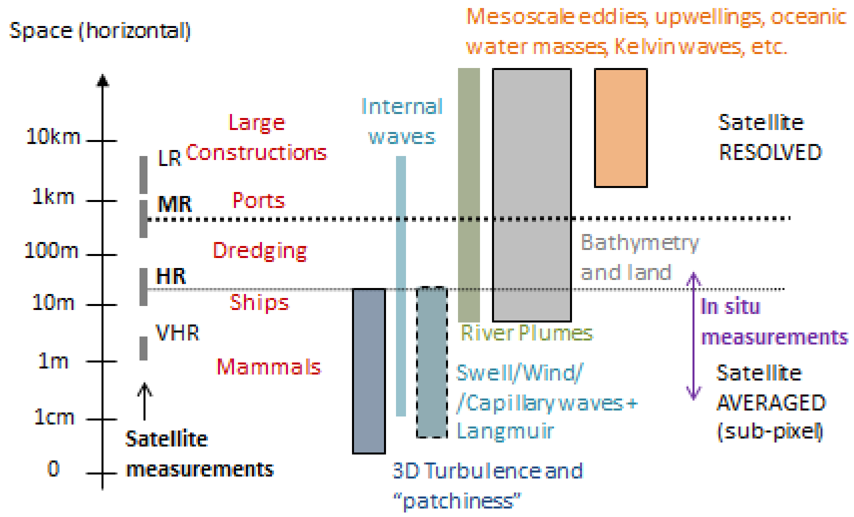

Figure 6-1. A schematic showing space scales of some important aquatic processes with optical relevance. The space scales of satellite measurements from Medium Resolution (MR), High Resolution (HR) satellite sensors are also shown, together with Very High Resolution (VHR: metre-scale) and Low Resolution length scales. LR data is typically obtained from spatial averaging of MR data. Some significant space scales relating to human activities (and large mammals) are shown in red. The spatial scales typical of in situ measurements are shown in violet and are generally shorter than MR satellite measurements but similar to HR or VHR length scales.

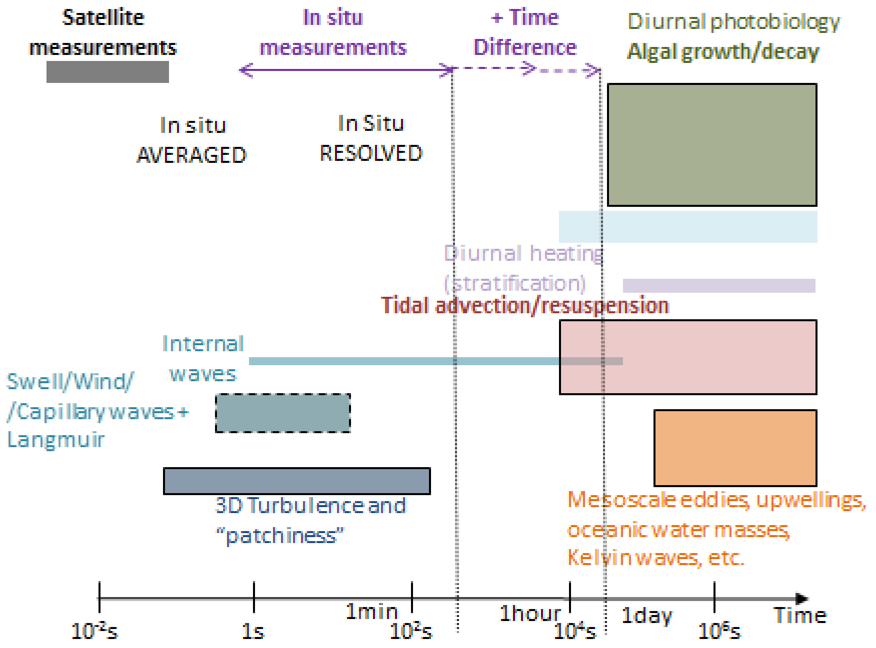

Figure 6-2. A schematic showing time scales of some important aquatic processes with optical relevance. Satellite measurements have very short time scales (1-100ms). The time scales typical of in situ measurements are shown in violet, but there is often also a time difference between in situ and satellite measurements, which may overlap with significant temporal variability of aquatic processes.

6.2 Definition of space and time scales for satellite data measurements

The space-time characteristics of satellite-mounted instruments are illustrated in Figure 6-1 and Figure 6-2 – these measurements are made very quickly in time, typically each pixel is measured in 1-100 milliseconds (depending on sensor design with faster speeds for higher resolution sensors), but with averaging of radiance over length scales of 250-1km for typical "medium resolution[14]" ocean colour sensors such as Sentinel-3/OLCI, MODIS, VIIRS and GOCI, and over length scales of 10-100m for typical "land-designed" optical sensors such as Sentinel-2/MSI and Landsat-8/OLI. Higher spatial resolutions, e.g. metre scale, can be reached by a few broad band satellite remote sensors such as Pléiades and Worldview[15].

Satellite image data is discretised horizontally into rectangular pixels[16], whose size is typically not smaller than the horizontal resolution of the satellite-borne optical system. **For the purposes of this report the pixel value for a radiometric parameter such as water-leaving radiance reflectance is considered to be an estimate of the parameter at**

[14] The terminology "km-scale" may be preferable to "medium resolution" in the long term in view of the now anachronistic naming of the Advanced "Very High Resolution" Radiometer series.
[15] Even high spatial resolutions, e.g. cm scale or less, may be reached by airborne sensors at lower altitude, e.g. on fixed-wing aircraft or drones.
[16] The instantaneous fields of view of the satellite sensor itself do not have a perfectly binary (0/1) response function over space and are more elliptical than rectangular when projected onto a horizontal surface from an off-nadir viewing direction. However, since the satellite data products are validated after processing and transformation to the rectangular pixel-based geometry it is the latter that is relevant for the validation analysis.

all points within the pixel. This assumption of uniformity within a pixel and discontinuous changes between adjacent pixels is analogous to the "nearest neighbour" remapping approach and is typical of the way that the satellite data is actually used by users. Clearly if there are applications where satellite data is used in a different way, e.g. with bilinear interpolation between pixel centres to represent sub-pixel scale variability, the same approach can be used to process the satellite data in the matchup validation analysis. Similarly if data from the same sensor is produced at different spatial resolutions, e.g. SeaWiFS Local Area Coverage (LAC: 1km) and Global Area Coverage (GAC: 4km) or MERIS Full Resolution (0.3km) and MERIS Reduced Resolution (RR: 1.2km), then a validation analysis can be made for each data product separately.

Also in the validation context, the location of the satellite measurement is taken at the location provided in the satellite data file. That location is itself subject to uncertainty, including possible geolocation biases, but from the users' point of view it is the stated location that is relevant for validation.

As regards vertical space, the L2R satellite data products are defined as surface values[17] and the in situ measurements are accordingly defined as surface values. Here, "surface" refers to the air-water interface, which may be irregular and may be at an altitude very different from the geoid, but is defined in the same way for both satellite and in situ data. Any uncertainties associated with vertical variability (e.g. extrapolation of underwater measurements to the surface) are incorporated in the in situ measurement uncertainty and so there are no additional uncertainties associated with differences in the vertical location of satellite and in situ data.

6.3 Definition of space and time scales for in situ data measurements

The space-time characteristics of in situ measurements are discussed per protocol in detail in this section, but generally have time scales from about 1s to about 10 mins, depending on the intrinsic sampling speed of the instrument and the number of samples required to achieve a single measurement (allowing for whatever temporal filtering, averaging or other processing is required according by the protocol). Horizontal length scales may vary from a few cm, for example for fixed depth radiometry from fixed platforms, to a metre or a few metres for abovewater radiometry to a few tens or hundreds of metres for measurements made from drifting platforms, including multicast free-fall vertical profilers or above water radiometry from moving ships[18].

The spatial basis for in situ measurements of L_w varies according to the deployment protocol and platform. Considering the protocols described in Chapters 3 and 4:

- Fixed depth measurements of L_w (section4.1) are typically made from quasi-fixed structures such as BOUSSOLE and MOBY with limited horizontal movement during the measurement duration. The horizontal extent of the "probe volume" of water contributing to light received by the highest L_w sensor could be estimated from geometrical scales such as sensor angular field of view and K_{Lu}, but is unlikely to exceed a few metres – see Figure 6-3. The horizontal basis for the in situ measurement can

[17] This cannot be said for L2W data for which the vertical location is generally less accurately defined.
[18] In the case of a horizontally-varying concentration field that is advected through the probe volume of a horizontally-fixed instrument the spatial variability will be measured as temporal variability and will be considered as such in this validation context.

then be effectively represented by the coordinates of a measurement "centre position", e.g. position at centre time, and a horizontal length scale combining sensor probe volume and any horizontal movement effects. This horizontal length scale will typically be quite small, perhaps between a few centimetres and a few metres, although could be more significant if fixed depth measurements are being made from a ship.

- Vertical profile measurements of L_w (section4.2) can be considered in a similar way to fixed depth measurements as regards horizontal space (centre position and horizontal length scale), although the horizontal length scale could typically be larger, for example in the case of ship-tethered multicast profiles or, *a fortoriori*, underwater drifting platforms (section 4.2.3) – see Figure 6-4.
- Abovewater radiometric measurements of L_w (section 4.3) made from a fixed platform, such as those of the AERONET-OC network, have a horizontal basis that is defined by the sensor field of view, the sensor height above water and the viewing zenith angle – see Figure 6-5. This can be represented effectively as a measurement centre position and horizontal length scale. This horizontal length scale will typically be small, e.g. a few tens of centimetres or a few metres, although will be more significant if measurements are made from a ship holding position or, a fortoriori, a "ferrybox-style" deployment on a ship of opportunity.
- Measurements of L_w made using a skylight blocked approach (section4.4) have a horizontal basis that is conceptually similar to that of fixed depth measurements. This can be represented by a horizontal centre position and horizontal length scale. The latter will be typically be small, e.g. a few tens of centimetres or a few metres, assuming that such systems are somehow anchored.

The horizontal basis for E_d should not contribute significant to any satellite vs in situ validation analysis because E_d should not have significant natural variability over the horizontal length scales of measurement (a few metres for fixed platforms or a few hundred metres for drifting systems). Horizontal variability of E_d induced by the deployment platform itself is considered already in the in situ measurement uncertainty budget (sections 4.1.2.3). Natural horizontal variability of E_d associated with clouds passing near the sun should be deduced from temporal variability of E_d and affected measurements should be removed in the quality control process.

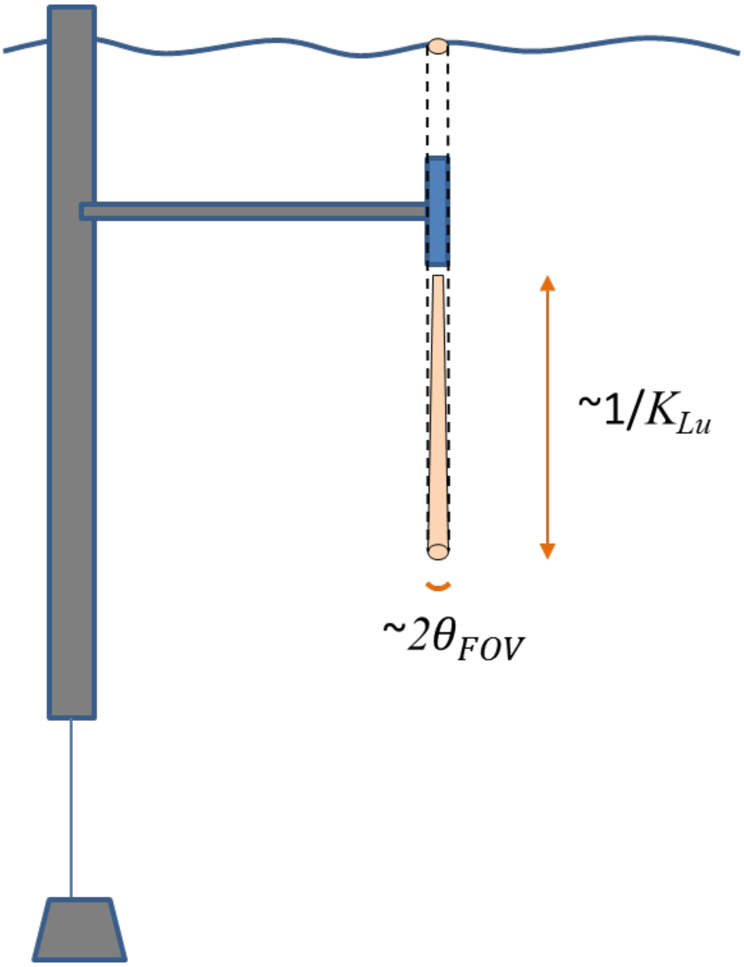

Figure 6-3 Schematic illustrating horizontal length scale for typical measurements made with fixed depth radiometry. K_{Lu} is the diffuse attenuation coefficient for upwelling radiance, θ_{FOV} is the half-angle field of view of the radiance sensor.

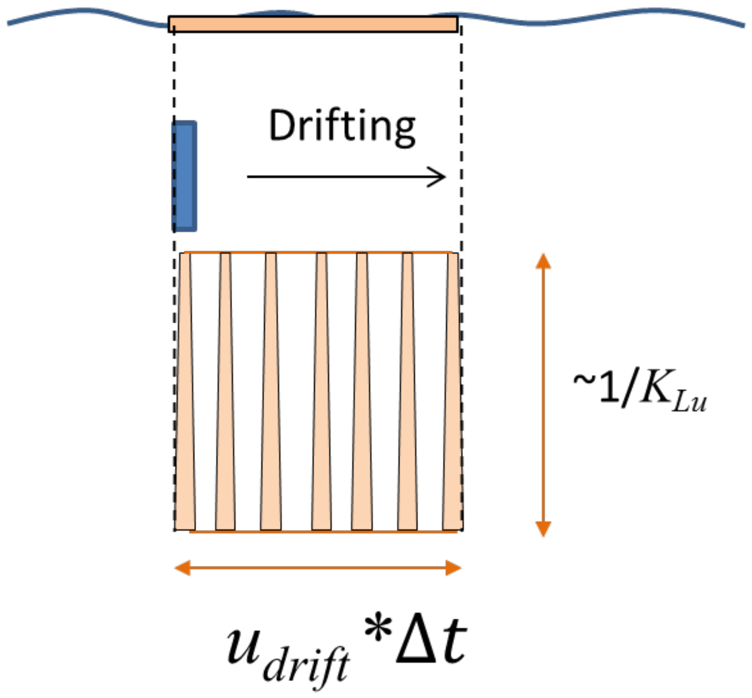

Figure 6-4 Schematic illustrating horizontal length scale for typical measurements made with "free-fall" vertically profiling depth radiometry. K_{Lu} is the diffuse attenuation coefficient for upwelling radiance, θ_{FOV} is the half-angle field of view of the radiance sensor. u_{drift} is the horizontal drift velocity (similar to current velocity) and Δt is the time interval for the whole measurement sequence.

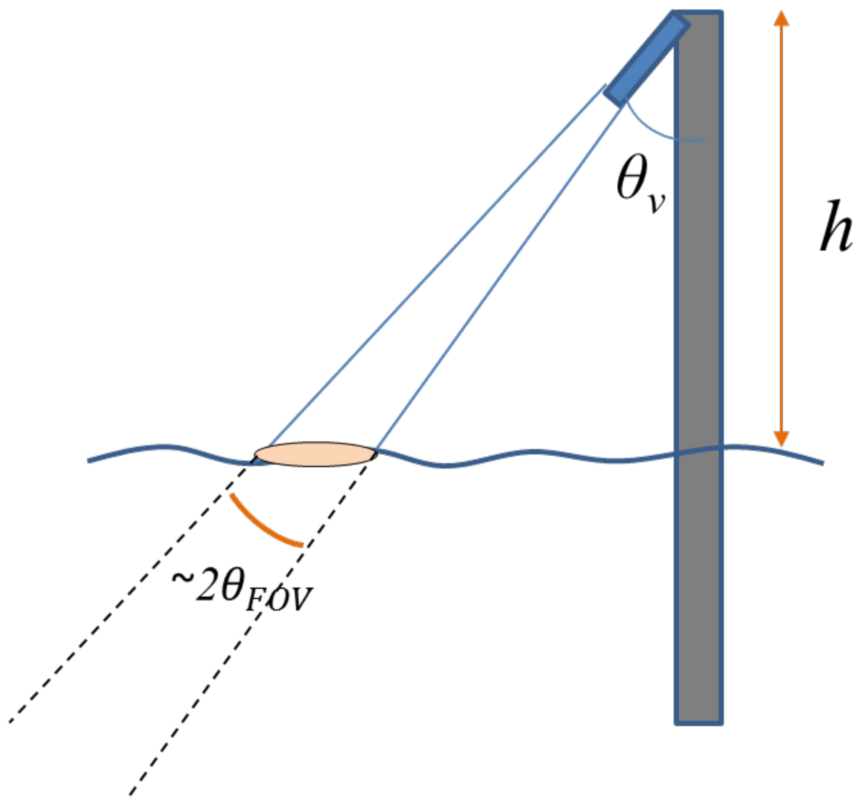

Figure 6-5 Schematic illustrating horizontal length scale for typical measurements made above water radiometry. h is the height of the sensor above water level, θ_{FOV} is the half-angle field of view of the radiance sensor. , θ_v is the zenith angle of the sensor.

6.4 Approaches for dealing with space-time differences when comparing satellite with in situ measurements

The time scale for in situ measurements is thus generally longer than for satellite measurements, whereas the length scale for in situ measurements is generally shorter than for satellite measurements. All spatial variability between the length scales of satellite and in situ measurements and all temporal variability between the time scales of satellite and in situ measurements is theoretically problematic because it will be averaged (in some way) by one instrument but resolved by the other.

6.4.1 Approaches to sub-pixel scale spatial variability

As regards spatial variability, there can be considerable sub-pixel scale variability within a satellite data pixel which is not captured by the in situ measurements, particularly for coastal, estuarine and inland waters. These processes are illustrated in Figure 6-1 and include firstly spatial variability in bathymetry (and coastline), which structures many hydrodynamical and hence optical processes – bathymetric features include continental shelf breaks, submerged sandbanks and many other features in coastal, estuarine and inland waters. River inputs also significantly affect hydrodynamics and suspended particulate matter distributions either smoothly or via fronts and patches. The longer scale mesoscale eddies, upwellings, oceanic water mass, and other features are generally less problematic in this context except at fronts, which will be smoothed in most satellite data. Shorter scale processes including 3D turbulence and other diverse processes causing "patchiness" may give significant difference between the in situ measurement over a few cms or metres and a much larger satellite data pixel. There is also considerably optical variability from the longer surface gravity waves at the intermediate length scales, although these surface effects should normally be removed from both under water and above water in situ measurements.

A common approach for dealing with spatial aspects of match up validation in medium resolution ocean colour imagery (Bailey and Werdell 2006) is to define a macro-pixel box around the location of the in situ measurements, e.g. 3*3 or 5*5 or 7*7. The spatial variability within the macro-pixel can then be assessed by considering for example standard deviation, minimum and maximum. Typically a threshold will be set on spatial variability of the satellite data for acceptability of a matchup. (Bailey and Werdell 2006) suggested use of a 5*5 box for SeaWiFS 1km data based on a limit for reducing the impact of noise in the satellite dataset (Hu, Carder, and Muller-Karger 2001).

Requirements may also be set on usability of data for a certain % of the pixels within a macro-pixel since some pixels may be unusable because of cloud, land or other factors. For example (Bailey and Werdell 2006) suggested that 50% of pixels should be usable with the relaxed criterion of 50% of usable non-land pixels for coastal waters.

In the case of multiple in situ measurements per macropixel (Bailey and Werdell 2006) also recommend a procedure for reducing to a single in situ measurement per macropixel by selecting first the in situ measurement nearest in time to the satellite acquisition and using further in situ measurements, if available, for subsequent macro-pixels.

It is noted here that the macropixel approach was designed following criteria based on noise reduction in the satellite data and not as a way of representing sub-pixel scale variability (although a noisy macropixel, if the spatial variability is not satellite data noise but is real natural variability either in the water or in the atmosphere, may indicate also that sub-pixel scale variability could be significant).

Along-track measurements of optically relevant parameters such as fluorescence or scattering may provide information on sub-pixel scale spatial variability if response times of the systems are fast enough. Time series measurements in a fixed point may also provide an indication of corresponding spatial variability if horizontal advection processes dominate and current speeds are known.

Alternatively, airborne data or very high resolution satellite data may be used if sensor noise is sufficiently low. An example of this is provided by (Quinten Vanhellemont and Ruddick n.d.)who use Landsat-8 imagery at 30m to study sub-pixel scale effects inside a 300m simulated Sentinel-3/OLCI pixel – see Figure 6-6 and Figure 6-7. That study also demonstrates the impact of sub-pixel scale offshore platforms (e.g. used for an AERONET-OC validation site) on satellite data, where a small object and/or its shadow with strong contrast to surrounding water (e.g. in the NIR/SWIR) can impact at medium resolution pixel level in a way that is not obvious to detect automatically. That study also mentions the possibility of platform-induced wakes which can generate further, artificial subpixel scale variability. In a comparison of possible validation sites in the extremely turbid La Plata Estuary (Dogliotti, A.I. et al. 2015) show that measurements made within a nearshore coastal current may be appropriate to validation of 30m satellite data but not 300m satellite data – see Figure 6-8.

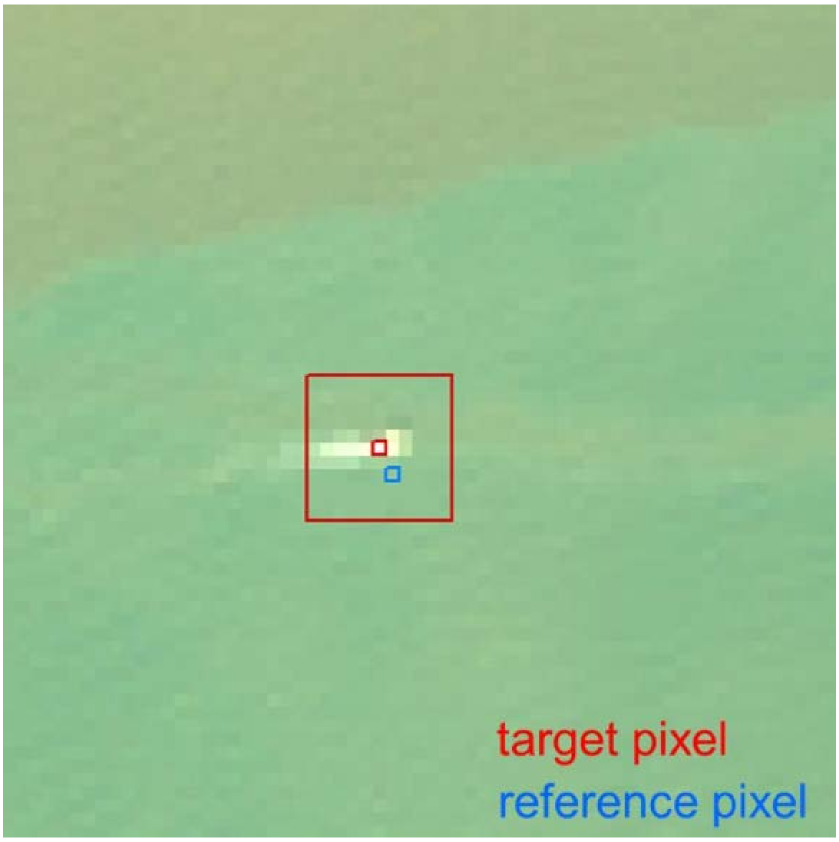

Figure 6-6 Subset of a Landsat-8 Top Of Atmosphere Red-Green-Blue image described in detail by (Q. Vanhellemont and Ruddick 2015). Pixel size is 30m. The small red pixel contains a ship. The larger red pixel simulates a 300m Sentinel3/OLCI pixel. The blue pixel containing unperturbed water, is considered as a reference pixel. A band of darker brown water is also visible across the top of the image – this turbidity front will clearly be under-resolved in 300m imagery. Some periodic structures can also be seen across the image caused by surface gravity waves.

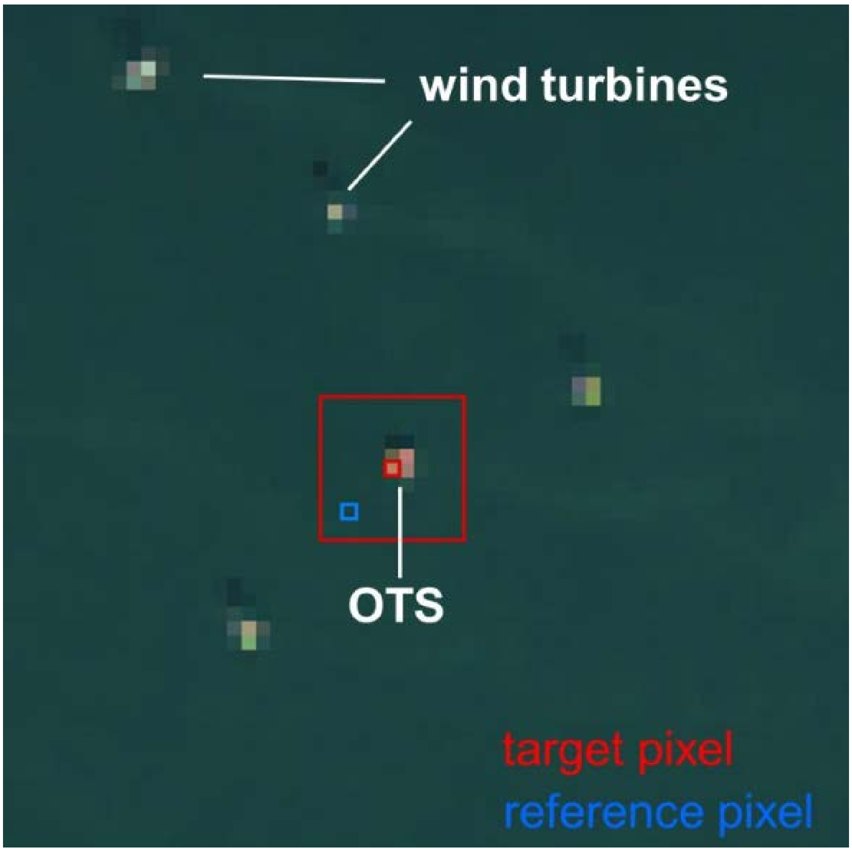

Figure 6-7 Subset of a Landsat-8 Top Of Atmosphere Red-Green-Blue image described in detail by (Q. Vanhellemont and Ruddick 2015). Pixel size is 30m. The small red pixel contains a large red offshore platform ("OTS") – it's shadow is also visible two pixels further North. The larger red pixel simulates a 300m Sentinel3/OLCI pixel. The blue pixel containing unperturbed water, is considered as a reference pixel. Individual wind turbines and their shadows are also clearly visible in this 30m imagery and will impact on 300m pixels. Some turbid wakes are visible to the East of the structures – see also (Q. Vanhellemont and Ruddick 2014).

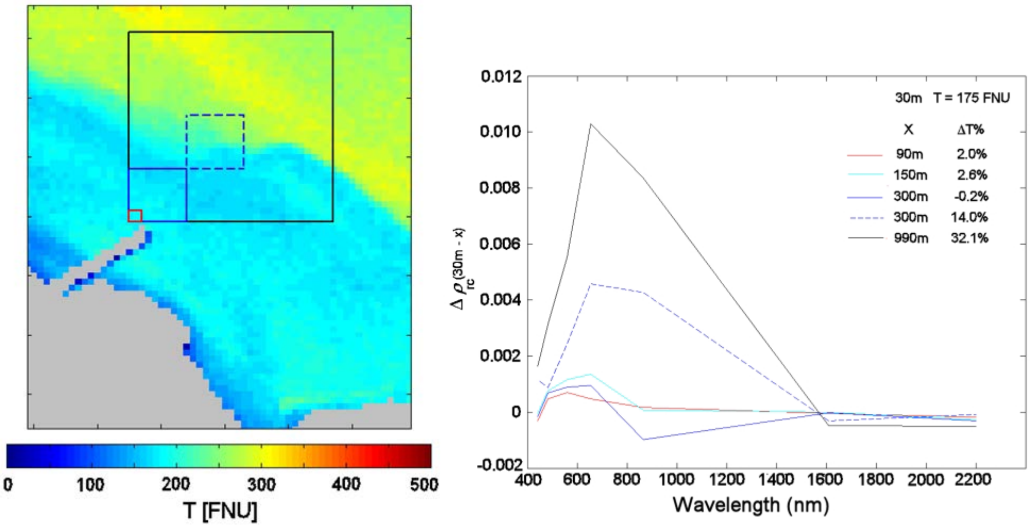

Figure 6-8. (left) Turbidity map from a Landsat-8 of 23/4/2015 in the La Plata estuary. (right) Rayleigh-corrected reflectance spectral difference between different window sizes and a single L8 pixel (30m). Reproduced from (Dogliotti et al, 2015).

6.5 Approaches for dealing with time differences when comparing satellite with in situ measurements

Temporal variability between the time scale of satellite acquisition (1-100ms) and that of in situ measurements (~10s-10mins) is generally not significant, except for the processes which are in any case spatially averaged by the satellite sensor and time-averaged in the in situ measurement (or simply removed as for surface waves). As regards time, the main problem for matchup validation arises from the logistic challenges of synchronising in situ measurements with satellite measurements, so it is the (centre) time difference between satellite and in situ measurements rather than the duration difference, which is of concern. This time difference may be a few minutes or even a few hours – see Figure 6-2.

A common approach for dealing with temporal aspects of match-up validation (Bailey and Werdell 2006) is to define an "acceptable" time window for in situ measurements, e.g. ±3 hours around the satellite acquisition time for relatively homogeneous oceanic water masses. This time window could be significantly smaller for waters where there is faster temporal variability, e.g. coastal waters with tidal effects where a time window for using in situ measurements could be e.g. ±1 hour or less.

Obviously a reliable threshold can only be set if there is knowledge of the true temporal variability of optical parameters in the water. This can be obtained from continuously measuring fluorimeters or turbidimeters, e.g. CEFAS Smartbuoys. This is illustrated in Figure 6-9 where a time series of in situ turbidimeter measurements every 15 minutes is presented as a time series with geostationary measurements made every 15 minutes and a single satellite data point from MODIS/AQUA. In these tidal waters a time difference of 3 hours between an in situ measurement and a satellite measurement can give up to a factor 2 difference.

Another example of how temporal difference between satellite and in situ data is shown in Figure 6-10, where in situ measurements made within 15 minutes of the satellite measurements have also been shown two hours before and two hours after the satellite measurement. The time difference clearly increases the scatter.

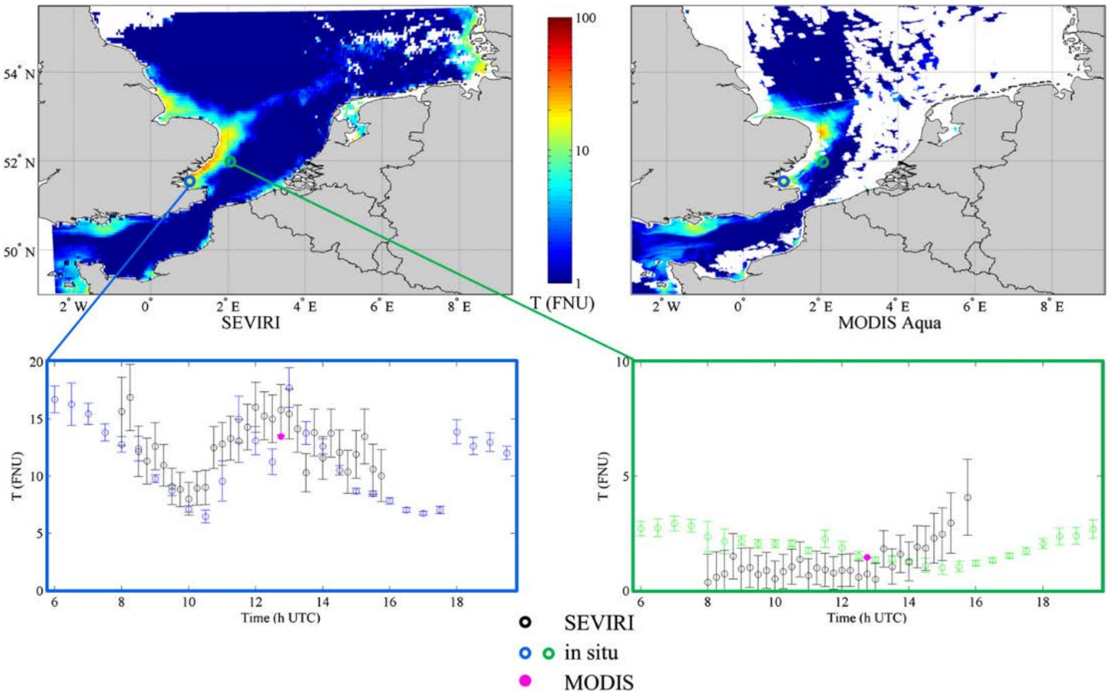

Figure 6-9 Reproduced from (Kevin Ruddick et al. 2014): Comparison of turbidity data derived from SEVIRI and MODIS-AQUA on 15th April 2008 using the processing of (Neukermans, Ruddick, and Greenwood 2012): (top-left) daily average from 34 SEVIRI images,(top-right) single MODIS-AQUA acquisition at 12:45 UTC. Corresponding time series of in situ and remotely sensed turbidity at (bottom left) the mouth of the Thames river (51.5235°N,1.0240°E) and (bottom right) further offshore (51.9802°N, 2.0828°E). In the time series, SEVIRI data is given as grey dots, in situ optical data is given as blue or green dots according to location, and MODIS data is given as a single magenta dot for each location.) Full details of processing, including definition of the uncertainty bars for SEVIRI and in situ data, are given in (Neukermans, Ruddick, and Greenwood 2012) and (Neukermans 2012).

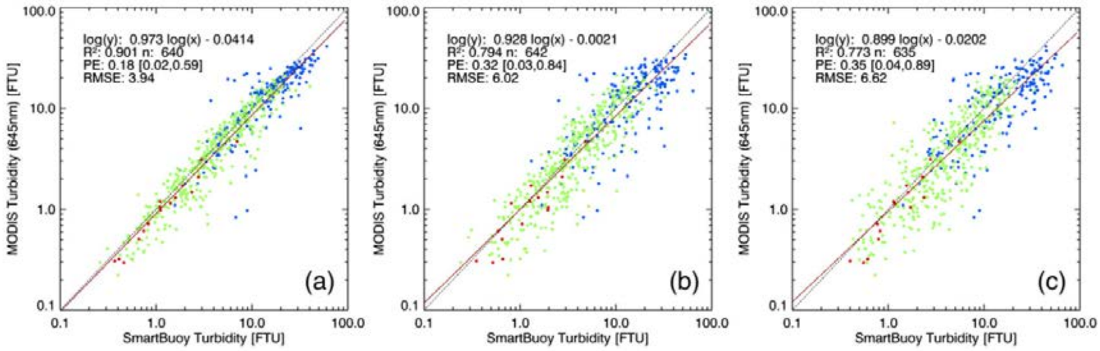

Figure 6-10 Reproduced from (Q. Vanhellemont, Neukermans, and Ruddick 2014): Comparison of MODIS derived turbidity with CEFAS/SmartBuoy turbidities from DOWS, WGAB and WARP (red, green and blue dots) at a) overpass time t0, b) two hours before, and c) three hours after t0. Matchups were extracted from mid-2002 to 2010, depending on buoy deployments. Red, green and blue dots are data from Dowsing, West Gabbard and Warp buoys respectively.

7 Conclusions and Recommendations

7.1 Maturity of requirements and protocols

The current review is based on strong heritage from previous protocol documents, including in particular the NASA Ocean Optics Protocols Revision 5 dated 2004. Inputs from the MERIS optical measurement protocols and from many individual studies since the last revision of the NASA protocols. However, there are a number of major developments over the period 2004-2017 that have helped shape the present document, including:

1. A maturing of methods for abovewater radiometry (although significant diversity still exists particularly for the skyglint correction),

2. A growing consensus that E_d^{0+} should be measured abovewater, even for protocols that derive L_w from the vertical extrapolation of underwater measurements. This allows significant simplification and restructuring with respect to the NASA Ocean Optics protocols – see Figure 2-2.

3. A move away from supervised measurements, typified by individual seaborne cruises, to unsupervised measurements (e.g. BOUSSOLE, MOBY, AERONET-OC and potential future drifting systems) because of obvious advantages in terms of measurements/year and the economies of scale for automated acquisition and processing.

4. A growing availability of high spatial resolution satellite data for inland and coastal water applications … and need for validation of such data. Conceptually there are no fundamental differences between the application of protocols for oceanic or inland waters, although different circumstances may occur more frequently in the latter that will impact the choice and/or performance of protocols, e.g. bottom reflectance, very high vertical attenuation, very shallow water, optical impacts of surrounding trees/buildings/terrain, fetch-limited surface gravity wave field, etc.

5. Reinforcement of **the need for measurements to be accompanied by a full uncertainty budget with traceability to SI standards**, introduction of the **terminology of Fiducial Reference Measurements** (see section 1.2) and the **detailed set of recommendations of the CEOS INSITU-OCR White paper**, reproduced in section 1.4.5. The current document in fact focusses on describing protocol elements that should be considered in an uncertainty budget rather than prescribing exactly how measurements should be made (see discussion of section 1.1.3).

The essential methods described here for measuring E_d^{0+} (3 generic methods) and L_w (4 generic methods), with the possible exception of the more recently-developed SBA approach for L_w, can be considered to have reached a reasonable degree of maturity in that they have existed for at least 10-15 years in some form. However, it is clear that there are many incremental improvements still occuring and still possible because of improved understanding/modelling of optical processes and new instruments and measuring platforms.

7.2 Recommendations for achieving FRM status from S3VT

It is clear that the requirements of Fiducial Reference Measurements as expressed in section 1.2 were not met by the majority of teams participating in the previous ENVISAT/MERIS Validation team and that considerable (and costly) work is required to achieve FRM status for many S3VT participants. At present, in view of the sparsity of any validation data for many regions and water types, it seems impractical to restrict validation data to only those data that meet FRM requirements, although this should certainly be a medium-term (~3-5 years?) aim.

In order to achieve FRM status as regards the measurement protocols, it is recommended to S3VT participants to:

- Consider the CEOS INSIT-OCR White Paper (reproduced partially in section 1.4.5) and the present document and provide comments for its improvement
- Analyse carefully their measurement protocol and construct a uncertainty budget including minimally the elements listed in the corresponding sections of this document
- Participate in intercoparison exercises to validate their uncertainty estimates against those of other methods/scientists.

and it is recommended to ESA and other space agencies to:

- facilitate discussion and adoption of best practice and uncertainty estimation by sponsoring intercomparison exercise with appropriate funding for post-measurement analysis of results
- in the medium term encourage and stimulate the adoption of FRM requirements and in the long term, when sufficient progress and consensus is achieved, use only FRM for the routine validation of satellite ocean colour data.

7.3 Other Recommendations - terminology

The International Ocean Colour Coordinating Group (IOCCG) has been the primary forum over the last 20 years for coordination, harmonisation and improvement of many aspects of satellite optical data, including validation. The NASA Ocean Optics Protocols have similarly led the community of validation scientists. However, the advent of freely available, high quality data at much higher spatial resolution, e.g. from Landsat-8 and Sentinel-2, has led to a massive expansion of interest in satellite optical data for coastal, estuarine and inland waters and hence a need for FRM for validation in such non-oceanic waters. Although certain conditions (e.g. shallow water, adjacency effects, certain phytoplankton species, vertical stratification, high CDOM absorption, etc.) may prevail more or less frequently in coastal/estuarine/inland waters as compared to oceanic waters there is no generic difference in terms of optical processes that may occur. In the specific case of the uncertainty budget of Fiducial Reference Measurements considered in this report many references have been drawn from the "ocean colour" community, but it is clear that the uncertainty elements that must be considered are quite applicable to all types of water. It is therefore recommended to the IOCCG and to the "ocean colour" community to:

- adopt a terminology that reflects this generic nature of aquatic optical processes: "air-water interface" instead of "sea surface", "water colour/reflectance" instead of "ocean colour", "aquatic/water optics protocols" instead of "ocean optics protocols", etc.

7.4 Any remaining issues and gaps in knowledge

7.4.1 Rare and expensive tools and expertise

During the discussion of this review with validation scientists it became obvious that the fundamental FRM4SOC requirement to provide a full and validated uncertainty budget for measurements is an extremely challenging task. For many validation the necessary modelling tools and/or expertise are simply not available in-house or would require many months of scientist-time to develop and implement or many thousands of euros. Examples of such "rare and expensive" tools/expertise include the modelling of sky and water radiances to analyse the effect of tilt on Ed measurements (section 3.1.2.1) or the modelling of radiative transfer in water between the uppermost measurement depth and the air-water interface for the estimation of depth extrapolation uncertainties (section 4.1.2.1). The validation community would benefit greatly if such tools/expertise could be mutualised in a way that both rewards appropriately the developers of such tools/expetise and allows the user validation scientists to remain independent.

7.5 Future evolution of requirements and protocols

It is probable that new findings and practices will lead to some obsolescence for the present document, e.g. over a 3-5 year timeframe, as is currently the case for the 2004 NASA Ocean Optics protocols. Some scientists advocate the use of a "living document", such as a constantly evolving web site, for measurement protocols to stay abreast of rapid developments in the field. However, traceability implies a need for clear versioning of any document and the possibility to easily see the differences between versions and reference the version that was relevant when any specific measurement was acquired/processed. A practical compromise between the needs for traceability and stability/maturity and the desire to take account of new developments may be achieved by a revision cycle for this document (or a similar IOCCG document) of 3-4 years, preferably associated with a 2-3 day international protocols workshop for detailed discussions within a limited number of scientists and a full community consultation, e.g. via a IOCS breakout.

8 References

Albert, A., and C. Mobley. 2003. "An Analytical Model for Subsurface Irradiance and Remote Sensing Reflectance in Deep and Shallow Case-2 Waters." *Optics Express* 11 (22):2873–90.

Antoine, D., P. Guevel, J-F. Desté, G. Bécu, F. Louis, A. J. Scott, and P. Bardey. 2008. "The 'BOUSSOLE' Buoy-a New Transparent-to-Swell Taut Mooring Dedicated to Marine Optics: Design, Tests, and Performance at Sea." *Journal of Atmospheric and Oceanic Technology* 25 (6):968–989.

Antoine, David, Fabrizio d'Ortenzio, Stanford B. Hooker, Guislain Bécu, Bernard Gentili, Dominique Tailliez, and Alec J. Scott. 2008. "Assessment of Uncertainty in the Ocean Reflectance Determined by Three Satellite Ocean Color Sensors (MERIS, SeaWiFS and MODIS-A) at an Offshore Site in the Mediterranean Sea (BOUSSOLE Project)." *Journal of Geophysical Research* 113 (C7). https://doi.org/10.1029/2007JC004472.

Austin, Roswell W., and George Halikas. 1976. "The Index of Refraction of Seawater." https://escholarship.org/uc/item/8px2019m.pdf.

Bailey, S.W., and P.J. Werdell. 2006. "A Multi-Sensor Approach for the on-Orbit Validation of Ocean Color Satellite Data Products." *Remote Sensing of the Environment* 102 (1–2):12–23.

Barker, K., C. Mazeran, C. Lerebourg, M. Bouvet, D. Antoine, M. Ondrusek, G. Zibordi, and S. Lavender. 2008. "MERMAID: The MEris MAtchup In-Situ Database." In *2nd MERIS/(A)ATSR User Workshop Proceedings*.

Beltrán-Abaunza, J. M., S. Kratzer, and C. Brockmann. 2014. "Evaluation of MERIS Products from Baltic Sea Coastal Waters Rich in CDOM." *Ocean Science* 10 (3):377–96. https://doi.org/10.5194/os-10-377-2014.

Brando, Vittorio E., Jenny L. Lovell, Edward A. King, David Boadle, Roger Scott, and Thomas Schroeder. 2016. "The Potential of Autonomous Ship-Borne Hyperspectral Radiometers for the Validation of Ocean Color Radiometry Data." *Remote Sensing* 8 (2):150.

Brown, Steven W., Stephanie J. Flora, Michael E. Feinholz, Mark A. Yarbrough, Terrence Houlihan, Darryl Peters, Yong Sung Kim, James L. Mueller, B. Carol Johnson, and Dennis K. Clark. 2007. "The Marine Optical Buoy (MOBY) Radiometric Calibration and Uncertainty Budget for Ocean Color Satellite Sensor Vicarious Calibration." In , edited by Roland Meynart, Steven P. Neeck, Haruhisa Shimoda, and Shahid Habib, 67441M. https://doi.org/10.1117/12.737400.

Carder, K.L., and R.G. Steward. 1985. "A Remote-Sensing Reflectance Model of a Red-Tide Dinoflagellate off West Florida." *Limnology and Oceanography* 30 (2):286–98.

CEOS. 2016. "Committee on Earth Obseravtion Satellites (CEOS) Working Group on Cailbration and Validation (WGCV) Terms of Reference."

Clark, D. K., H. R. Gordon, K. J. Voss, Y. Ge, W. Broenkow, and C. Trees. 1997. "Validation of Atmospheric Correction over the Oceans." *J. Geophys. Res* 102 (17):209–17.

Clark, D.K., M.A. Yarbrough, M. Feinholz, S. Flora, W. Broenkow, Y.S. Kim, B. C. Johnson, S.W. Brown, M. Yuen, and J. L. Mueller. 2003. "MOBY, A Radiometric Buoy for Performance Monitoring and Vicarious Calibration of Satellite Ocean Color Sensors: Measurement and Data Analysis Protocols. Chapter 2." http://ntrs.nasa.gov/search.jsp?R=20030063145.

Claustre, H., S. Bernard, J.-F. Berthon, J. Bishop, E. Boss, C. Coaranoan, F. D'Ortenzio, K. Johnson, A. Lotliker, and O. Ulloa. 2011. *Bio-Optical Sensors on Argo Floats*. IOCCG Report 11.

Cox, C., and W. Munk. 1954. "Measurements of the Roughness of the Sea Surface from Photographs of the Sun's Glitter." *Journal of the Optical Society of America* 44:834–50.

D'Alimonte, D., G Zibordi, and J.-F. Berthon. 2001. "The JRC Data Processing System." In *Results of the Second SeaWiFS Data Analysis Round Robin, March 2000 (DARR-00)*, 15:52–56. SeaWiFS Postlaunch Technical Report Series Volume 15, NASA Technical Memorandum 2001-206892.

D'Alimonte, Davide, and Tamito Kajiyama. 2016. "Effects of Light Polarization and Waves Slope Statistics on the Reflectance Factor of the Sea Surface." *Optics Express* 24 (8):7922. https://doi.org/10.1364/OE.24.007922.

D'Alimonte, Davide, Eugeny B. Shybanov, Giuseppe Zibordi, and Tamito Kajiyama. 2013. "Regression of In-Water Radiometric Profile Data." *Optics Express* 21 (23):27707–27733.

D'Alimonte, Davide, Giuseppe Zibordi, Tamito Kajiyama, and José C. Cunha. 2010. "Monte Carlo Code for High Spatial Resolution Ocean Color Simulations." *Applied Optics* 49 (26):4936–4950.

Darecki, Miroslaw, Dariusz Stramski, and Maciej Sokólski. 2011. "Measurements of High-Frequency Light Fluctuations Induced by Sea Surface Waves with an Underwater Porcupine Radiometer System." *Journal of Geophysical Research: Oceans* 116 (C7).

Deschamps, P.-Y., B. Fougnie, R. Frouin, P. Lecomte, and C. Verwaerde. 2004. "SIMBAD: A Field Radiometer for Satellite Ocean Color Validation." *Applied Optics* 43 (20):4055–69.

Deuzé, J. L., M. Herman, and R. Santer. 1989. "Fourier Series Expansion of the Transfer Equation in the Atmosphere-Ocean System." *Journal of Quantitative Spectroscopy and Radiative Transfer* 41 (6):483–494.

Doerffer, R. 2002. "Protocols for the Validation of MERIS Water Products" PO-TN-MEL-GS-0043 Issue 1 Revision 3, 25th January 2002.

Dogliotti, A.I., J.I. Goosn, Vanhellemont, Q., and K. G. Ruddick. 2015. "Evaluation of Two Sites for Ocean Color Validation in the Turbid Waters of the Rio de La Plata (Argentina) (2015) Submitted for the Proceedings of The." In . Vol. ESA Special Publication SP-734.

Donlon, Craig J., W. Wimmer, I. Robinson, G. Fisher, M. Ferlet, T. Nightingale, and B. Bras. 2014. "A Second-Generation Blackbody System for the Calibration and Verification of Seagoing Infrared Radiometers." *Journal of Atmospheric and Oceanic Technology* 31 (5):1104–27. https://doi.org/10.1175/JTECH-D-13-00151.1.

Doxaran, David, Nagur C. Cherukuru, Samantha J. Lavender, and Gerald F. Moore. 2004. "Use of a Spectralon Panel to Measure the Downwelling Irradiance Signal: Case Studies and Recommendations." *Applied Optics* 43 (32):5981. https://doi.org/10.1364/AO.43.005981.

Doyle, John P., and Giuseppe Zibordi. 2002. "Optical Propagation within a Three-Dimensional Shadowed Atmosphere–ocean Field: Application to Large Deployment Structures." *Applied Optics* 41 (21):4283–4306.

Early, E. A., P. Y. Barnes, B. C. Johnson, J. J. Butler, C. J. Bruegge, S. F. Biggar, P. R. Spyak, and M. M. Pavlov. 2000. "Bidirectional Reflectance Round-Robin in Support of the Earth Observing System Program." *Journal of Atmospheric and Oceanic Technology* 17 (8):1077–91. https://doi.org/10.1175/1520-0426(2000)017<1077:BRRRIS>2.0.CO;2.

Fan, Yongzhen, Wei Li, Kenneth J. Voss, Charles K. Gatebe, and Knut Stamnes. 2016. "Neural Network Method to Correct Bidirectional Effects in Water-Leaving Radiance." *Applied Optics* 55 (1):10–21.

Foster, Robert, and Alexander Gilerson. 2016. "Polarized Transfer Functions of the Ocean Surface for Above-Surface Determination of the Vector Submarine Light Field." *Applied Optics* 55 (33):9476. https://doi.org/10.1364/AO.55.009476.

Fougnie, B., R. Frouin, P. Lecomte, and P.-Y. Deschamps. 1999. "Reduction of Skylight Reflection Effects in the Above-Water Measurement of Diffuse Marine Reflectance." *Applied Optics* 38 (18):3844–56.

Garaba, Shungudzemwoyo P., Daniela Voß, Jochen Wollschläger, and Oliver Zielinski. 2015. "Modern Approaches to Shipborne Ocean Color Remote Sensing." *Applied Optics* 54 (12):3602. https://doi.org/10.1364/AO.54.003602.

Georgiev, Georgi T., and James J. Butler. 2004. "The Effect of Incident Light Polarization on Spectralon BRDF Measurements." In , edited by Roland Meynart, Steven P. Neeck, and Haruhisa Shimoda, 492. https://doi.org/10.1117/12.565686.

———. 2007. "Long-Term Calibration Monitoring of Spectralon Diffusers BRDF in the Air-Ultraviolet." *Applied Optics* 46 (32):7892–7899.

Gerbi, Gregory P., Emmanuel Boss, P. Jeremy Werdell, Christopher W. Proctor, Nils Haëntjens, Marlon R. Lewis, Keith Brown, et al. 2016. "Validation of Ocean Color Remote Sensing Reflectance Using Autonomous Floats." *Journal of Atmospheric and Oceanic Technology* 33 (11):2331–52. https://doi.org/10.1175/JTECH-D-16-0067.1.

Gergely, Mathias, and Giuseppe Zibordi. 2014. "Assessment of AERONET-OC L_{WN} Uncertainties." *Metrologia* 51 (1):40–47. https://doi.org/10.1088/0026-1394/51/1/40.

Gernez, Pierre, Dariusz Stramski, and Miroslaw Darecki. 2011. "Vertical Changes in the Probability Distribution of Downward Irradiance within the Near-Surface Ocean under Sunny Conditions." *Journal of Geophysical Research* 116 (October). https://doi.org/10.1029/2011JC007156.

Gohin, F., B. Saulquin, H. Oger-Jeanneret, L. Lozac'h, L. Lampert, A. Lefebvre, P. Riou, and F. Bruchon. 2008. "Towards a Better Assessment of the Ecological Status of Coastal Waters Using Satellite-Derived Chlorophyll-a Concentrations." *Remote Sensing of the Environment* 112 (8):3329–40.

Gordon, Howard R. 1985. "Ship Perturbation of Irradiance Measurements at Sea 1: Monte Carlo Simulations." *Applied Optics* 24 (23):4172. https://doi.org/10.1364/AO.24.004172.

———. 2005. "Normalized Water-Leaving Radiance: Revisiting the Influence of Surface Roughness." *Applied Optics* 44 (2):241. https://doi.org/10.1364/AO.44.000241.

Gordon, Howard R., and Kuiyuan Ding. 1992. "Self-Shading of in-Water Optical Instruments." *Limnology and Oceanography* 37 (3):491–500. https://doi.org/10.4319/lo.1992.37.3.0491.

Gordon, H.R., and D.K. Clark. 1981. "Clear Water Radiances for Atmospheric Correction of Coastal Zone Color Scanner Imagery." *Applied Optics* 20 (24):4175–80.

Gould, R.W., R.A. Arnone, and M. Sydor. 2001. "Absorption, Scattering and Remote-Sensing Reflectance Relationships in Coastal Waters: Testing a New Inversion Algorithm." *Journal of Coastal Research* 17 (2):328–41.

Gregg, Watson W., and Kendall L. Carder. 1990. "A Simple Spectral Solar Irradiance Model for Cloudless Maritime Atmospheres." *Limnology and Oceanography* 35 (8):1657–1675.

Groetsch, Philipp M. M., Peter Gege, Stefan G. H. Simis, Marieke A. Eleveld, and Steef W. M. Peters. 2017. "Validation of a Spectral Correction Procedure for Sun and Sky Reflections in Above-Water Reflectance Measurements." *Optics Express* 25 (16):A742. https://doi.org/10.1364/OE.25.00A742.

GUM, ISO. 2008. "Guide to the Expression of Uncertainty in Measurement, (1995), with Supplement 1, Evaluation of Measurement Data, JCGM 101: 2008." *Organization for Standardization, Geneva, Switzerland*.

Harmel, Tristan, Alexander Gilerson, Alberto Tonizzo, Jacek Chowdhary, Alan Weidemann, Robert Arnone, and Sam Ahmed. 2012. "Polarization Impacts on the Water-Leaving Radiance Retrieval from above-Water Radiometric Measurements." *Applied Optics* 51 (35):8324. https://doi.org/10.1364/AO.51.008324.

Hieronymi, M., and A. Macke. 2012. "On the Influence of Wind and Waves on Underwater Irradiance Fluctuations." *Ocean Science* 8 (4):455–71. https://doi.org/10.5194/os-8-455-2012.

Hieronymi, Martin. 2016. "Polarized Reflectance and Transmittance Distribution Functions of the Ocean Surface." *Optics Express* 24 (14):A1045. https://doi.org/10.1364/OE.24.0A1045.

Hlaing, Soe, Tristan Harmel, Amir Ibrahim, Ioannis Ioannou, Alberto Tonizzo, Alexander Gilerson, and Samir Ahmed. 2010. "Validation of Ocean Color Satellite Sensors Using

Coastal Observational Platform in Long Island Sound." In *Remote Sensing*, 782504–782504. International Society for Optics and Photonics. http://proceedings.spiedigitallibrary.org/proceeding.aspx?articleid=725099.

Holben, B., and e. al. 1998. "AERONET - A Federated Instrument Network and Data Archive for Aerosol Characterization." *Remote Sensing of the Environment* 66 (1):1–16.

Hommersom, A., S. Kratzer, M. Laanen, I. Ansko, M. Ligi, M. Bresciani, C. Giardino, et al. 2012. "Intercomparison in the Field between the New WISP-3 and Other Radiometers (TriOS Ramses, ASD FieldSpec, and TACCS)." *Journal of Applied Remote Sensing* 6:063615–22pp.

Hooker, S. B., J. H. Morrow, and A. Matsuoka. 2013. "Apparent Optical Properties of the Canadian Beaufort Sea; Part 2: The 1% and 1 Cm Perspective in Deriving and Validating AOP Data Products." *Biogeosciences* 10 (7):4511.

Hooker, S.B. 2010. "The Telescopic Mount for Advanced Solar Technologies (T-MAST)." In *Advances in Measuring the Apparent Optical Properties (AOPs) of Optically Complex Waters*. Vol. 215856. NASA/TM.

Hooker, S.B., and G. Lazin. 2000. "The SeaBOARR-99 Field Campaign" TM 2000-206892, Volume 8 (SeaWiFS Postlaunch Technical Report Series):46.

Hooker, S.B., and A. Morel. 2003. "Platform and Environmental Effects on Above-Water Determinations of Water-Leaving Radiances." *Journal of Atmospheric and Oceanic Technology* 20:187–205.

Hooker, S.B., G Zibordi, and S. Maritorena. 2001. "The Second SeaWiFs Ocean Optics DARR (DARR-00)." In *Results of the Second SeaWiFS Data Analysis Round Robin, March 2000 (DARR-00)*, 15:4–45. SeaWiFS Postlaunch Technical Report Series Volume 15, NASA Technical Memorandum 2001-206892.

Hooker, Stanford B., Germar Bernhard, John H. Morrow, Charles R. Booth, Thomas Comer, Randall N. Lind, and Vi Quang. 2012. "Optical Sensors for Planetary Radiant Energy (OSPREy): Calibration and Validation of Current and Next-Generation NASA Missions." https://ntrs.nasa.gov/search.jsp?R=20130003503.

Hooker, Stanford B., Gordana Lazin, Giuseppe Zibordi, and Scott McLean. 2002. "An Evaluation of Above- and In-Water Methods for Determining Water-Leaving Radiances." *Journal of Atmospheric and Oceanic Technology* 19 (4):486–515. https://doi.org/10.1175/1520-0426(2002)019<0486:AEOAAI>2.0.CO;2.

Hooker, Stanford B., and Stephane Maritorena. 2000. "An Evaluation of Oceanographic Radiometers and Deployment Methodologies." *Journal of Atmospheric and Oceanic Technology* 17 (6):811–830.

Hu, Chuanmin, Kendall L Carder, and Frank E Muller-Karger. 2001. "How Precise Are SeaWiFS Ocean Color Estimates? Implications of Digitization-Noise Errors." *Remote Sensing of Environment* 76 (2):239–49. https://doi.org/10.1016/S0034-4257(00)00206-6.

International Ocean Colour Coordinating Group (IOCCG). 2007. "Ocean Colour Data Merging" 6 (IOCCG Report):68.

Johnson, B. C., H. Yoon, J.P. Rice, and A.C. Parr. 2014. "Principles of Optical Radiometry and Measurement Uncertainty." In *Optical Radiometry for Ocean Climate Measurements*, edited by G. Zibordi, C. Donlon, and A.C. Parr.

Joseph Rhea, W., and Curtiss O. Davis. 1997. "A Comparison of the SeaWiFS Chlorophyll and CZCS Pigment Algorithms Using Optical Data from the 1992 JGOFS Equatorial Pacific Time Series." *Deep Sea Research Part II: Topical Studies in Oceanography* 44 (9–10):1907–25. https://doi.org/10.1016/S0967-0645(97)00062-3.

Kalisch, John, and Andreas Macke. 2008. "Estimation of the Total Cloud Cover with High Temporal Resolution and Parametrization of Short-Term Fluctuations of Sea Surface Insolation." *Meteorologische Zeitschrift* 17 (5):603–11. https://doi.org/10.1127/0941-2948/2008/0321.

Kallio, Kari, Sampsa Koponen, Antonio Ruiz-Verdú, Thomas Heege, Kai Sørensen, Timo Pyhälahti, and Roland Doerffer. 2007. “Development of MERIS Lake Water Algorithms Document Title: Validation Protocol (WP 2.4).” https://www.brockmann-consult.de/beam-wiki/download/attachments/1174/MERIS_LAKES_Validation_Protocol_V1.0.doc.

Kutser, Tiit, Ele Vahtmäe, Birgot Paavel, and Tuuli Kauer. 2013. “Removing Glint Effects from Field Radiometry Data Measured in Optically Complex Coastal and Inland Waters.” *Remote Sensing of Environment* 133:85–89.

Lee, Zhong Ping, Keping Du, Kenneth J. Voss, Giuseppe Zibordi, Bertrand Lubac, Robert Arnone, and Alan Weidemann. 2011. “An Inherent-Optical-Property-Centered Approach to Correct the Angular Effects in Water-Leaving Radiance.” *Applied Optics* 50 (19):3155–67.

Lee, ZhongPing, Yu-Hwan Ahn, Curtis Mobley, and Robert Arnone. 2010. “Removal of Surface-Reflected Light for the Measurement of Remote-Sensing Reflectance from an above-Surface Platform.” *Optics Express* 18 (25):26313. https://doi.org/10.1364/OE.18.026313.

Lee, ZhongPing, Nima Pahlevan, Yu-Hwan Ahn, Steven Greb, and David O’Donnell. 2013. “Robust Approach to Directly Measuring Water-Leaving Radiance in the Field.” *Applied Optics* 52 (8):1693. https://doi.org/10.1364/AO.52.001693.

Leeuw, Thomas. 2014. “Crowdsourcing Water Quality Data Using the IPhone Camera.” Master of Science, University of Maine.

Li, Linhai, Dariusz Stramski, and Rick A. Reynolds. 2016. “Effects of Inelastic Radiative Processes on the Determination of Water-Leaving Spectral Radiance from Extrapolation of Underwater near-Surface Measurements.” *Applied Optics* 55 (25):7050. https://doi.org/10.1364/AO.55.007050.

Loisel, H., and A. Morel. 2001. “Non-Isotropy of the Upward Radiance Field in Typical Coastal (Case 2) Waters.” *International Journal of Remote Sensing* 22 (2):275–95.

Maritorena, S., and S.B. Hooker. 2001. “The GSFC Data Processing System.” In *Results of the Second SeaWiFS Data Analysis Round Robin, March 2000 (DARR-00)*, 15:46–51. SeaWiFS Postlaunch Technical Report Series Volume 15, NASA Technical Memorandum 2001-206892.

McClain, C.R., M.L. Cleave, G.C. Feldman, W.W. Gregg, S.B. Hooker, and N. Kuring. 1998. “Science Quality SeaWiFS Data for Global Biosphere Research.” *Sea Technology* 9:10–16.

Milton, Edward J., Michael E. Schaepman, Karen Anderson, Mathias Kneubühler, and Nigel Fox. 2009. “Progress in Field Spectroscopy.” *Remote Sensing of Environment* 113 (September):S92–109. https://doi.org/10.1016/j.rse.2007.08.001.

Mobley, C.D. 1994. *Light and Water: Radiative Transfer in Natural Waters*. London: Academic Press.

———. 1999. “Estimation of the Remote-Sensing Reflectance from above-Surface Measurements.” *Applied Optics* 38:7442–55.

Mobley, Curtis D. 2015. “Polarized Reflectance and Transmittance Properties of Windblown Sea Surfaces.” *Applied Optics* 54 (15):4828. https://doi.org/10.1364/AO.54.004828.

Morel, A. 1980. “In-Water and Remote Measurements of Ocean Colour.” *Boundary Layer Meteorology* 18:177–201.

Morel, A., and B. Gentili. 1991. “Diffuse Reflectance of Oceanic Waters: Its Dependence on Sun Angle as Influenced by the Molecular Scattering Contribution.” *Applied Optics* 30 (30):4427–38.

———. 1993. “Diffuse Reflectance of Oceanic Waters II. Bidirectional Aspects.” *Applied Optics* 32:6864–79.

———. 1996. “Diffuse Reflectance of Oceanic Waters. III. Implications of Bidirectionality for the Remote Sensing Problem.” *Applied Optics* 35 (24):4850–62.

Morel, A., and J. L. Mueller. 2003. "Normalized Water-Leaving Radiance and Remote Sensing Reflectance: Bidirectional Reflectance and Other Factors." In *Ocean Optics Protocols for Satellite Ocean Color Sensor Validation, Revision 4, Volume III: Radiometric Measuremens and Data Analysis Protocols*, 32–59. NASA/TM.

Morrow, John H., Stanford B. Hooker, Charles R. Booth, Germar Bernhard, Randall N. Lind, and James W. Brown. 2010. "Advances in Measuring the Apparent Optical Properties (AOPs) of Optically Complex Waters." *NASA Tech. Memo* 215856:42–50.

Mouw, Colleen B., Steven Greb, Dirk Aurin, Paul M. DiGiacomo, Zhongping Lee, Michael Twardowski, Caren Binding, et al. 2015. "Aquatic Color Radiometry Remote Sensing of Coastal and Inland Waters: Challenges and Recommendations for Future Satellite Missions." *Remote Sensing of Environment* 160:15–30.

Mueller, J. L. 2003. "In-Water Radiometric Profile Measurements and Data Analysis Protocols (Chapter 2)." In *Ocean Optics Protocols for Satellite Ocean Color Sensor Validation, Revision 4, Volume III: Radiometric Measurements and Data Analysis Protocols*, 7–20. NASA/TM.

———. 2004. "Shadow Corrections to In-Water Upwelled Radiance Measurments: A Status Review." In *Ocean Optics Protocols for Satellite Ocean Color Sensor Validation, Revision 5, Volume VI: Special Topics in Ocean Optics Protocols, Part 2*, 1–7. NASA/TM.

Mueller, J., J. L. MuelIer, C. Pietras, S. B. Hooker, D. K. Clark, A. Morel R. Frouin, B. G. Mitchell, et al. 2002. "Ocean Optics Protocols For Satellite Ocean Color Sensor Validation, Revision 3, Volumes 1 and 2." *NASA Tech. Memo* 210004. https://www.researchgate.net/profile/Malgorzata_Stramska/publication/255606432_Determination_of_spectral_absorption_coefficients_of_particles_dissolved_material_and_phytoplankton_for_discrete_water_samples/links/00b7d53c634b3b38d9000000.pdf.

Mueller, James L., and Roswell W. Austin. 1992. "SeaWiFS Technical Report Series. Volume 5: Ocean Optics Protocols for SeaWiFS Validation." https://ntrs.nasa.gov/search.jsp?R=19920020950.

Mueller, J.L., C. Davis, R. Arnone, R. Frouin, K. Carder, Z.P. Lee, R.G. Steward, S. Hooker, C.D. Mobley, and S. McLean. 2003. "Above-Water Radiance and Remote Sensing Reflectance Measurements and Analysis Protocols (Chapter 3)." In *Ocean Optics Protocols for Satellite Ocean Color Sensor Validation Revision 4, Volume III*, 21–31. Greenbelt, Maryland: National Aeronautical and Space Administration.

Mueller, J.L., G.S. Fargion, and C.R. McClain. 2003. *Ocean Optics Protocols for Satellite Ocean Color Sensor Validation*. Technical Memorandum TM-2003-21621/Revision 4. NASA.

———. 2004. *Ocean Optics Protocols for Satellite Ocean Color Sensor Validation*. Technical Memorandum TM-2003-21621/Revision 5. NASA.

Neukermans, G. 2012. "Optical In-Situ and Geostationary Satellite-Borne Observations of Suspended Particles in Coastal Waters." PhD Thesis, Université du Littoral Côte d'Opal. Academic and Scientific Publishers, Brussels, Belgium (ISBN 978 90 7028 949 2),.

Neukermans, G., K. G. Ruddick, and N. Greenwood. 2012. "Diurnal Variability of Turbidity and Light Attenuation in the Southern North Sea from the SEVIRI Geostationary Sensor." *REMOTE SENSING OF ENVIRONMENT* 124 (September):564–80. https://doi.org/10.1016/j.rse.2012.06.003.

Ondrusek, Michael, Veronica Peterson Lance, Robert Arnone, Sherwin Ladner, Wesley Goode, Ryan Vandermeulen, Scott Freeman, et al. 2016. "Report for Dedicated JPSS VIIRS Ocean Color December 2015 Calibration/Validation Cruise." U.S. Department of Commerce, National Oceanic and Atmospheric Administration, National Environmental Satellite, Data, and Information Service. https://doi.org/10.7289/V5/TR-NESDIS-148.

Park, YJ, and K Ruddick. 2005. "Model of Remote-Sensing Reflectance Including Bidirectional Effects for Case 1 and Case 2 Waters." *APPLIED OPTICS* 44 (7):1236–49. https://doi.org/10.1364/AO.44.001236.

Preisendorfer, Rudolph W., and Curtis D. Mobley. 1986. "Albedos and Glitter Patterns of a Wind-Roughened Sea Surface." *Journal of Physical Oceanography* 16 (7):1293–1316. https://doi.org/10.1175/1520-0485(1986)016<1293:AAGPOA>2.0.CO;2.

Ruddick, K., C. Brockmann, R. Doerffer, Z. Lee, V. Brotas, N. Fomferra, S. Groom, et al. 2010. "The Coastcolour Project Regional Algorithm Round Robin Exercise." In *REMOTE SENSING OF THE COASTAL OCEAN, LAND, AND ATMOSPHERE ENVIRONMENT*, edited by Frouin, RJ and Yoo, HR and Won, JS and Feng, A. Vol. 7858. Proceedings of SPIE-The International Society for Optical Engineering. SPIE; Korea Ocean Res & Dev Inst; Korea Ocean satellite Ctr; Incheon Tourism Org; Natl Aeronaut & Space Adm; Natl Inst Informat & Commun Technol; Sci Technol Corp; Indian Space Res Org; Indian Natl Ctr Ocean Informat Serv. https://doi.org/10.1117/12.869506.

Ruddick, K., V. De Cauwer, and B. Van Mol. 2005. "Use of the near Infrared Similarity Spectrum for the Quality Control of Remote Sensing Data." In , edited by R.J. Frouin, M. Babin, and S. Sathyendranath. Vol. 5885. SPIE. https://doi.org/10.1117/12.615160.

Ruddick, Kevin, Geneviève Lacroix, Christiane Lancelot, Bouchra Nechad, Youngje Park, Steef Peters, and Barbara Van Mol. 2008. "Optical Remote Sensing of the North Sea." In *Remote Sensing of the European Seas*, edited by V. Barale and M. Gade, 79–90. Springer-Verlag.

Ruddick, Kevin, Griet Neukermans, Quinten Vanhellemont, and Dominique Jolivet. 2014. "Challenges and Opportunities for Geostationary Ocean Colour Remote Sensing of Regional Seas: A Review of Recent Results." *REMOTE SENSING OF ENVIRONMENT* 146 (SI):63–76. https://doi.org/10.1016/j.rse.2013.07.039.

Ruddick, KG, V De Cauwer, YJ Park, and G Moore. 2006. "Seaborne Measurements of near Infrared Water-Leaving Reflectance: The Similarity Spectrum for Turbid Waters." *LIMNOLOGY AND OCEANOGRAPHY* 51 (2):1167–79.

Santer, R., F. Zagolski, K. Barker, and J.-P. Huot. 2012. "Correction of the above Water Radiometric Measurements for the Sky Dome Reflection, Accounting for Polarization." In *Roceedings of MERIS/(A) ATSR & OLCI/SLSTR Preparatory Workshop*.

Segal-Rosenheimer, M., P. B. Russell, B. Schmid, J. Redemann, J. M. Livingston, C. J. Flynn, R. R. Johnson, et al. 2014. "Tracking Elevated Pollution Layers with a Newly Developed Hyperspectral Sun/Sky Spectrometer (4STAR): Results from the TCAP 2012 and 2013 Campaigns." *Journal of Geophysical Research: Atmospheres* 119 (5):2013JD020884. https://doi.org/10.1002/2013JD020884.

Shang, Zhehai, Zhongping Lee, Qiang Dong, and Jianwei Wei. 2017. "Self-Shading Associated with a Skylight-Blocked Approach System for the Measurement of Water-Leaving Radiance and Its Correction." *Applied Optics* 56 (25):7033. https://doi.org/10.1364/AO.56.007033.

Simis, Stefan G.H., and John Olsson. 2013. "Unattended Processing of Shipborne Hyperspectral Reflectance Measurements." *Remote Sensing of Environment* 135 (August):202–12. https://doi.org/10.1016/j.rse.2013.04.001.

Slivkoff, Matthew Michael. 2014. "Ocean Colour Remote Sensing of the Great Barrier Reef Waters." Thesis, Curtin University. https://espace.curtin.edu.au/handle/20.500.11937/798.

Smith, Raymond C., Charles R. Booth, and Jeffrey L. Star. 1984. "Oceanographic Biooptical Profiling System." *Applied Optics* 23 (16):2791–2797.

Stiegman, Albert E., Carol J. Bruegge, and Arthur W. Springsteen. 1993. "Ultraviolet Stability and Contamination Analysis of Spectralon Diffuse Reflectance Material." *Optical Engineering* 32 (4):799–804.

Tanaka, Akihiko, Hiroaki Sasaki, and Joji Ishizaka. 2006. "Alternative Measuring Method for Water-Leaving Radiance Using a Radiance Sensor with a Domed Cover." *Optics Express* 14 (8):3099. https://doi.org/10.1364/OE.14.003099.

Tartu Observatory, SYKE, CNR, and Water Insight. 2015. "Global Lake Sentinel Services (GLASS) Technical Report about Measurement Protocols." http://www.glass-project.eu/assets/Downloads/GLaSS-inland-waters-protocols-2015.pdf.

Thorpe, Stephen A. 2007. *An Introduction to Ocean Turbulence*. Cambridge University Press.

Thuillier, G., M. Herse, D. Labs, T. Foujols, W. Peetermans, D. Gillotay, P.C. Simon, and H. Mandel. 2003. "The Solar Spectral Irradiance from 200 to 2400 Nm as Measured by the SOLSPEC Spectrometer from the ATLAS and EURECA Missions." *Solar Physics* 214 (1):1–22.

Tilstone, G., G. Moore, K. Sorensen, R. Doerffer, R. Rottgers, K.G. Ruddick, R. Pasterkamp, and P.V. Jorgensen. 2003. "REVAMP Regional Validation of MERIS Chlorophyll Products in North Sea Coastal Waters: Protocols Document." In . Vol. WPP-233. European Space Agency.

Van der Zande, D., G. Lacroix, X. Desmit, and K. Ruddick. 2011. "Impact of Irregular Sampling by MERIS on Eutrophication Monitoring Products for WFD and MSFD Applications." In . Sopot, Poland.

Vanhellemont, Q., G. Neukermans, and K. Ruddick. 2014. "Synergy between Polar-Orbiting and Geostationary Sensors: Remote Sensing of the Ocean at High Spatial and High Temporal Resolution." *Remote Sens. Environ.* 146:49–62.

Vanhellemont, Q., and K. Ruddick. 2015. "Assessment of Sentinel-3/OLCI Sub-Pixel Variability and Platform Impact Using Landsat-8/OLI." In . ESA Special Publication SP-734.

Vanhellemont, Q., and K.G. Ruddick. 2014. "Turbid Wakes Associated with Offshore Wind Turbines Observed with Landsat 8." *Remote Sens. Environ.* 145:105–15.

Vanhellemont, Quinten, and Kevin Ruddick. n.d. "ASSESSMENT OF SENTINEL-3/OLCI SUB-PIXEL VARIABILITY AND PLATFORM IMPACT USING LANDSAT-8/OLI." Accessed January 8, 2016. http://odnature.naturalsciences.be/downloads/publications/vanhellemontruddick2015_s3fs_proceedings_header47.pdf.

Voss, K. J., and Stephanie J. Flora. 2017. "Spectral Dependence of the Seawater-Air Radiance Transmission Coefficient." *Journal of Atmospheric and Oceanic Technology*, 1203–5.

Voss, K. J., H. R. Gordon, S. Flora, B. C. Johnson, M.A. Yarbrough, M. Feinholz, and T. Houlihan. 2017. "A Method to Extrapolate the Diffuse Upwelling Radiance Attenuation Coefficient to the Surface as Applied to the Marine Optical Buoy (MOBY)," (in press).

Voss, Kenneth J. 1988. "Radiance Distribution Measurements In Coastal Water." In , edited by Marvin A. Blizard, 56–66. https://doi.org/10.1117/12.945709.

Voss, Kenneth J., and Albert L. Chapin. 2005. "Upwelling Radiance Distribution Camera System, NURADS." *Optics Express* 13 (11):4250. https://doi.org/10.1364/OPEX.13.004250.

Voss, K.J., J.W. Nolten, and G.D. Edwards. 1986. "Ship Shadow Effects on Apparent Optical Properties." In *Ocean Optics VIII*, 186–90. SPIE.

Waters, Kirk J., Raymond C. Smith, and Marion R. Lewis. 1990. "Avoiding Ship-Induced Light-Field Perturbation in the Determination of Oceanic Optical Properties." *Oceanography* 3 (2):18–21.

Zaneveld, J. Ronald, Emmanuel Boss, and Paul Hwang. 2001. "The Influence of Coherent Waves on the Remotely Sensed Reflectance." *Optics Express* 9 (6):260. https://doi.org/10.1364/OE.9.000260.

Zaneveld, J. Ronald V., Emmanuel Boss, and Andrew Barnard. 2001. "Influence of Surface Waves on Measured and Modeled Irradiance Profiles." *Applied Optics* 40 (9):1442. https://doi.org/10.1364/AO.40.001442.

Zhang, Xiaodong, Shuangyan He, Afshin Shabani, Peng-Wang Zhai, and Keping Du. 2017. “Spectral Sea Surface Reflectance of Skylight.” *Optics Express* 25 (4):A1. https://doi.org/10.1364/OE.25.0000A1.

Zibordi, G., S. Bailey, D. Antoine, P. Goryl, E.J. Kwiatkowska, M. Wang, B. Franz, et al. 2012. “International Network for Sensor Inter-Comparison and Uncertainty Assessment for Ocean Color Radiometry (INSITU-OCR).” INSITU-OCR White Paper.

Zibordi, G., and G.M. Ferrari. 1995. “Instrument Self-Shading in Underwater Optical Measurements: Experimental Data.” *Applied Optics* 34 (15):2750–54.

Zibordi, G., B. Holben, I. Slutsker, D. Giles, D. D’Alimonte, F. Mélin, J.-F. Berthon, et al. 2009. “AERONET-OC: A Network for the Validation of Ocean Color Primary Product.” *Journal of Atmospheric and Oceanic Technology* 26:1634–51.

Zibordi, G., S.B. Hooker, J.F. Berthon, and D. D’Alimonte. 2002. “Autonomous Above-Water Radiance Measurements from an Offshore Platform: A Field Assessment Experiment.” *J. Atmos. Oceanic Technol.* 19:808–19.

Zibordi, G., K. Ruddick, I. Ansko, G. Moore, S. Kratzer, J. Icely, and A. Reinart. 2012. “In Situ Determination of the Remote Sensing Reflectance: An Inter-Comparison.” *OCEAN SCIENCE* 8 (4):567–86. https://doi.org/10.5194/os-8-567-2012.

Zibordi, G., and K. J. Voss. 2014. “In Situ Optical Radiometry in the Visible and Near Infrared.” In *Optical Radiometry for Ocean Climate Measurements*, edited by G. Zibordi, C. Donlon, and A.C. Parr, 248–305.

Zibordi, Giuseppe, Jean-François Berthon, and Davide D’Alimonte. 2009. “An Evaluation of Radiometric Products from Fixed-Depth and Continuous In-Water Profile Data from Moderately Complex Waters.” *Journal of Atmospheric and Oceanic Technology* 26 (1):91–106. https://doi.org/10.1175/2008JTECHO619.1.

Zibordi, Giuseppe, Davide D’Alimonte, and Jean-François Berthon. 2004. “An Evaluation of Depth Resolution Requirements for Optical Profiling in Coastal Waters.” *Journal of Atmospheric and Oceanic Technology* 21 (7):1059–1073.

Zibordi, Giuseppe, John Piero Doyle, and Stanford B. Hooker. 1999. “Offshore Tower Shading Effects on In-Water Optical Measurements.” *Journal of Atmospheric and Oceanic Technology* 16 (11):1767–79. https://doi.org/10.1175/1520-0426(1999)016<1767:OTSEOI>2.0.CO;2.